Thesis submitted for M.A. in Geography November 2012

by

Bernie Mc Carthy
B.A. (Coláiste Mhuire Gan Smál)
Mary Immaculate College
University of Limerick

Supervisor: Dr. Angela Hayes

An Roinn Tíreolaíochta
Coláiste Mhuire Gan Smál
Ollscoil Luimnigh
An Cuarbhóthar Theas
Luimneach
Éire

Department of Geography
Mary Immaculate College
University of Limerick
South Circular Road
Limerick
Ireland

Table of Contents

Author's Declaration

I, Bernie Mc Carthy, declare that this thesis is my own work and has never been previously submitted by me or any other individual for the purpose of obtaining a qualification.

Signed:

Date:

Acknowledgements

Particular thanks to my supervisor Dr. Angela Hayes for inspiring and guiding me on a palaeoenvironmental path as an undergraduate and postgraduate student. For all her help and guidance, a sincere thank you. Thanks also to Prof. Des McCafferty, Dr. Brendan O Keeffe, Dr. Helene Bradley and Dr. Catherine Dalton for their help and support throughout this research. To Hellen Gallagher who was always so kind.

To all my collegues in Mary Immaculate College, Ruth Guiry, Darren Barry, Teresa Broggy, Shane O Sullivan, Enda Keenan, Karin Sparber, Filippo Cassina, Margaret Browne and Gráinne Dwyer, a special thank you for the entertaining news, gossip and general fun.

My greatest debt is to my family and I dedicate this work to my husband Gerry, my son Michael, and my daughters, Sinéad, Eilís, Gráinne and Méabh, without you I could not have completed this thesis. I really appreciated your constant support and encouragement in times of need.

List of Figures

List of Tables

Abstract

Late Quaternary palaeoenvironmental reconstruction of the Ionian Sea in the eastern Mediterranean

By Bernie Mc Carthy

Three eastern Mediterranean deep-sea cores, all from the Ionian Sea, have been investigated to assess late Quaternary palaeoenvironmental change. The high resolution record of planktonic foraminiferal variations for the three Ionian Sea deep cores provides a significant insight into the late Quaternary in relation to palaeoenvironmental and palaeoclimatic conditions. The timing of climatic events is further strengthened by a Sea Surface Temperature (SST) reconstruction based on the utilisation of the transfer function, Artificial Neural Network (ANN) and the calibration dataset of Hayes *et al.* (2005). Radiocarbon (^{14}C) gives an absolute age of planktonic foraminiferal shell formation within the late Pleistocene and Holocene.

The Ionian Sea palaeoenvironmental reconstruction allowed the presentation of four distinct time frames, the late Pleistocene (~20,000-13,000 cal yrs BP), the glacial/interglacial transition (~13,000-9,000 cal yrs BP), Sapropel 1 (~9,000-6,000 cal yrs BP) and the late Holocene (~6,000 to present cal yrs BP). High concentrations of warm water planktonic foraminiferal species, in particular *G. ruber*, is evident throughout the Holocene and late Pleistocene. A general consistency in the fluctuation of cold water species is observed in the faunal assemblages from the Ionian Sea during the late Pleistocene. Overall, a general cooling is observed from the start of the record, with a pronounced temperature increase at the beginning of the Holocene.

Comparison of the intervals and climatic events shows some correlation with other eastern Mediterranean studies, however, some discrepancies have also been observed.

Chapter 1: Introduction

1.1 Background

The Quaternary period, the most recent of the three periods of the Cenozoic Era, comprises the last 2.6 million years of Earth's history. This period consists of two geological epochs: the Pleistocene and Holocene. The world's climate changed from one of arctic harshness during the Pleistocene to the warmer conditions of the present interglacial Holocene. The late Pleistocene and Holocene represents a time with the most prolific and precise information on palaeoenvironmental and palaeoclimatic inconsistency. Since the 1940s the range of radiocarbon dating (~45,000 cal yrs BP) underpins the accuracy of information in relation to palaeoenvironmental studies (Bell and Walker, 2005). The commencement of this research begins at ~20,000 cal yrs BP to the present day late Holocene. The three cores (964A, 973A and 969A) studied originated in the Ionian Sea in the eastern Mediterranean basin. This sea is characterised by the modification of the major water masses, namely, by the moderately fresh Atlantic Water (AW), the extremely saline Levantine Intermediate Water (LIW) and the colder and deeper Eastern Mediterranean Deep Water (EMDW) (Malonotte-Rizzoli *et al*., 1997).

A generalised climatic evolution of the previous ~20,000 cal yrs BP is evident in the three Ionian cores examined. The long-term trend during this record is from the cold, glacial conditions of the late Pleistocene to the warmer interglacial conditions of the Holocene. Superimposed on this long term trend are the shorter climatic events, namely, Heinrich events, the Younger Dryas and the '8.2 cal yrs BP cold event' (Robinson *et al*., 2006). These cold events had a significant effect on climatic conditions in the northern Hemisphere. Robinson *et al*. (2006) acknowledged that their origin may have occurred as a result of a significant cold freshwater input into the North Atlantic Sea, resulting in oceanic circulation and local climatic regime disturbances. A short period of intense cooling depicts the Heinrich events and in the eastern Mediterranean region, as a result of the cold-freshwater input which led to a reduction in evaporation and precipitation, caused cooling and an evaporation excess

over the Levant region (Robinson *et al.*, 2006).

The Bølling-Allerøid warm interval (~15-13 cal yrs BP) is consistent with warmer and wetter conditions (Rossignol-Strich, 1995). However, the eastern Mediterranean record of this time is unclear but warm temperatures (~18°C) have been recorded at site 967 at ~16.5 cal yrs BP by Emeis *et al*., 2000.

The transition from glacial to interglacial is influenced by increasing temperatures and sea level rises. The climate of the present interglacial is reasonably stable when compared to the previous glacial interval, with the exception of the 8.2 cal yrs BP cold event (Ellison *et al*., 2006). These authors have revealed another similar cold event at ~8400 cal yrs BP, both of these cooling intervals prevailed at times when reduced SSTs dominated between ~8,000 - 8,900 cal yrs BP (Ellison *et al*., 2006). It has been also been noted by the previous authors that abrupt cooling at ~8,400 cal yrs BP occurred and lasted ~80 years which underpinned a 0.6 per mil (‰) depletion in planktonic foraminiferal §^{18}O values (Ellison *et al*., 2006). The effects of sea level rise during interglacial intervals can be catastrophic as regards salinity ranges within the eastern Mediterranean basin. Increased salinity levels gives rise to poor deep water ventilation and affects the hydrological and ecological systems (Rohling *et al*., 1994). Furthermore, a nutrient depletion effect on the surface waters as a result of this change reduces planktonic foraminiferal species (Rohling and Gieskes, 1989).

1.2 Area of Study: The Mediterranean Sea

The Mediterranean Sea is a semi-enclosed, mid-latitude sea situated between Europe and Africa occupying an area of approximately 2,542 million km² (Figure 1.1) (La Violette, 1994). Divided by the Straits of Sicily, the Mediterranean Sea consists of the western and eastern basins which are further subdivided into several smaller basins. The Strait of Gibraltar provides the only natural connection to the open ocean. At its narrowest, this strait is approximately 14km wide and up to 800m in depth (Rohling *et al.,* 2009). The Mediterranean Sea is a concentration basin with evaporation rates exceeding precipitation, resulting in high temperature and salinity rates from west to east (Hayes *et al*., 1999).The topography surrounding this sea tends to influence and strengthen seasonal atmospheric changes. The Atlantic Ocean, Eurasian and North African pressure systems also exert significant control on the weather patterns in specific locations within the Mediterranean Sea (Rohling *et al.,* 2009). Temperatures and salinities control the stability of the water column and hence the distribution of nutrients. This therefore impacts on the distribution of planktonic foraminifera (Hayes

et al., 1999). Using the principle of uniformitarianism researchers use the present day distribution of these organisms to aid in the reconstruction of past climates and environments.

Figure 1.1: Satellite image illustrating the Mediterranean Sea and surrounding countries. Both the western and eastern basins are highlighted along with several of the smaller sub-basins such as the Alboran, Adriatic and Aegean Seas (Courtesy of Earth Threats 2012).

Over the past few decades, numerous studies have been undertaken by many scientists in relation to the eastern Mediterranean Sea. This is as a result of the discovery, in 1947 during the Swedish Deep Sea Expedition, of dark, often laminated organic-rich sediments known as sapropels (Rohling *et al*., 2009). In general, these sapropels are only prevalent in the eastern Mediterranean making this basin attractive to scientists. While numerous models have been proposed to explain this phenomenon, it still remains controversial. To explain the formation of organic carbon enrichment in these sapropels, two theories have been put forward: an increased preservation rate of organic matter under anoxic conditions and increased productivity of organic matter in the photic zone (Murat and Got, 2000). Some interesting studies have focused more so on planktonic foraminifera as they are a more reliable proxy in relation to changes in marine ecosystems. Their distribution is suggestive of the time span involved in the

onset of anoxic conditions and the return of oxygenated waters (Schmiedl *et al*., 2003, Stefanelli *et al*., 2005).

To examine eastern Mediterranean palaeoenvironmental reconstruction in the late Quaternary, this study uses planktonic foraminifera as a palaeoproxy. These microfossils are extensively used in modern research as the launch of deep sea drilling in the 1950s incited their use as palaeoceanographic indicators (Bé, 1977; Haslett, 2002). Planktonic foraminifera are one of the most common tools utilised in palaeoceanography to reconstruct palaeoenvironmental constraints such as sea surface temperatures (SST) and other parameters such as depth of the pycnocline and of the chlorophyll maximum, the thickness of the mixed layer and convective mixing, among others (Pujol and Vergnaud Grazzini, 1995). Pioneer studies of the distribution and seasonality of living planktonic foraminifera were undertaken initially by such scientists as, Bé (1977) and Bé and Tolderlund (1971). Previous studies have acknowledged local seasonal distribution. Cifelli, (1974) presented a general account of planktonic foraminiferal distribution throughout the Mediterranean Sea. Previous studies have focused on the relationship between planktonic foraminifera and the temperature and salinity of the overlying water masses (Thiede, 1978, Thunell, 1978). Pujol and Vergnaud Grazzini, (1989).

1.3 Aims of this Research

To date while a number of studies focus on palaeoclimatic studies on the Mediterranean Sea, there is limited spatial coverage in the Ionian Sea. As such this research aims to enhance the coverage.

The aim of this research is to investigate, using micropalaeontological analyses, palaeoenvironmental change in the eastern Mediterranean Sea throughout the late Quaternary. To achieve this, this research aims to:

- To provide a high resolution record of planktonic foraminiferal variations for the three Ionian Sea deep cores.
- Examine the palaeoclimatic and palaeoenvironmental changes throughout the late Quaternary.
- Constrain the timing of any climatic events by constructing a well-defined age model based on AMS ^{14}C dating.
- Use an advanced computational transfer function -Artificial Neural Network (ANN) and the calibration dataset of Hayes *et al*. (2005) to reconstruct sea surface temperatures.

Chapter 2: Literature Review

2.1 Present Day Climatology

Situated between 30 and 45°N, the Mediterranean Sea occupies a transitional location in terms of its climatic regime. The arid climate of North Africa lies to the south, while the wet temperate climate of central Europe lies to the north of the western basin and the cold European climate to the north of the eastern basin (Giorgi and Lionello, 2008). Thus the Mediterranean climate is influenced by interactions between both mid-latitude and equatorial atmospheric processes. In the northern hemisphere, at approximately 30°N, descending air associated with the mid latitude and Hadley cells create a system of high pressure known as the Subtropical High. In the Atlantic Ocean this system is known as the Azores high pressure system. During the summer months the climate of the Mediterranean Sea is controlled by the presence of the Azores high pressure system resulting in hot arid conditions particularly over the southern Mediterranean region (Baudin *et al*., 2007; Frigola *et al*., 2007). In contrast, during the winter the Azores high pressure system is displaced southwards allowing the westerly winds to dominate the climate. As such the winter climate is generally controlled by the westward movement of storms originating over the Atlantic Ocean and impacting upon the western European coasts (Giorgi and Lionell, 2008).

The mountain ranges and plateaux surrounding the Mediterranean Sea also influence the regions climate. Local winds are orographically channelled towards the Mediterranean Sea thus influencing the climate and circulation regimes (Rohling *et al.*, 2009).

2.2 Mediterranean Winds

There are approximately 45 identified localised winds affecting the Mediterranean region of which the most common winds known are the Mistral, Levante, Bora, Bora/Etesian, Westerly and Sirocco (Figure 2.1). Winds within the Mediterranean region are influenced by the surrounding mountainous topography. The mountains channel wind towards the basin, frequently creating strong gales (Istrianet, 2012).

Mistral: These are cold north-westerly winds flowing into the Mediterranean Sea through the Gulf of Lion from the south of France. The wind is characterised by cold air sinking over the mountains which is channelled through the openings between the Alps, the Massif Central and the Pyrenees. Mistrals are at their strongest during the spring and winter months and frequently their effects are seen to continue to the eastern basin through the Strait of Sicily. In the winter, wind speeds of over 100 knots often advance over the south coast of France. Strong mistrals frequently develop when cyclogenesis occurs over the Gulf of Genoa with the effects extending into west and central Mediterranean. These winds are considered dangerous because of their high speeds (Istrianet, 2012).

Westerly winds: These cold winds flow through the Strait of Gibraltar from the Atlantic Ocean and are channelled between the Sierra Nevada Mountains in Spain and the Moroccan Atlas Mountains. Cyclones frequently form in the North Atlantic Ocean during winter and these cyclones are often guided towards the Mediterranean Sea creating precipitation (Istrianet, 2012). There are two types of westerly winds:

- Vendaval

These are strong southwesterlies ahead of cold fronts that occur with a low progression from the west. Thunderstorms are frequently associated with these winds (Istrianet, 2012).

- Poniente

These are northwesterly winds behind cold fronts flowing off the south-east coast of Spain and into the Alboran Channel and into the Strait of Gibraltar (Istrianet, 2012).

Levante winds: These are warm easterly winds and are associated with high levels of moisture. These winds are channelled from Corsica into the Alboran Sea and through the Strait of Gibraltar. Levantes can extend from the Balearic Islands into the Gulf of Cadiz. Levante winds can develop in three ways:

- They occur as a result of high pressure over central Europe and fairly low pressure over the south-west Mediterranean.
- They can develop as a consequence of high pressure over the Balearic Islands.
- The Levante winds occur due to an imminent cold front from the west towards the Strait of Gibraltar (Naval Research Laboratory, 2012).

During winter months, gale-force Levante winds frequently follow the end of gale-force Mistrals. In summer, these gale-force Levantes are normally restricted to the Strait of Gibraltar (Naval Research Laboratory, 2012).

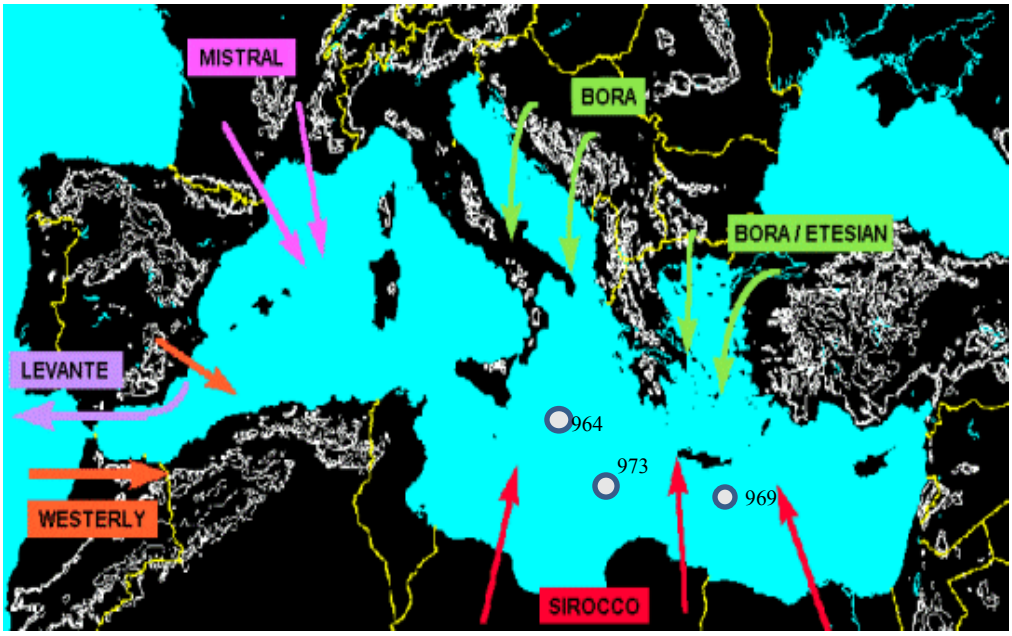

Figure 2.1: Map depicting major winds affecting the Mediterranean region. Pink arrows depict Mistral winds; green arrows depict Bora and Bora/Etesian winds; purple arrows depict Levante winds; orange arrows depict westerly winds and red arrows depict the Sirocco winds. The white shading depicts the mountain terrain surrounding the Mediterranean Sea. The core locations of those utilised in this study (ODP cores 964, 973 and 969) are also highlighted on the map (Courtesy of Istrianet, 2012).

Sirocco Winds: These are south-westerly warm winds and are the only wind not channelled by mountainous terrain. They flow from the desert regions between Egypt, Libya and Tunisia into the south-eastern and south-central Mediterranean Sea. These winds produce fog and rain in northern parts of the Mediterranean region. Gale-force Sirocco winds are often common in spring due to a low moving into the Gulf of Gabes from Tunisia, combined with the passage of a deep 500 mb trough expanding into northern Africa and located off the western side of the Gulf of Gabes (Naval Research Laboratory, 2012).

Bora Etesian Winds: These are northerly monsoonal summer and early fall winds which are forced through the Rhodope Mountains in Turkey and the Greek Pindus Mountains and carried to the Aegean Sea extending to the eastern Mediterranean Sea. Gale-force Etesians can develop as a consequence of thermal lows deepening over Turkey; however, this seldom occurs except when the winds are funnelled through passes (Naval Research Laboratory, 2012).

Boro Adriatic Winds: These are cold, north north-east winds, and are forced through gaps in the Dinaric Alps flowing into the Adriatic Sea east of Italy. These winds can occur as a result of cold polar air building up over the Balkans or when high pressure over the Balkans interacts with a low in the Ionian Sea. These winds are generally associated with stormy weather with winds frequently reaching 100 knots. Boro Adriatic Winds are usually restricted to the Adriatic Sea area, the northern Alps and the western Apennines (Naval Research Laboratory, 2012).

The above named gale-force winds have two individual seasons, 'winter' from October 1 to May 31 and 'summer' from June 1 to September 30. The strength of these winds varies between the seasons. The winter season correlates more with ridges and troughs, in contrast to the summer season which correlates more with calmer conditions (Naval Research Laboratory, 2012).

2.3 Cyclonic systems

A cyclone is a low pressure area in the atmosphere in which winds spiral inwards. Cyclones have two characteristics, firstly, the winds spiral in towards the centre and secondly, the atmospheric pressure is also lowest at the centre. The Mediterranean region is an active cyclone area with the most concentrated area of cyclonic activity being in the western basin. The Gulf of Genoa is a specific area of cyclonic activity and to a lesser degree the Catalan-Balearic basin, the Gulf of Lion and the Algerian Sea (Figure 2.2). Cyclones represent the most important manifestation of mid-latitude high frequency variability and playing a major role in atmospheric horizontal and vertical mixing altering sea-air interactions (Lionello *et al.,* 2006). Cyclonic circulations in the Mediterranean Sea, due to their frequency, strength and duration, play a vital role in the weather and climate of this entire region. The formation and passage of cyclonic disturbances in the Mediterranean greatly influences temperature, wind, fog and thunderstorms. Shallow, high intensity cyclones normally occur during summer. The Mistral wind has an impact on the formation of deep cyclones in winter and these deep cyclones are correlated with more severe weather conditions (Campins *et al.*, 2006).

2.4 The North Atlantic Oscillation

The North Atlantic Oscillation (NAO) is an important climate phenomenon or teleconnection in the Atlantic Ocean and has a distinct influence on the Mediterranean climate. This oscillation refers to changes in the atmospheric pressure difference between the Atlantic and the Arctic (Hurrell *et al*., 2003). It is understood to be the

main driver of seasonal temperature and precipitation over the Mediterranean region (Frigola *et al.,* 2007). Coupled with the Icelandic Low pressure system and the Azores High subtropical anticyclone, differences in atmospheric pressure conclude in a large scale circulation pattern which explains the North Atlantic Oscillation (Hurrell *et al*., 2003).

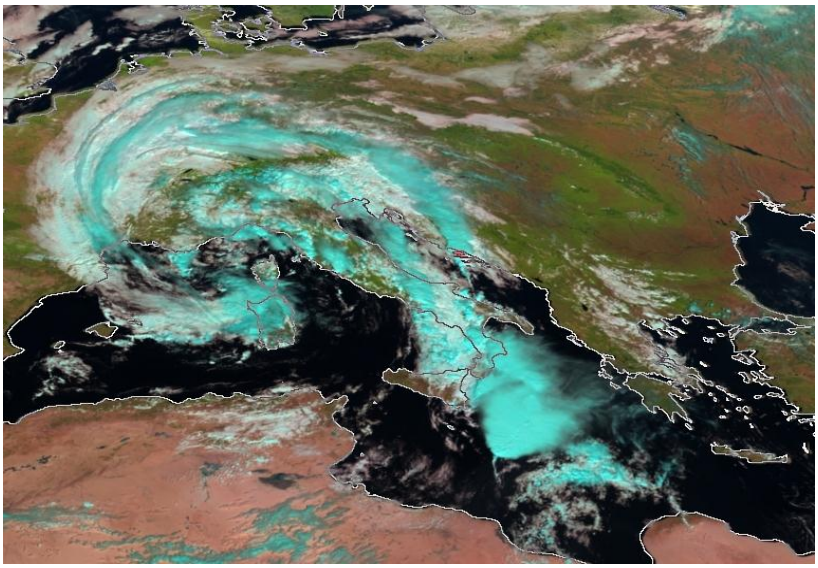

Figure 2.2:.Satalite image of the development of a cyclone "Genoa Low" October 2005. This image depicts the formation of a large convective system over the Mediterranean Sea to the south-east of Sicily (Courtesy of Eumestat, 2012).

The climate differences associated with the NAO are stronger during the boreal winter months however; the NAO alternates between positive and negative phases depending on the orientation and location of the dominant pressure cell (Figure 2.3). The positive phase of the NAO is characterised by strong westerly air flows across the North Atlantic particularly in winter when warm, moist maritime air moves over parts of Europe and the Mediterranean region. This positive NAO index increases the

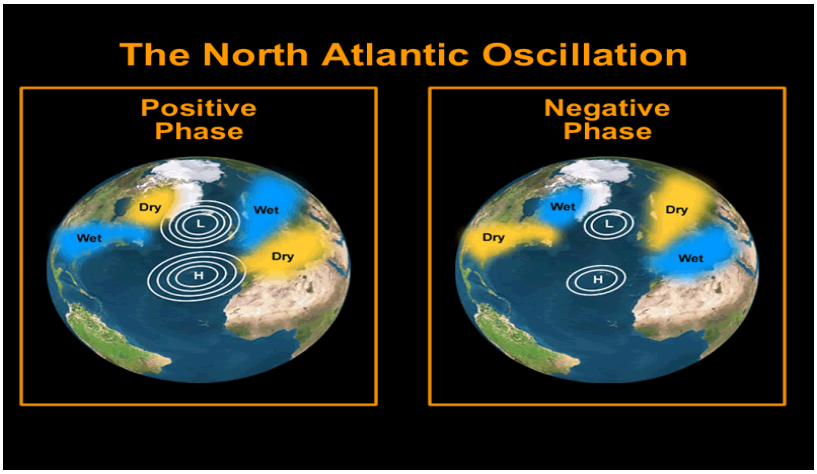

Figure 2.3: Images depicting the NAO in both the (a) negative and (b) positive phases (Courtesy of UCAR, 2012).

strength of the Westerlies creating cool dry summers in this area. In contrast, the negative phase of NAO creates a weakening of the Westerlies allowing Atlantic Ocean storm tracks to drift in a further southerly direction towards the Mediterranean basin. Subsequently, this results in increased storm activity and mild wet winters in the Mediterranean region as more precipitation than normal falls from Iceland through Scandinavia (Hurrell *et al*., 2003). According to Jalut *et al.* (2008), excess winter rainfall in the western Mediterranean is attributed to NAO, while rainfall to the east and south is less significant.

2.5 Present Day Oceanography

The circulation system of the Mediterranean Sea is intricate and is mainly characterised by a thermohaline circulation system. Fundamental processes in relation to the general circulation of the global oceans occur within the Mediterranean basin (Robinson *et al.,* 2001). Evaporation exceeds precipitation in the Mediterranean basin which increases the sea surface salinity particularly in an easterly direction (Robinson *et al.*, 2001). The resultant net buoyancy loss creates a two level exchange at the Strait of Gibraltar. This exchange is characterised by a saline subsurface outflow and a comparatively fresh surface inflow (Rohling *et al.*, 2009). This system is largely driven by the inter-relationships between temperature, density, wind-stress, salinity, water exchanges with the North Atlantic Ocean and surface water buoyancy fluxes (Robinson *et al.,* 2001). Deep water ventilation in the Mediterranean Sea is predominantly salt and temperature driven (Rohling *et al.*, 2009).

The dominant water masses within the Mediterranean Sea are the Atlantic Inflow (AI) from the Atlantic Ocean, a surface layer of Modified Atlantic Water (MAW), a subsurface layer of Levantine Intermediate Water (LIW), and the western and eastern Mediterranean deep-waters (WMDW and EMDW) (Figure 2.4). Bottom water (BW) occurs at depths greater than 3000m (La Violette, 1994).

2.6 Atlantic Inflow (AI) and Modified Atlantic Water (MAW)

Atlantic Inflow (AI) enters the Mediterranean Sea through the Strait of Gibraltar and flows on top of the denser saltier out flowing Mediterranean water (La Violette, 1994). This inflow, with its origin in the Atlantic Ocean, has a low salinity of approximately 36.2‰ and a temperature of between 15-16˚C (Rohling *et al.*, 2009). This water can be

traced throughout the Mediterranean Sea in the upper water column to a depth of 200m (La Violette, 1994). Many conditions modify the direction and strength of this two-way system, namely wind stress on the sea surface, the sinking of dense water in the Straits of Gibraltar and Sicily and atmospheric pressures in the Atlantic Ocean and Mediterranean Sea (La Violette, 1994). AI mixes with the upwelled Mediterranean Intermediate Water (MIW) to create the Modified Atlantic Water (MAW) causing minimum increases in temperature (16ºC) and salinity (36.5%) levels. This water mass is found near the surface during winter and at a depth of approximately 50-70m during the summer (La Violette, 1994). MAW presents itself as a strong jet along the Spanish coast in the Alboran Sea. This strong jet has the capacity to instigate the creation of two anticyclonic gyres, the western and eastern Alboran gyres. MAW converges with resident Mediterranean waters as it flows eastwards to Almeria (Rohling *et al.*, 2009), resulting in a distinct frontal zone along the eastern threshold of the eastern Alboran gyre. This Almeria-Oran Front has an approximate depth of 200m and has a width of approximately 35km (Cheney and Doblar, 1982; Rohling *et al.*, 2009). To the east of the Alboran Sea, the MAW is transported by the narrow Algerian Current (30-50km) (Robinson *et al.*, 2001). This current frequently generates 'coastal eddies', the cyclonic eddies to the north of the Algerian Current are usually short-lived. Anticyclones are generated to the south of the Algerian Current and unlike the cyclonic eddies they can normally last for months (Robinson *et al.*, 2001).

MAW flows into the eastern Mediterranean Sea through the Strait of Sicily, with salinity values of 37-38.5‰, however, as a result of excess evaporation these salinity values increase as it continues to flows eastwards (Malanotte-Rizzoli and Hecht, 1988; Rohling *et al.*, 2009). In the eastern basin MAW sustains the Ionian Current and the Mid-Mediterranean Jet (MMJ). Cyclones and anticyclones are generated by the MMJ, of which one outlet flows to Cyprus and then north and westwards to become the Asia Minor Current (Robinson *et al.*, 2009). MAW is frequently used as a term to identify the entire western Mediterranean water surface layer however; surface water in the Alboran Sea is less saline than the surface water at the Strait of Sicily. Equally MAW entering the Tyrrhenian Sea is fresher and differs from the water leaving the basin in the north as this water had a longer residency time allowing greater mixing to occur (La Violette, 1994).

2.6.1 Levantine Intermediate Waters

Surface waters in the Levantine Basin undergo enhanced mixing and evaporation due to the strong cold winds and dry air masses surrounding the eastern Mediterranean during the winter months (Ozsoy, 1981). This winter cooling reduces sea surface temperatures to approximately 11-13°C (Rohling, 2001). Low temperatures (~17°C) and high salinities (~39‰**)** (Figure 2.5) in the surface waters underpins the favourable conditions for vertical thermohaline convection, which results in the formation of Levantine Intermediate Water (LIW). This water mass flows westwards through the Ionian and Adriatic Seas. On approaching the Strait of Sicily and at intermediate depths (between ~200 and 800m), part of this water mass is re-circulated back into the eastern basin, while the remainder enters the western Mediterranean basin (Figure 2.4) (Lascaratos *et al.,* 1993). LIW has now undergone change due to the mixing process, resulting in a lower temperature (14°C) and lower salinities (38.75‰) (Ozturgut, 1976). LIW then flows into the Tyrrhenian Sea in a cyclonic fashion at a depth between ~200-600m prior to entering the Strait of Sardinia (Katz, 1972). Until recently it was thought that the western basin didn't have equivalent intermediate water. Western Mediterranean Intermediate Waters (WIW) forms at a temperature minimum above the LIW in the Gulf of Lions, and is usually located between 100-300m. The temperatures of this water mass range between 12.5 and 13°C while the salinity ranges between 37.9-38.3‰ (Monserrat *et al*., 2008; Vargas-Yanez *et al*., 2012). In cold winters, Monserrat *et al*. (2008) acknowledged that as WIW moves southwards reaching the Balearic Channels, it deflects the warmer more saline LIW coming from the eastern Mediterranean. However, during warmer winters the contrary has been highlighted by the above authors. They concluded that less WIW is formed during warmer winters allowing the flow of LIW through the channels prior to this water mass appearing at its normal intermediate depths.

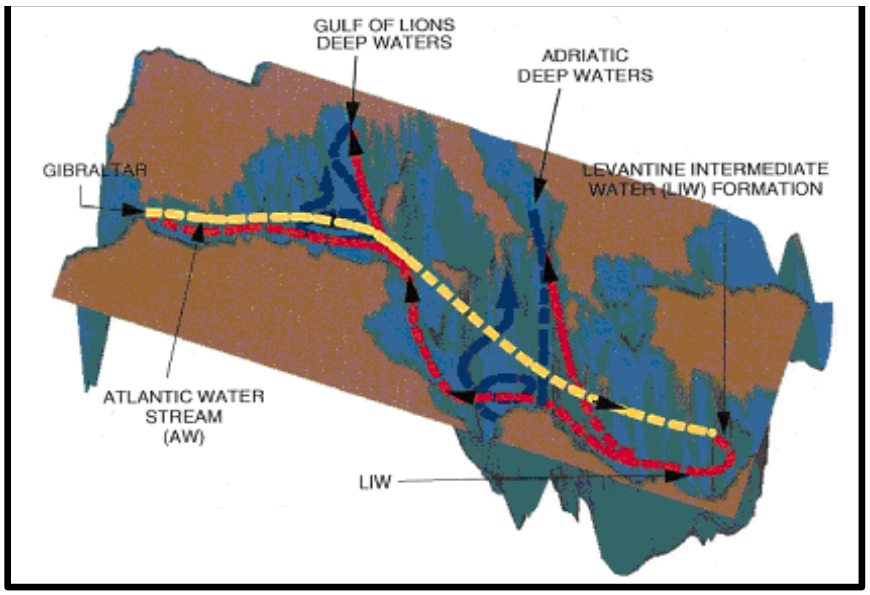

Figure 2.4: Schematic diagram depicting Levantine Intermediate Water formation. The red dashed line depicts the mid-depth Levantine Intermediate Water (LIW). The yellow dashed line depicts Atlantic Waters (AW) which is the surface indicator of the zonal conveyor belt of the Mediterranean. The dark blue line depicts the meridional cells generated by Adriatic Deep Waters. LIW branching from the zonal conveyor belt connects meridional and zonal conveyor belts (Courtesy of Pinardi and Masetti, 2000).

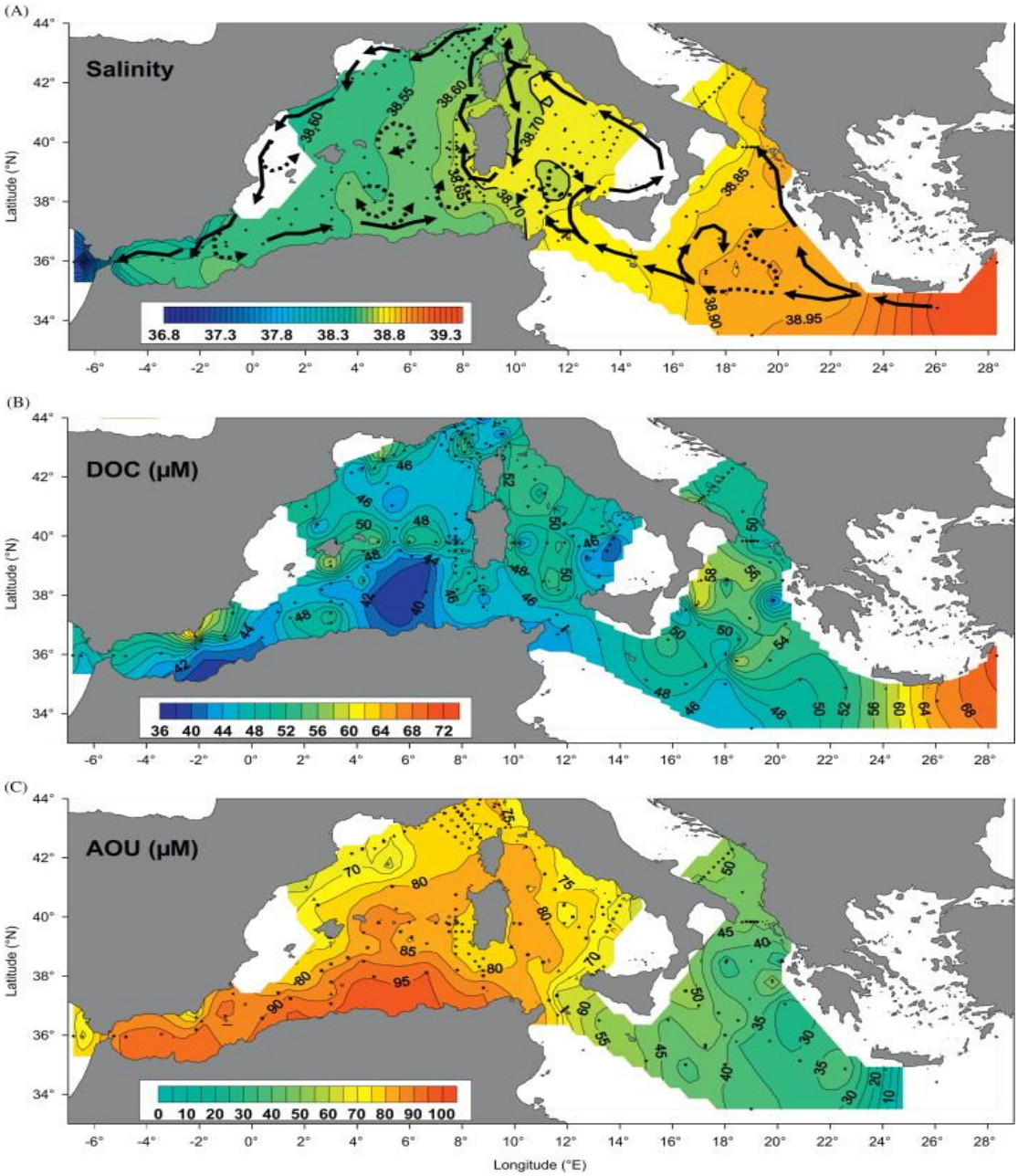

Figure 2.5: Maps illustrating the horizontal distributions of (a) Salinity, **(**b**)** DOC (µM) and **(c)** AOU (µM) in the core of the LIW. Map A is of particular relevance to this section as it outlines the salinity of the LIW at a depth of 200-700m. The black arrows on this map indicate the flow path of LIW (Courtesy of Santinelli *et al*., 2010).

2.7 Deep Water Formation

2.7.1 Western Mediterranean Deep Water

Western Mediterranean Deep Water (WMDW) is formed in the Gulf of Lion. A cyclonic gyre characterises the surface circulation in this area (Rohling *et al.,* 2009). Cold winter conditions, driven by cold polar and continental air streams channelled through the Rhone Valley, gives rise to the 'Mistral' winds (Rohling, 2001). Surface waters are cooled and the MAW and the LIW mix to form the largest water mass in the Western Mediterranean. The end product is known as WMDW and is found between

800 and 3000m (Table 2.1). This water mass migrates westwards, before exiting the Mediterranean Sea via the Strait of Gibraltar (La Violette, 1994). Its characteristics differ from MAW and LIW in that it has a lower temperature of between 10-12ºC and salinity levels of 38.4‰ (Rohling *et al.*, 2009).

Three phases have been observed during the formation of WMDW: the preconditioning phase, the violent mixing phase and the sinking and spreading phase.

- The preconditioning phase is initiated by the onset of winter cooling and the prominence of the 'Mistral' winds which reduces surface water temperatures (10-12°C) increasing water density (29.1g m^{-3}) and salinity (38.40‰) and initiating instability within the water column (Rohling *et al.*, 2009). The basin's cyclonic circulation is intensified causing a shallowing of the pycnocline from a depth of 200-250m, to less than 100m (Rohling *et al.*, 2009).

- The violent mixing phase is characterised by continued cooling and evaporation resulting in a large surface buoyancy loss. The decrease in density causes the stratification between surface and intermediate layers to breakdown. Consequently, this results in deep 'chimneys' of convective mixing to depths of more than 2000m developing within the centre of the gyre (Rohling *et al.*, 2009). Deep vertical mixing permits the exchange of properties namely, heat, oxygen and salt between the surface layers and the deep ocean.

- The final phase of sinking and spreading occurs when the mixed water mass sinks rapidly and diffuses to form WMDW. This large water mass is characterised by its high oxygen content of 4.4-4.7 ml l^{-1} as it flows horizontally between 1,500-3,000m into the Tyrrhenian Sea and Balearic basin (Rohling *et al.,* 2009). On penetrating the Alboran Sea, this water mass forms a narrow boundary current along the Moroccan coast (Rohling *et al.*, 2009) before exiting through the Strait of Gibraltar as part of the subsurface outflow.

2.7.2 Eastern Mediterranean Deep Water

Similar to the formation of WMDW, the formation of Eastern Mediterranean Deep Water (EMDW) can be regarded as a secondary component of the Mediterranean thermohaline circulation as both water masses include the entrainment and cooling of the LIW (Wu *et al., 2000*). EMDW is formed in both the Adriatic and Aegean Seas. During the winter, strong north-easterly Bora winds cause extreme cooling of the North Adriatic low salinity shelf waters (Rohling *et al.*, 2009). This facilitates the sinking of surface water below the LIW as it flows towards the southern part of the Adriatic basin (Rohling *et al.*, 2009). Here it mixes with the more warm and saline MIW, resulting in the formation of Adriatic Deep Water (ADW) which is characterised by a lower salinity (<38.7%) than the MIW and cooler temperatures of 13.0-13.6˚C (Rohling *et al.*, 2009). The resultant EMDW flows through the Ionian Sea before entering the Levantine Basin. The importance of the Aegean Sea to EMDW formation has been strongly debated. Recent findings have shown that it has become more important in relation to deep water formation. The observation of Miller (1963) led to the belief that Aegean Deep Water supports the formation of EMDW, which is also produced periodically in the Aegean Sea before flowing into the Levantine basin via the Straits of Kasos and Karpathos (Rohling *et al.*, 2009). Prior to 1987, the Aegean Sea was only considered to be of minor significance, but recent research now suggests otherwise. Lascaratos *et al*. (1999) reviewed the different mechanisms put forward for the formation of new deep waters in the Aegean Sea between 1987 and 1995. They recognised cold winters as the primary cause of new deep water formation. Theocharis *et al*. (1999b) and Wu *et al*. (2000) noted changes in net evaporation due to river diversion but established that low precipitation during 1989-1993 was the primary cause of the new salty deep water in the Aegean Sea. Georgopoulos *et al*. (2000) argued that the process of eddy ventilation led to the formation of Aegean deep water. Boscolo and Bryden, (2001) have stated that two processes were involved in the formation of new deep waters in the Aegean Sea. Firstly, a long, slow salinity increase and secondly, a destructive deep water formation event during a harsh cold, dry winter led to the formation of Aegean Deep Water. Table 2.1 summarises the characteristics of the water masses of the Mediterranean Sea.

Western Mediterranean Water Masses	Eastern Mediterranean Water Masses
Modified Atlantic Water (MAW) Source: Strait of Gibraltar. Temperature: 15-16°C. Salinity: 36-37.5‰. Depth: 0-200m.	
Western Mediterranean Intermediate Water (WIW) Source: Gulf of Lions Temperature:12.5-13°C Salinity: 37.9-38.3‰ Depth: 100-300m	Levantine Intermediate Water (LIW) Source: Strait of Gibraltar for western Mediterranean Basin and the Levantine Basin for the eastern Basin. Temperature: 13.5-16°C. Salinity: 38.45-39.5‰. Depth: 400-800m.
Western Mediterranean Deep Water Source: Gulf of Lion. Temperature: 12.75-12.90°C. Salinity: 38.40-38.48‰. Depth: 800-3000m.	Eastern Mediterranean Deep Water Source: Adriatic and Aegean Seas. Temperature: 13°C. Salinity: 38.65‰. Depth: 800-3000m.
Bottom Water (BW) Source: North-western Mediterranean. Depth: + 3000	

Table 2.1: Table depicting the main attributes of the western and eastern water masses in the Mediterranean Sea.

2.8 Sapropels

Sapropels are visually distinctive recurring organic-rich sediments that vary from olive green to black in colour and are often laminated (Figure 2.6). Sapropels are defined as sediments containing a total organic carbon (TOC) content of >2 wt % (Rohling, 2001; Martinez-Ruiz *et al.*, 2003). Sapropels have long been identified in the sedimentary sequences throughout the entire eastern Mediterranean Sea. These organic-rich layers or deposits have also been observed at western Mediterranean sites from the Ocean Drilling Programme (ODP) Leg 161 (Comas *et al.*, 1996; Martinez-Ruiz *et al.,* 2003). Sapropels range in thickness from a few millimetres to several centimetres. Their formation over the last 5.3 million years within sedimentary sequences is cyclic and they can be correlated to variations in the eccentricity of the Earth's orbit, in the tilt and in the precession of the Earth's axis (Rohling and Hilgen, 1991). Sapropel deposition in the eastern Mediterranean has been the subject of numerous studies for decades. Kullenberg (1952) first discovered such deposits in cores recovered from the Mediterranean seafloor during the 1947-48 Swedish deep-sea expedition. Olausson in 1961 entrusted them the name 'sapropelic layers' **(**Nijenhuis, 1999**)**. The deposition of sapropels in the eastern Mediterranean terminated approximately 6,000 years ago. In general the Mediterranean Sea is nutrient-poor, with sediments containing insignificant amounts of organic matter. Approximately every 21,000 years there are periods of enhanced solar radiation, resulting in intense rainfall and increased influx into the Mediterranean Sea. Subsequently, these periods are reflected in the high content of organic matter that is observed in sapropels (Gallego-Torres *et al.,* 2010). Sapropel formation therefore occurred in response to changes in climate, water circulation and biogeochemical cycling (Dick *et al.,* 2002).

Figure 2.6: Photograph illustrating a sapropel layer from ODP core 964A (one of the cores utilised in this research). The sapropel is distinguished by its olive green to black colouring with respect to the surrounding sediment (Courtesy of Sancetta, 1999).

Assemblages of fossils and pollen are evident within sapropels which bear witness to the scenarios that sapropel formation required fast deposition and ensuing preservation of the organic material, usually under anoxic conditions (<0.5mg L^{-1} O^2) (Dick *et al.*, 2002). Anoxic conditions refer to a total decrease and depletion in the level of oxygen in the water column. In contrast, the term oxic refers to waters that have normal

dissolved oxygen concentrations (0.5-2mg L^{-1} O^2) while dysoxic conditions prevail when dissolved oxygen becomes reduced in concentration to a degree where it becomes detrimental to all marine organisms. Faunal characteristics in sapropels are unusual; populations of planktonic foraminifera, such as *Globigerina bulloides* and *Neogloboquadrina* are the norm (Rohling *et al.*, 1993; Stefanelli *et al.,* 2005). The presence of benthic foraminifera can be attributed to dysoxic conditions and some species can even survive in anoxic environments. However, the complete absence of benthic foraminifera is symbolic of continuous anoxic conditions. Rohling *et al.* (1993) concluded that the substantial presence of benthic foraminifera within an Upper Pliocene sapropel (C2) suggested improved bottom water oxygenation. Possible alternation between dysoxic and anoxic conditions would allow for particular low-oxygen resistant benthic species such as *Bulimina marginata* to exist (Rohling *et al.*, 1993).

2.8.1 Sapropel Formation

Much information is now available concerning the formation of sapropels in the Mediterranean, in particular the eastern Mediterranean. Initially, it was thought that sapropel formation was as a result of increased freshwater from the Black Sea into the Mediterranean system due to post-glacial sea level rise (Shaw and Evans, 1984; Rossignol-Strick, 1987; Cramp *et al.*, 1988). These theories are generally not proven but hypotheses rejected as numerous studies have provided evidence that sapropels have been deposited in both glacial and inter-glacial periods (Vergnaud-Grazzini *et al.*, 1977; Rossignol-Strick, 1985; Rohling *et al.*, 1993a). Many studies suggested that lower surface water salinities commenced the formation of a well stratified water column. In turn, this lead to the constraint of large scale convection and the displacement of oxygen to the bottom waters leading to an anoxic environment (Olausson, 1961; Rohling and Hilgen, 1991; Kroon *et al.*, 1998). Since this conclusion, sapropel existence has been associated with water column stratification (Nijenhius and de Lange, 2000). Evidence in favour of the stagnation theory is frequently based on faunal assemblages. Isotopic analysis of foraminiferal tests and oceanographic factors have provided essential evidence for reduced surface water salinity and increased surface water temperatures at periods of sapropel formation, which is believed to spearhead such water column stratification (Emeis *et al.*, 1991). Rossignol-Strick *et al.* (1982) concluded that the timing of sapropel formation was also triggered as a direct response to heavy flooding and African monsoons. Again in 1985, Rossignol-Strick

was the first to suggest a relationship existed between sapropel formation and orbital forcing. They claimed that sapropel S1 coincided with a period of heavy monsoonal precipitation in Africa, which was channelled into the eastern Mediterranean basin by the River Nile. Rossignol-Strick (1982, 1985) invented a monsoon index (M) as a measure of monsoonal intensity related to variations in solar radiation throughout the Quaternary Period. These variations were sought from astronomical calculations regarding cycles in the Earth's orbital boundaries. Dick *et al.* (2002) agreed that sapropel depositions coincided with periods of maximum insolation and heavy flooding. This flooding generated a layer of nutrient-rich water in which phytoplankton bloomed on the surface of the eastern Mediterranean, possibly causing anoxia (Dick *et al.,* 2002). During the process of respiration at nightime, the dense population of phytoplankton blooms reduces dissolved oxygen. When phytoplanktons die, they sink to the ocean floors and are decomposed by bacteria. This process further reduces the oxygen levels within the water column leading to the anoxic conditions. Expansion on Rossignol-Strick's (1982, 1985) ideas by Calvert in 1983, argued that sapropel formation did not solely happen as a result of hydrographic changes leading to stagnation, bottom water oxygen depletion and improved preservation. In his studies, he proved that productivity must be equally as important however, increased productivity in the eastern Mediterranean is curtailed due to the anti-estuarine circulation where the supply of nutrients are transferred with deep water formation and are therefore unavailable in the photic zone (Calvert, 1983; Nijenhius and de Lange, 2000; Gallego-Torres *et al.*, 2006). To counteract this problem, Nijenhius and de Lange (2000) argued that a solution lies in the Deep Chlorophyll Maximum (DCM) model in which deep water nutrients become available for primary production (PP) as a result of shoaling of the pycnocline into the photic zone or 'nutrient desert'. In general, the above theories are not proven but it is now almost a consensus that the climate setting, humidity conditions and the resulting changes in river run-off at the time of sapropel deposition were major factors in sapropel formation (Gallego-Torres *et al.*, 2006).

A new model for sapropel formation was put forward by Rohling and Gieskes (1989). To explain sapropel formation, this model combined decreased deep water production with increased productivity and a broader evaluation of the eastern Mediterranean's vertical density system. This study provided evidence that a decrease in Levantine Intermediate Water (LIW) density, induced by increased freshwater overflow would affect the rate of formation of Eastern Mediterranean Deep Water (EMDW), subsequently weakening the circulation (Rohling, 1991). The hypotheses of

restricted deep water ventilation being the principal mechanism involved in sapropel formation have been argued (Rohling and Hilgen, 1991). Convection is reduced as a result of a more stable stratification due to higher temperatures or lower surface water salinities at the sites of deep water formation. Low $\delta^{18}O$ values within the sapropels strongly suggest lowered surface water salinities. Increased freshwater overflow into the basin would lower salinity rates and enhance the input of nutrients and organic material (Rohling and Hilgen, 1991).

Currently there are two possible explanations that are at the core of a major debate to understand the processes associated with sapropel formation:

1. The Stagnation Model

The 'Stagnation Model' is based on the external physical processes of temperature, circulation and evaporation, as a cause of sapropel formation. It is proposed that such physical processes created intense vertical gradients of temperature and salinity, resulting in stable stratification, reduced ventilation of deep water, anoxic conditions and enriched organic matter preservation (Sarmiento *et al.,* 1988; Martinez-Ruiz *et al.*, 2003). The stagnation model is explained by a density stratification of the water column that restricts vertical mixing and aeration of the deep water (Olausson, 1961; Thunnel *et al.*, 1984; Murat and Got, 2000). At the onset of S1 deposition approximately 9000 years BP, warm climatic conditions were re-establishing and surface salinity had decreased by almost 4‰ which initiated the formation of a clear stratified water column (Tang and Stott, 1993). Murat and Got (2000) have verified, from their study on S1, that sapropel formation was partly a result of a well oxygenated surficial layer (0-350/400 m) and a stagnant deep water layer. When stagnation was established water exchanges were minimal or non-existent. Organic flux decreased with depth through the stagnant deep water layer. Furthermore, the transfer of oxygen to the bottom waters was inhibited by large scale convection leading to anoxic conditions. At the end of this stagnation period vertical mixing increased and deep nutrient-rich waters were mixed with surficial waters (Murat and Got, 2000).

2. The Productivity Model

The alternative mechanism is explained by the 'Productivity Model' and is based on increased export production and the brisk supply of organic matter to the sediment. Moreover, it is now accepted that sapropel formation is as a result of astronomically forced climate changes, coinciding closely with minima in the precession index, which

occurs approximately every 21,000 years (Figure 2.7) (Rohling, 1991; Hilgen, 1991; Emeis *et al.*, 2000; Martinez-Ruiz *et al.,* 2003 amongst others). These astronomical cycles altered palaeoceanographic conditions in the Mediterranean Sea and increased precipitation and wetter conditions, creating a much higher run-off into the basin; this in turn provided the Mediterranean system with more freshwater and land-derived nutrients (Gallego-Torres *et al.*, 2006). Martinez-Ruiz *et al*. (2003) proposed that productivity, which is induced by astronomical cycles, was the main triggering factor controlling sapropel formation. Bottom water oxygen depletion could result as a response to increased productivity. In Pliocene sediments, absent and limited oxygen is associated with increased or high productivity. However, these conditions prevail even after the resumption of normal productivity levels. According to Gallego-Torres *et al.* (2006) this infers reduced ventilation of bottom waters or lags in the response of deep water oxygen. The integration of multi-proxy data makes it possible to reach a decision regarding sapropel formation and deposition in the eastern Mediterranean during the Pliocene-Holocene period. Organic matter is extensively deposited in the sediments as a consequence of enhanced export production. However, organic matter is quickly decomposed thus suggesting that Barium (Ba) derived from marine barite is a more reliable indicator of palaeoproductivity (Gallego-Torres *et al.*, 2006). This proxy has been utilised in numerous palaeoproductivity studies since Dymond *et al.* (1992) and Francois *et al*. (1995) proposed the palaeoproductivity algorithms to quantify palaeoproductivity from the accumulation rate of biogenic Ba in marine sediments. Ba has been demonstrated well for S1 (Paytan *et al*., 2004). Contrary to this finding, some limitations were evident for its use in older sapropels (Van Os *et al*., 1991). With regards to Ba peaks just above most sapropel layers Van Os *et al*. (1991) concluded that one must be wary when utilising Ba as a palaeoproductivity indicator due to diagenetic remobilisation of a primary Ba signal altering the relationship between Ba and organic production (Murat and Got, 2000).

Proxies show that Pliocene sapropels have lower oxygen concentrations, contributing to the prevailing anoxic conditions. On the otherhand, proxies display higher oxygen levels for the Quaternary sapropel which were deposited under oxic to dysoxic bottom water conditions (Gallego-Torres *et al.*, 2006).

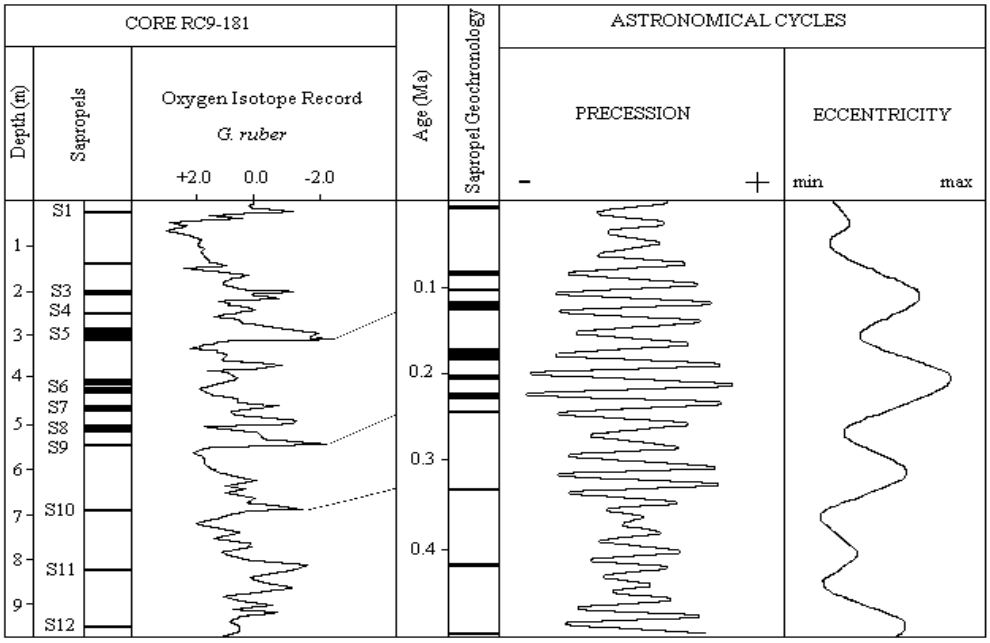

Figure 2.7: Phase relationships between the sapropel record and associated δ ^{18}O record from core RC9-181 and the precessional and eccentricity orbital cycles (Berger, 1978) (Courtesy of Hilgen, 1991).

2.8.2 Timing of Sapropels

Nine sapropelic layers were analysed at high resolution from ODP core 964A (Gallego-Torres *et al.,* 2006). This core was taken from a site located on the Pisano Plateau near the Ionian Abyssal on a small bathymetric high at a depth of 3650m. Sapropels from different time periods were selected, spanning from the Pliocene to the Holocene. Quaternary sapropels, S1, S3, S5 and S6 are defined at this location. The occurrence of at least 12 sapropels have been recorded and dated to the late Quaternary. Sapropel S1 is the most recent sapropel, and is the only sapropel within the time range where the radiocarbon dating method is well calibrated and precise (Thomson *et al.*, 1999). S1 occurred within the warm Holocene Climatic Optimum which followed the last major retreat of Northern Hemisphere continental ice sheets (Rohling and Hilgen, 1991). A number of insolation cycles are recognised by various authors and are thought to be a key factor in the timing and termination of sapropel formation and deposition (Rossignol-Strick *et al.*, 1982, 1985). These insolation cycles are numbered and are associated with variations in the Earth's orbit. It has been discovered that a correlation exists between sapropel formation and these insolation cycles, with the amount of insolation varying with periods of approximately 21,000 years, 40,000 years and 400,000 years (Figure 2.7). Rohling and Hilgen (1991) believe that orbital forcing of the climate controls the formation of sapropels with the cycle of precession being of major importance. Numerous studies have been devoted to sapropel S1, as this layer is

easily accessible by piston coring. Quite often the onset of S1 in the sediment record appears to be affected by oxidation and as such it can be difficult to determine the precise time upon which deposition started. However, a formation period between 3000 and 4000 years is understood to be a reasonable estimate (Rohling and Hilgen, 1991; Nijenhuis and de Lange, 2000)

Pleistocene sapropels are older than Holocene sapropels and cannot be dated directly and their formation time may vary by ~ 2000 years. Pleistocene sapropels S3, S4, S5 and S6, when analysed, correlated respectively to insolation cycles 12, 16, 18 and 20 (Table 2.2).

Sapropel	Insolation Cycle	Date (kyr BP)
S3	12	124
S4	16	172
S5	18	195
S6	20	216

Table 2.2: Pleistocene sapropels and their associated calibrated ages and insolation cycles. The data was obtained from Lourens, (2004) and Gallego-Torres *et al.* (2006).

2.9 Geochemical Characteristics of Sapropels

Mediterranean sapropels are visually distinctive in that they range in colour from dark green to black. A high content of organic matter (>2%) and iron sulphide minerals define their dark colouration (Figure 2.6). Hilgen (1991) describes the term "sapropel" as having more than 0.5% TOC (Murat and Got, 2000). The most obvious geochemical characteristics of sapropels are the high organic carbon (C_{org}) and Ba contents. In contrast, carbonates and manganese are found in relatively low levels (Thomson *et al.*, 1995; Nijenhius *et al.*, 1999). The geochemistry of S1 was analysed by Thomson *et al.*, (1995), revealing that $CaCO_3$ values were lower in sapropel S1 than in the surrounding marls. A marked enrichment of sulphite associated elements such as, sulphur (S), iron (Fe), molybdenum (Mo), and ardennite (V) were visible. Chalcophile elements were also present, namely copper (Cu), nickel (Ni), lead (Pb) and zinc (Zn) (Thomson *et al.*, 1995). When the older sapropel S3 was examined, similar characteristics were revealed. Nijenhuis and de Lange (2000) studied the geochemistry of numerous sapropels from four sites in the eastern Mediterranean, sites 964, 966, 967 and 969. These sites were representative of various water depths. The motivation behind this study was to seek out the conceivable circumstances under which the sapropels were created in the Plio-

Pleistocene. The seventeen sapropels which were recovered during ODP leg 160 and from the four sites mentioned, provided vital information with regards to the characteristics of eastern Mediterranean sapropels. High concentrations of organic carbon were found to be present; this is seen as a reflection of both increased productivity and improved preservation of the organic matter. High carbon/nitrogen (C/N) ratios suggested that productivity may have been N-limited (Nijenhuis and de Lange, 2000). When the sapropel characteristics were compared with the homogeneous intervals, the sapropels were shown to have almost 30% more C_{org} and a lower ratio of Ca**.** Sapropels on average are enriched in Ba and these sapropels were no exception in that they reached values of almost 5,200‰, this correlated considerably with the C_{org} contents (Nijenhuis and de Lange, 2000). Van Os *et al.* (1991), in their study of Ba and its distribution in Mediterranean sapropels concluded that Ba peaks do not occur within sapropel layers but directly above most layers. As a result of this occurrence it is important to be aware that the relationship between Ba and organic production can be disturbed, consequently caution should be employed when using Ba as a palaeoproductivity indicator (Murat and Got, 2000). Higher contents of opal, another trace element, were found while aluminium (Al) contents were usually lower in the sapropel sediment. The marked enrichment of the sapropels with Ba and opal, suggests that production was increased during sapropel formation. Research by Thomson *et al.,* (1995, 1999), has shown that elevated levels of Barium/Titanium (Ba/Ti) coincided with the high levels of organic carbon indicating increased productivity. François *et al.* (1995) proposed that since a good correlation exists between Ba and C_{org} content, Ba can be relied upon as an indicator for palaeoproductivity. Opal has been utilised extensively to indicate increased productivity levels and is easily dissolvable; therefore a greater sedimentation rate and a high opal flux are two requirements for its preservation. As opal is precipitated by algae in highly productive surface waters, its presence can indicate a high productivity rate. However, its absence, according to François *et al.* (1995), does not exclude the possibility of a high production ratio. These authors analysed three sapropels for opal content and subsequently found up to 4% opal in sapropels i-176A and i-282C and a high enrichment of up to 26% opal in sapropel i-176B, leading to the conclusion that a high opal value may suggest an increase in productivity at times of sapropel deposition (Nijenhuis and de Lange, 2000). Ti and Al occurred at irregular intervals in sites 964 and 969 however, these minerals are considered to be cyclic in sites 966 and 967. Sapropels from the four sites were well

enriched with trace elements such as Mo, aluminium (Al), V/Al, and Ni/Al (Nijenhuis and de Lange, 2000).

Three million year old well-developed sapropels from the Metochia on Gavdos, Greece, were selected for a geochemical study by Schenau *et al.* (1999). The results were consistent with those of the above studies. These old sapropels were again characterised by high organic carbon and low carbonate content. High ratios of Ba indicated that productivity was high during sapropel formation. A high percentage of the planktonic species, *Neogloboquadrina acostaensis* also suggests that productivity was high. However, these theories must be considered with care as Ba dissolution and reprecipitation may ensue during sulphate reduction. Enrichment of Mo and V in these sapropels is characteristic of fine grained organic-rich sediments which are sometimes deposited in depleted oxygen bottom water conditions (Schenau *et al.,* 1999*).* Low levels of Ti and Al implies an alternating dominance of fluvial sapropels (Schenau *et al.,* 1999). Carbonate depletion was possibly caused by the increased freshwater input and increased sedimentary rate during sapropel formation. The presence of trace elements Ni and Cu correlate well with the organic matter content indicating increased surface water productivity.

A consistency exists in many studies related to the geochemical characteristics of sapropels. Similar geochemical characteristics could be recognised in the most recent sapropel S1, in the older sapropel S3 and in the three million year old sapropels. This consistency suggests that all sapropels deposited in at least the past 10 million years are the result of a single mechanism that is orbital forcing (Schenau *et al.,* 1999).

2.10 Planktonic Foraminiferal Species within Sapropels

Extensive studies have been devoted to planktonic foraminiferal species associated with Mediterranean sapropels. These single-celled organisms have registered an abnormally high percentage of *Neogloboquadrina pachyderma* and *Neogloboquadrina dutertrei* especially in the late Quaternary sapropel layers. Previous authors interpreted this association between *neogloboquadrinids* and sapropels as reflecting reduced surface water salinity during sapropel formation (Ryan, 1972; Cita *et al.*, 1973). Stefanelli *et al.* (2005) explained that the abundance of these species suggested a seasonal shallowing of the thermocline within the photic zone. The development of a well-defined basin-wide DCM (Figure 2.8) in the thermocline of the Mediterranean basin is strongly associated with peak abundances of *neogloboquadrinids.* This

abundance is fuelled by LIW formation and the subsequent appearance of the pycnocline and associated DCM which creates the upward mixing of nutrients from deeper waters (Rohling and Gieskes, 1989; Rohling *et al.*, 1993). Previous authors also observed an abundance of *neogloboquadrinids* during glacial periods associated with non sapropelic sediments (Negri *et al.*, 1999; Stefanelli *et al.*, 2005). Sapropelic assemblages in colder climatic conditions are characterised by an enrichment of *N. dutertrei*. However, S1 is almost devoid of *neogloboquadrinids* (Rohling and Gieskes, 1989; Ariztegui *et al*., 2000).

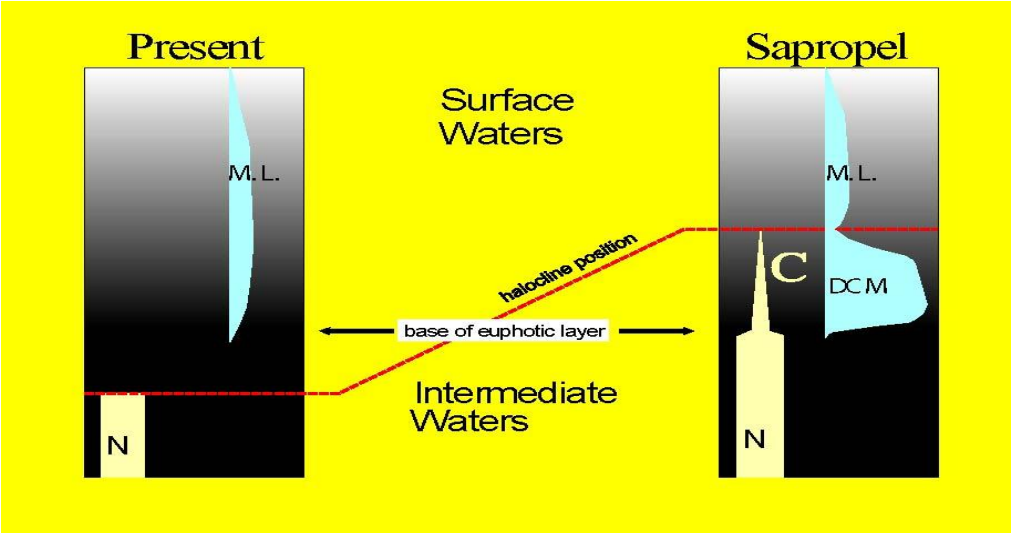

Figure 2.8: Difference in the depth of the surface to intermediate water interface between the present and times of sapropel deposition, relative to the depth of light penetration (base euphotic layer = 1% light intensity level). N indicates nutrients, C indicates consumption of nutrients for photosynthesis, DCM stands for Deep Chlorophyll Maximum association, and M.L. for Mixed Layer association (Courtesy of Rohling, 2001).

The absence of *neogloboquadrinids* in the Holocene sapropel S1 is related to the disappearance of a DCM layer. During deposition of S1, the pycnocline had disappeared well below the euphotic zone due to the completion of MIW formation resulting in the non-development of a DCM. As a consequence of this there is no deep phytoplankton assemblage to sustain *neogloboquadrinids* (Rohling and Gieskes, 1989).

The absence of *Globorotalia inflata* in Late Quaternary sapropels infers a lack of mixing in the water column, with year round stratification. *G. inflata* have a preference for cool, well-mixed waters with transitional to high nutrient levels (Stefanelli *et al.,* 2005). Ariztegui *et al.* (2000) suggested that the absence of *G. inflata* in S1 indicates a limited water exchange between the western and eastern basins at the

time of formation. An increase of this species in the Alboran Sea between 7000-8000 BP has been interpreted as the re-establishment of vertical mixing during winter in the Adriatic and Levantine basins, an enhanced inflow of MAW with the onset of modern hydrographic conditions (Pujol and Vergnaud-Grazzini, 1989; Rohling *et al.*, 1995; Ariztegui *et al.*, 2000). During the deposition of most sapropels, warm water planktonic species prevailed in the surface waters. A general consistency in the fluctuations of *Globigernoides ruber* which was observed in S1 and S5 reflects optimum temperature conditions during deposition periods (Rohling and Gieskes, 1989; Rohling *et al.*, 1993a). The distinct presence of *G. ruber* (pink) in S1 indicates optimum temperature conditions during the deposition and formation of this sapropel (Thunell *et al*., 1977; Rohling *et al*., 1993). An increase in *G. ruber and Globigerinoides sacculifer* indicates that surface waters were dominated by an oligotrophic mixed layer for most of the year (Ariztegui *et al.*, 2000). On the other hand, cold water species were more prevalent in sapropels S6 and S8, leading to the conclusion that both of these sapropels were deposited under relatively cool conditions. *N. pachyderma, Globorotalia scitula, Turborotalia quinqueloba* and *N. dutertrei* prevail in S6 indicative of cold and highly productive surface conditions (Trcantaphyllou *et al.*, 2010).

2.11 Benthic foraminiferal species in sapropels

From the 1950s, much research has been carried out on benthic foraminiferal species and data have been used to reconstruct a wide range of oceanographic parameters. Sapropels have been deposited in dysoxic to anoxic bottom waters, leading to the preservation of organic matter and the near absence of benthic species (Rohling and Hilgen, 1991). This has led to the suggestion that low oxygen environments are inhabited by specific faunal assemblages usually with a low diversity. Intervals devoid of benthic foraminiferal species are usual within the Mediterranean since the Upper Miocene. The presence of laminations within sapropels suggests a total or near total absence of benthic fauna (Rohling, 2001; Jorissen, 1999). X-radiographs reveal that intensive burrowing takes place in well-oxygenated intervals. This data indicates that thriving fauna existed within the sediments.

Oxygen is one of the most important factors that influence species diversity and abundance in the benthic marine realm (Stefanelli *et al.*, 2005). Benthic foraminiferal species usually inhabit a well-oxygenated to strongly hypoxic sediment layer. Distinct species normally have a preference for a specific depth interval but most species will experience an extensive range of oxygen concentrations during their life-

span. *Crenostrea wuellerstorfi,* epifaunal taxa, lives abundantly in well-oxygenated bottom waters however, Jorissen (1999) provided evidence that a significant number of these taxa were present in the Sulu Sea where bottom water oxygen concentrations were well below 2ml/l. Nijenhuis *et al.* (1996) conducted a major study of benthic foraminifera within an Upper Miocene sapropel and its surrounding sediments. Low-oxygen benthic species were characteristic of this sapropel, suggestive of near bottom water oxygen depletion. In comparison, the sediments between the sapropels, were found to contain benthic species characteristic of oxic environments (Nijenhuis *et al.,* 1996). A benthic foraminiferal study for the Late Quaternary Mediterranean sapropels S1, S5 and S6 was also carried out by Nijenhuis (1999). This research concluded that the main factor governing the benthic foraminiferal successions that occurred prior to and post sapropel deposition was the commencement of anoxic conditions and the re-oxygenation of the benthic environment (Nijenhuis, 1999). *Globobulimina* and *Chilostomella* were the two dominant benthic species found in these Late Quaternary sapropels, suggestive of either a gradual decrease or a slow increase in bottom water oxygenation (Nijenhuis, 1999). Stefanelli *et al.* (2005) in their research of benthic and planktonic foraminiferal assemblages investigated across the Early-Middle Pleistocene, IM/Fosso 5 Agosto section, identified two sapropel sediment layers. Their data reveal that preceding the deposition of these sapropels, changes occurred in the benthic foraminiferal population due to a decrease in bottom water oxygenation even prior to sapropel formation. Bottom water recovery was brisk, owing to the fact that stratification terminated at the finish of the sapropel occurrence, normal circulation resumed and the benthic foraminiferal species instantaneously utilised this resource (Stefanelli *et al.*, 2005). It appears that benthic foraminifera are more tolerant to a low oxygen environment than most other metazoan and macrofauna. However, an enrichment of some benthic species may dwell in dysoxic conditions. Other benthic species have been observed to survive in anoxic conditions but prolonged anoxia proves lethal to this species (Rohling *et al*., 1993).

2.12 Foraminifera

Foraminifera are single-celled aquatic organisms made up of two basic units: the cell, consisting of the soft cytoplasm which encloses the functional parts of the cell, and the shell or test which varies in shape and outward appearance. These single-celled organisms are capable of conducting the various functions necessary for life and reproduction. Belonging to the phylum Protozoa, the majority of foraminifera are found

in marine environments, where populations can be extremely diverse (Doyle, 2005). In contrast only a few species can survive in fresh water environments. For millions of years large quantities of sediment composed of biogenic and terrigenous materials have been accumulating on the ocean floors (Bradley, 1999). Contained within this sediment are the fossilised remains of planktonic and benthic foraminifera. Planktonic organisms are normally free floating within the water column and tend to occupy the open ocean environment. Benthic (bottom-dwelling) organisms normally reside at the sediment water interface (Geraga *et al.*, 2008). Both types are characterised by their modes of life and the absence of tissues and organs (Armstrong and Brasier 2005).

Appearing in the fossil record since the mid Jurassic period, planktonic foraminifera are one of the most frequently used tools in palaeoceanography. In particular certain species can be utilised to reconstruct palaeoenvironmental variables such as sea-surface temperature (SST), sea surface salinity (SSS) or productivity (Mulitza *et al.*, 1998). In fact the fossil record of planktonic foraminifera provides a multitude of valuable palaeoproxies in relation to climate change over geological time. Having a longer geological range, from the early Cambrian period to the present day, benthic foraminifera can also be utilised in stratigraphical studies and palaeoenvironmental analysis (Doyle, 2005).

2.13 Planktonic and Benthic Foraminifera

2.13.1 The Life Cycle

The life cycle of foraminifera is characterised by sexual and asexual reproduction and can be alternated between two generations, an agamont generation reproducing asexually and a gamont generation reproducing sexually (Figure 2.9) (Armstrong and Brasier, 2002). In asexual reproduction cytoplasm enters the test, the cytoplasm then splits creating numerous haploid daughter cells. A single parent cell breaks up to produce numerous daughter cells and each cell contains a nucleus but with only half the chromosomal compliment evident in the parent nucleus (Armstrong and Brasier, 2002). When a new chamber is formed, the new gamont generation is then released into the water to diffuse. Gametogenesis is the division of the cytoplasm to form gametes. Gametes retain the same haploid chromosome number as the parent. Two gametes may fuse when released from the parent test and this is known as sexual reproduction (Armstrong and Brasier, 2002).

In larger benthic foraminifera, a schizont generation is thought to be combined to the conventional life cycle. These are diploid and multinucleate. They are produced

by meiosis and the life cycle here is understood to take from one to several years to complete (Armstrong and Brasier, 2002). In contrast it is understood that planktonic foraminifera reproduce sexually approximately every 28 days as dictated by the lunar cycle and under favourable conditions. However some shallow dwelling species such as *Globigerina bulloides* are known to reproduce once or twice per month in the upper water column, releasing approximately 200,000 to 400,000 gametes. Intermediate to deep dwelling species, reproduce less often, while *Globorotalia truncatulinoides*, the deepest dwelling species to date, is thought to reproduce only once per year (Schiebel and Hemleben, 2005). Scientists believe that planktonic foraminifera do not produce asexually.

Other deviations in the life cycle occur latitudinally. In tropical latitudes it is thought that most life cycles are completed within a year whereas in polar latitudes the life cycle may take over two years to complete, however there are many variations in both planktonic and benthic forms (Armstrong and Brasier, 2002).

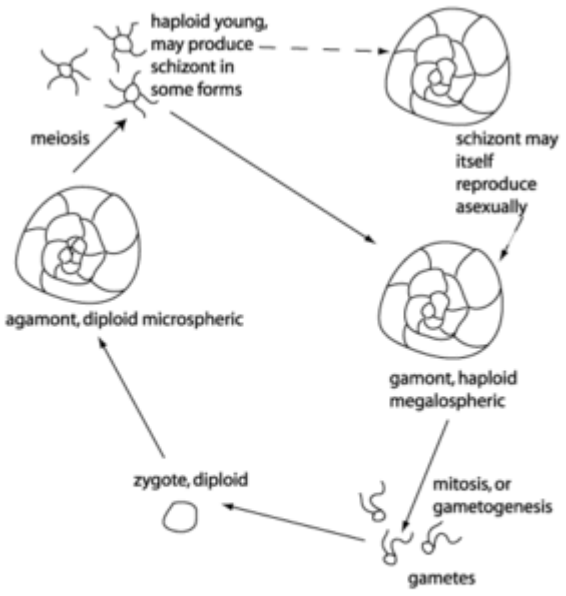

Diagram showing a generalised foraminifera life cycle note alternation between a haploid megalospheric from and a diploid microspheric form.

Redrawn from Goldstein 1999.

Figure 2.9: Schematic diagram illustrating a generalised foraminifer's life cycle (Foraminifera, 2012).

2.13.2. Foraminiferal shell composition morphology and structure

Many studies have been carried out on foraminiferal shell composition over the last few decades, making them ideal bioindicators for the dynamic marine environments

through geochemical analyses (Schiebel and Hemleben, 2005). Changes in foraminiferal composition is utilised to analyse sea-water depth and changes relating to the water masses, salinity and climate (Armstrong and Brasier, 2005).

Shell morphology plays a vital role in revealing past climates and environments. Evolutionary changes can be easily traced by the unique foraminiferal morphology. For example, *Neogloberina pachyderma* and *G. truncatulinoides* are characterised by a distinct coiling direction (dextral and sinstral). *N. pachyderma,* a cold water species, sometimes by its coiling direction can dictate if the species originated in polar or sub polar waters (Armstrong and Brasier, 2005). In a study based on plankton tows from the Pacific coasts of Japan, Kuroyanagi and Kawahata (2004) found that the distribution of *N. pachyderma* was mainly controlled by SST, however, the authors concluded that the coiling direction was not influenced by temperature alone but can be linked to genetic differences (Kucera *et al*., 2002).

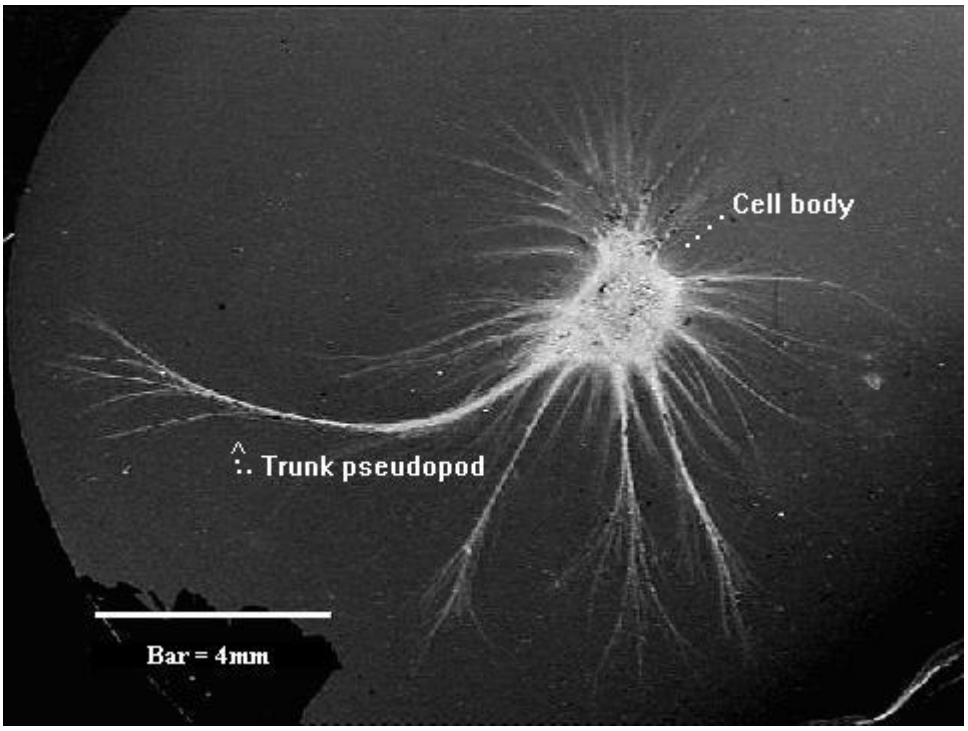

Figure 2.10: Scanning electron micrograph illustrating the foraminiferal cell and pseudopodia of a benthic foraminifera (Foraminifera, 2011).

Foraminifera are made up of two basic units: the cell and the test (shell). The single cell is capable of carrying out all the functions necessary for life and reproduction (Doyle, 2005). The cell is divided into dark granular endoplasm and transparent ectoplasm. The ectoplasm forms a thin mobile film around the test which gives rise to long, stiff fine granular branches called pseudopodia (meaning 'false feet') (Doyle, 2005). These pseudopodia (Figure 2.10) are utilised by foraminifera to capture

and engulf food material. Vacuoles containing waste products are carried by the cytoplasmic flow along the pseudopodia (Doyle, 2005). Food requirements consist of bacteria, other protozoa, diatoms, molluscs, nematodes and other small organisms. Some foraminifera are understood to be parasitic, while many other species feed selectively. In addition, pseudopodia are used for anchorage and for pulling the test along, although this happens more in benthic forms (Armstrong and Brasier, 2005). The ectoplasm is connected to the test by means of an aperture, which is a hole or opening. The passage of food, excretory products, cytoplasm and reproductive cells is possible through this aperture. The endoplasm is the storehouse of the cell and is sheltered by the test (Armstrong and Brasier, 2005).

The test or shell varies in form and may consist of single (unilocular) or multiple chambers (multilocular) with a single opening or aperture. Multilocular tests comprise of two or more chambers which are separated by septa. The aperture acts as a means of communication penetrating each chamber. Each individual chamber is identified as a growth stage (Doyle, 2005). Chambers can appear in a variety of shapes and forms. The two basic patterns are serial and spiral and these patterns are critical for identification purposes. Test size varies through time and space and is thought to reduce biological, chemical and physical stress. Biological stresses include the risk of ingestation by worms, gastropods or fish. Physical stresses include the effects of excess solar radiation and water turbulence on the foraminifera. Chemical stresses incorporate poisons in the water and fluxes in salinity, oxygen, pH and carbon dioxide levels (Armstrong and Brasier, 2005). Should any of these stresses occur, the cytoplasm can vacate into the inner chambers whereby the outer chambers then act as defensive guards.

A test may have an organic, agglutinated, or calcareous wall (Pawlowski, 2009). Agglutinated walls are rigid and the tests are formed from foreign particles bound together with a variety of cements secreted by the organism. Organic wall structures are composed of protein and sugar compounds. Calcite walls can be categorised into three main types, micro granular, porcellaneous or hyaline (Figure 2.11). Micro granular walls may appear fibrous as the calcite grains can be arranged haphazardly or at right angles to the surface (Doyle, 2005). Porcellaneous walls are of an opaque appearance whereas hyaline walls have perforations and appear glassy. It is important to note that two foraminiferal groups can be recognised by their different wall structure: *Arenaceous* and *calcareous* foraminifera.

2.13.3 Arenaceous foraminifera

Arenaceous foraminifera can have numerous shapes and sizes. They have the widest geographical distribution because of their survival mechanism which allows them to live below the carbonate compensation depth. They have a sandy appearance and above all they have a completely benthic form of life (Doyle, 2005).

2.13.4 Calcareous foraminifera

- *Calcareous* foraminifera have a rigid wall of calcium carbonate, which characterises the major groups.
- *Fusulinids* are coiled and oval in shape with a sugary appearance. The aperture is often unrecognisable.
- *Miliolids* are distinguished by their milky-white appearance and are generally characterised by milioline coiling and there are two key types. Firstly, there are the small, plain form with obvious milioline coiling, a single clear aperture with the addition of a tooth (Doyle, 2005). The second group are larger and oval in shape with small obvious apertures.
- *Rotalines* tend to vary in form, but are usually characterised and identified by a glassy appearance. They have a perforated wall and a completely benthic form of life.
- *Globigerinids* are similar to rotalines especially the wall structure. They possess a perforated hyaline wall, a multilocular test, multiple apertures, coiled spiral chambers and unlike *Rotalines* they have a completely planktonic form of life (Doyle, 2005).

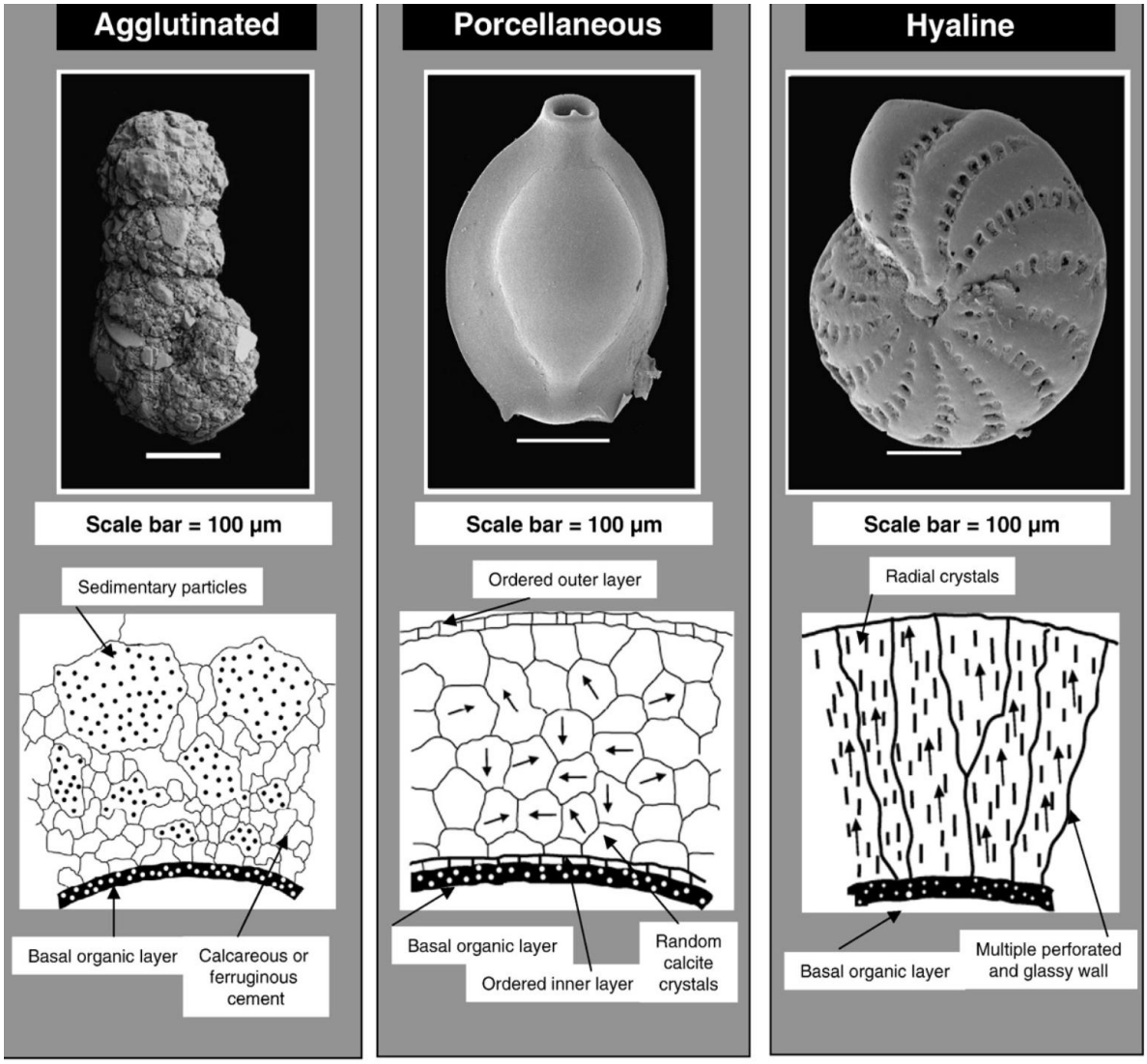

Figure 2.11: Agglutinated, Porcellaneous and Hyaline foraminiferal walls (Mamo *et al.*, 2009).

2.14 Factors affecting the distribution of planktonic foraminifera

A broad range of environmental variables can influence the distribution of planktonic foraminifera such as temperature, oxygenation and nutrients, salinity, water depth and the calcite compensation depth. The remainder of this section will refer only to planktonic foraminiferal species.

2.14.1 Temperature

According to Doyle (2005), planktonic foraminifera are quite tolerant to temperature variations and are present in all world oceans and seas. However, Cifelli (1971) claims that temperature is the primary control which regulates the distribution of planktonic foraminiferal species. Unfavourable temperatures can hamper growth and reproduction, therefore, organisms cannot survive. Planktonic foraminifera and latitude show a certain degree of equilibrium. In the past, planktonic foraminiferal species were grouped into three assemblages according to SST, nowadays; the species are related to

specific water masses which illustrate latitudinal distribution patterns mirroring the effect of temperature (Cifelli, 1971; Capotondi *et al*., 1999). As a result of this, five water masses have been identified; tropical, subtropical, temperate, polar and subpolar (Figure 2.12**)**.

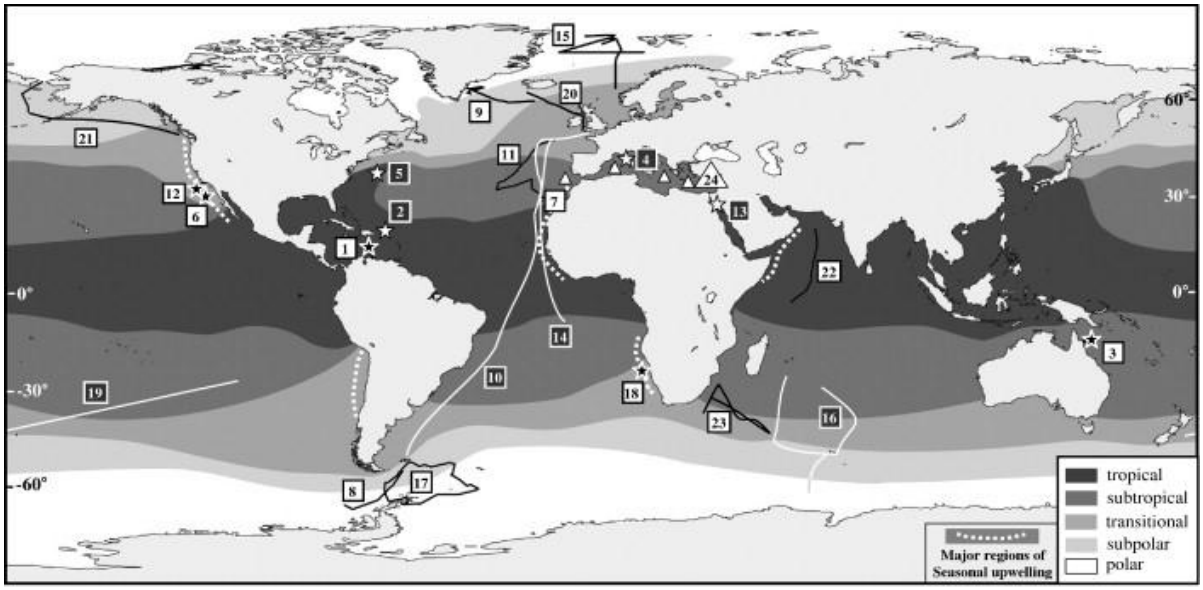

Figure 2.12: Map illustrating the latitudinal distribution of water masses based on sea surface temperature (courtesy of Beavington and Racey, 2004).

Planktonic foraminifera have numerous characteristics, such as size and shape that may be governed by temperature and it is known that some species exist at deeper levels within the water column (Doyle, 2005). For example, surface tropical waters can reach 28°C while water at lower depths may average less than 4°C.

Mulitza *et al.* (1998), used isotope measurements from Holocene planktonic foraminiferal samples to deduce temperature responsiveness and optimum temperature of *Globigerinoides ruber* (pink) and *Globigerinoides sacculifer.* Two experiments concluded that *G. sacculifer* is less sensitive to temperature change than *G. ruber* (pink). The optimum temperature of *G. sacculifer* was 22ºC while *G. ruber* (pink) was 27ºC. Meanwhile, *Žarić et al.* (2005) presented the first universal collection of foraminiferal flux and relative abundance data obtained from sediment traps. From this compilation they derived SST as the most important governing factor in relation to foraminiferal flux and relative abundance. During glacial periods when large volumes of water were stored in continental ice sheets, planktonic foraminifera may have migrated upwards to warmer surface waters in order to survive. Likewise, during interglacials they may have migrated downwards to cooler water (Bradley, 1999).

2.14.2 Salinity

Planktonic foraminifera are normally found in marine environments with salinities ranging between ~30-40‰ and these species have adapted well under these conditions (Doyle, 2005). Two cold phases, The Younger Dryas, (13-12.5 kyr BP) and Heinrich Event H2, (approximately 24 kyr BP) are two specific times when surface water salinity and SST decreased limiting the distribution of these species (Melki *et al*., 2009). An influence of salinity on foraminiferal Mg/Ca ratios has been observed in many studies and the Mediterranean Sea provides the ideal setting for these investigations. Williams *et al*. (2008), concluded that *Orbulina Universa* grown at salinities of 26, 35 and 44 psu showed a weak increase of Mg/Ca (4± 3% per psu), whereas *G. sacculifer* grown at the same salinity rates had a significant increase of Mg/Ca (~100%). Tang and Stott (1993) investigated temporal variations in surface water salinities in the eastern Mediterranean Sea. In this study, these scientists discovered low salinity conditions during the past 13,000 yrs BP. At the onset of S1, surface salinity had decreased by ~4‰ in this eastern basin, moreso during the winter season. This in turn may inhibit the production of Levantine Intermediate water, prevent the formation of Adriatic deep water and reduce ventilation of the eastern Mediterranean (Tang and Stott, 1993). Inevitable adaptation by the planktonic foraminiferal species is likely under such conditions.

2.14.3 Water Depth

Doyle (2005) claims that like temperature and salinity levels, water depth plays an important role in the distribution of planktonic foraminifera. The maximum concentration of planktonic life survives in shallow depths of the photic zone, where light penetrates and microscopic plants can survive to provide food for these minute animals (Fortey, 2002). Most species live near the surface but among living planktonic organisms there is sometimes stratification according to water depth (Fortey, 2002). Shallow species tend to reside in the upper 50m of the photic zone and compared to deeper residing species they tend to be smaller in size with thinner walls (Armstrong and Brasier, 2002). Intermediate species, such as *O. universa* and *G. bulloides*, tend to dominate depths between 50 and 100m. Species residing below a depth of 100m are referred to as deep water species and are adapted to the cooler, denser water masses that occupy these areas. Examples of such species include *Globorotalia menardii* and *G. truncatulinoides* (Armstrong and Brasier, 2002).

2.14.4 Oxygen and Nutrients

Phosphate and nitrate are the primary nutrients associated with foraminiferal productivity in oceans and seas. Food supply is generally low in the deep sea therefore foraminiferal density is low but diversity may be high (Armstrong and Brasier, 2002). However, in areas where nutrient supply is high (e.g. upwelling zones), foraminiferal densities increase but diversities decrease (Armstrong and Brasier, 2002. In general, on a seasonal scale, food is understood to be the main factor governing the distribution of planktonic foraminifera (Fraile *et al.*, 2008) with each individual species having a different food preference. Planktonic foraminifera can be divided into two groups, one group bearing thin long calcite spines (spinose) while the other group remains spineless and smooth (non-spinose). For example, spinose species have a preference for animal prey such as copepods, while non-spinose species are mainly herbivorous (Fraile *et al.*, 2008).

Large scale primary production in the surface waters can often cause anaerobic bacterial blooms on the sea floor and in the mid-water zone. Planktonic foraminifera have a low oxygen demand therefore oxygen deficiency does not totally reduce them from low oxygen water ranges (Armstrong and Brasier, 2002).

2.14.5 The Calcite Compensation Depth

The calcite compensation depth (CCD) is the depth at which calcium carbonate cannot be recorded in the sediment as the rate of dissolution is greater than the rate of precipitation. Shallow marine waters are normally saturated in calcium carbonate ($CaCO_3$). Shells of dead organisms fall downwards to deeper waters and generally remain intact until reaching the lysocline where the rate of dissolution increases significantly. The CCD exists just below the lysocline, here only a relative small proportion of calcite is preserved (Schiebel and Hemleben, 2005). As many foraminiferal species are susceptible to dissolution below the CCD, their fossilised skeletons are often absent from deep sea sediments. Temperature is known to influence the rate of calcium carbonate solubility, for example the CCD is shallower in sub Polar Regions than in tropical regions (Armstrong and Brasier, 2005). The shallowest known CCD levels of approximately 3,400m are found in low latitudes (Emwlyanov, 2005). However, only a limited amount of calcareous species are found below 3,000m in depth (Armstrong and Brasier). Sediments from depths below the CCD level are considered unsuitable for palaeoclimatic studies (Bradley, 1999).

2.15 Present Day Distribution of Planktonic Foraminifera in the Mediterranean Sea

Distribution patterns of planktonic foraminifera differ significantly across the Mediterranean Sea. These patterns are mirrored by fertilisation patterns which are ultimately controlled by hydrographical systems (Pujol and Vergnaud Grazzini, 1995). Eddies and fronts play a major role in the control of these patterns and give rise to a higher diversity of species. The western basin shows a higher density of planktonic species in winter than summer (3,700 specimens/1000 m^3 in winter compared to 200-600 specimens/1000 m^3 in summer) (Pujol and Vergnaud Grazzini, 1995). Overall, the western basin has a higher production rate than the eastern basin with the eastern basin having long been established as an area of low productivity. Nutrient levels are low in the eastern basin especially in the upper 10m, limiting phytoplankton growth in both summer and winter. Oligotrophic conditions may prevail here because of the surrounding physical features and the arid climate producing very little nutrient rich runoff (Pujol and Vergnaud Grazzini, 1995). Predatory species such as *G. ruber* and *O. universa* tend to prevail in such environmental conditions. Peak production has been observed in the central Mediterranean during late summer with approximately 1000-2000 species/ 1000 m^3 (Pujol and Vergnaud Grazzini, 1995). *Globigerinoides ruber alba,* and *G. ruber rosea,* dominate the assemblages here. According to Geraga *et al.* (2008), the distribution and productivity patterns of planktonic foraminifera differ in summer and winter. Standing stocks are higher in winter than in summer in the western basin. *G. ruber alba,* and *G. ruber rosea,* dominate the eastern basin while *G. trilobus* and *O. universa* control the standing stock in the western basin at the end of summer in a mixed layer (Pujol and Vergnaud Grazzini, 1995). *G. truncatulinoides* and *Globorotalia inflata,* dominate the western basin during winter. In late summer, foraminiferal production is found to be low as a result of the surface and mixed layers being nutrient poor (Pujol and Vergnaud Grazzini, 1995). In late winter, productivity is found to be high as a result of deep water mixing and nutrients being conveyed to the thermocline (Pujol and Vergnaud Grazzini, 1995). The North African coasts, near Crete and in the Ionian Sea, are the three areas where high densities of foraminifera are located in late summer.

In conclusion, it is important to note that understanding the ecological preferences and resultant distribution of various planktonic foraminiferal species is recognised as a modern analogue which can be subsequently used in palaeoenvironmental reconstructions. The observations of Pujol and Vergnaud Grazzini

(1995) indicate that the geographic and depth distribution of planktonic foraminifera in both western and eastern basins, cannot be fully explained as poor correlation with the surrounding temperatures and salinity gradients were noted. Hydrography regulates the water columns in both basins. Nutrient supply and production are mainly regulated by the strength of the pycnocline, the depth of the mixed layer and stratification (Pujol and Vergnaud Grazzini, 1995) Therefore; planktonic foraminiferal assemblages may be considered a commendable tool in relation to general hydrographic variability from the sedimentary record. Palaeoenvironmental inferences are the fundamental principle underlying the principle of uniformitarianism, where the present is the key to the past (Stanley, 2005). Moreover, this principle of uniformitarianism, discounts evolutionary adaptation and change. Without dismissing the usefulness of planktonic foraminifera as a palaeoproxy, it is frequently necessary to utilise certain transfer functions, (which are based on the principle of uniformitarianism) in palaeoenvironmental reconstructions.

2.16 Transfer Functions

Transfer functions are mathematical functions that compare fossils in ocean or sea sediments to their present day descendants. With the advancement of methods to measure the relationship between planktonic faunal assemblages and environmental variables, The Imbrie-Kipp (IKTF) and the modern analogue technique (MAT) have both been used to reconstruct Quaternary SSTs in the Mediterranean Sea (Hayes *et al.*, 2005). Using the Imbrie-Kipp technique, CLIMAP (1976) was the first project to reconstruct Mediterranean glacial sea surface temperatures however; this has since been updated due to the advancement of palaeoenvironmental knowledge (Hayes *et al.*, 2005). Recently, improvements in the modern analogue method (MAT) and the revised analogue method (RAM) have led to a more detailed reconstruction of the Mediterranean Sea. These developments were further complimented by progress in computer technology. Studies are now relying more on the artificial neural networks (ANN) which is a computer based method. Hayes *et al.* (2005) utilised this method in their study to provide a specific and thorough sea surface temperature reconstruction of the entire Mediterranean Sea. The calibration data set included 145 core tops from the Mediterranean. 129 cores from the North Atlantic database were also utilised in the study to provide analogues for glacial Mediterranean assemblages, which contain planktonic foraminiferal species that do not exist in the Mediterranean Sea today (Hayes *et al.*, 2005). These transfer functions will be discussed further in Chapter 3 'Materials and Methods'.

Chapter 3: Materials and Methods

3.1 Introduction

This chapter will deliver a comprehensive account of the materials and methods applied during the course of this research. Firstly, it will deal with the Mediterranean deep-sea cores, their individual locations and specifications. Secondly, it will present information on the laboratory processes and finally, provide an overview of the transfer function used in this research.

3.2 Materials

3.2.1 The Deep-Sea Cores

Since the beginning of the 1960s and largely under the auspices of the Ocean Drilling Programmes, complex deep-sea drilling techniques have been extracting foraminiferal enriched sediment cores. Quaternary scientists turned to the deep oceans where sedimentation was continuous over millions of years and this has now provided an almost uninterrupted record of data into the Tertiary period (Walker, 2005). With the development of coring equipment on individually designed ships, sediment cores were easily obtained from water depths of over 3km.

To implement this investigation sediment from three eastern Mediterranean deep-sea cores were utilised (Figure 3.1). This sediment was extracted from the oldest and deepest part of the Mediterranean Sea, where several kilometres of sediment has been deposited on the oceanic crust surface (Cita and Alosi, 2000). These cores, (964A), (973A) and (969A), were collected from The Ionian Sea at varying depths (Tables 3.1 and 3.2). Site 964 is situated at the foot of the Calabrian Ridge in water 3650m deep and is located close to the Ionian Abyssal Plain. It is also positioned near the present day sources of deep-water formation in the Adriatic Sea (Emeis *et al.*, 1996). The lithology of this site comprises of ash layers and turbidites with some of the light coloured intervals being depicted as normal graded turbidites. The host sediments contain clayey nannofossil ooze varying in colour from brown to green. Tuffs are present and volcanic glass is evident throughout this site. Sapropel S1 is present in the uppermost part and is enriched in pyrite, plant material and amorphous organic matter. The sedimentation rate at site 964 averages at ~30 m/m.y. (Emeis *et al.*, 1996). Site 969 is found on the inner, shallower, undeformed part of the Mediterranean Ridge.The lithology of site 969 comprises of nannofossil clay and ooze over calcareous silty clay. The age versus depth relationship as studied by Emeis *et al.* (1996), suggests that the

sedimentation rate at site 969 is approximately 22 m/m.y. Site 973 is situated on the lower part of this Mediterranean Ridge. The upper 84m of this site is dominated by nannofossil ooze and nannofossil clay with sapropels and three minor ash layers (Emeis *et al.*, 1996). Fine to medium turbidites are apparent as well as interbeds of sands, silts and nannofossil clays. The underlying section is governed by red-coloured clayey nannofossil ooze overlaying a calcareous silty claystone**.** A thin black layer mainly comprised of gypsum is evident and is considered a relict sapropel (Emeis *et al.*, 1996).

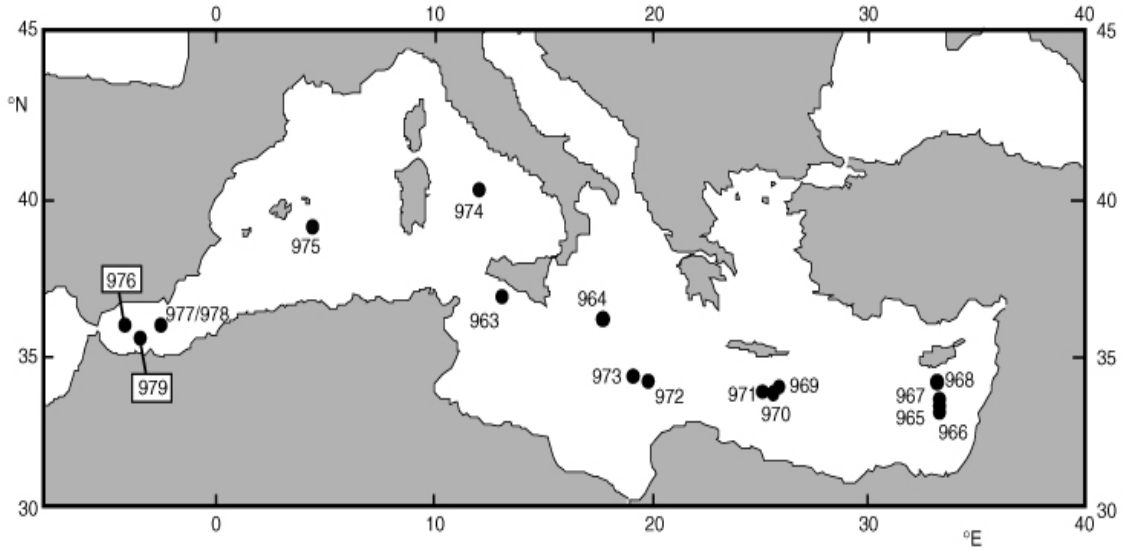

Figure 3.1: Map depicting the sites of Leg 160 and Leg 161. Illustrated in this map are the three cores, 964A, 973A and 969A which were utilised in this project (Ocean Drilling Programme, 2012).

Core	Position	Sub-Basin	Length of core (m)	Lithology	Earliest Age
964A	36°15.623'N, 17°44.990'E	Ionian Basin	106.1	Foraminifer-bearing nannofossil ooze	Early Pliocene
973A	35°46.820'N, 18°56.889'E	Ionian Basin	148.5	Clayey calcareous siltstone	Early Pliocene
969A	33°50.399'N, 24°53.065'E	Ionian Basin	108.3	calcareous silty clay	Pliocene-Pleistocene

Table 3.1: Specifications of the three deep-sea cores.

Core	Length of core examined (cm)	Sampling Resolution (cm)	Radiocarbon Dated
964A	134.5	4	Yes
973A	102.5	4	Yes
969A	70.5	2	

Table 3.2: Sampling and radiocarbon dating details of the three deep-sea cores.

3.3 Methods

The samples utilised for the purpose of this research had undergone initial wet laboratory processing techniques prior to the start of this project. All laboratory procedures for these cores were undertaken at Mary Immaculate College, Limerick and will be described in full in the following sections.

3.3.1 Laboratory Procedures

Firstly, all micropalaeontological samples were taken from storage in a laboratory refrigerator, removed from their packaging and placed into labelled petri dishes. They were then dried overnight in the laboratory oven at 40°C (Figure 3.2). For small samples (<5g) 24 hours drying between temperatures of 40°C should suffice. Samples are never dried above these temperatures as loss of some foraminiferal tests may occur due to cracking by high temperatures (National Oceanography Centre, 2012). Following on from this procedure, the samples were disaggregated in deionised water and wet sieved through a 63 µm sieve (Figure 3.3). When washing was completed, the sample was poured into a clean labelled container. The sieve was thoroughly washed between each sample to avoid any contamination. The samples were again put into petri dishes and dried overnight in the laboratory oven which allowed the water to evaporate off at the unchanged temperature of 40°C. Afterwards the samples were weighed to gain a dry fraction weight. It is good practice to weigh the petri dishes before the previous procedure, then the dried samples can be utilised immediately for weighing. Furthermore, the weight of the petri dish may be subtracted to leave the sample dry weight (National Oceanography Centre, 2012). Each sample was then dry sieved through a 150 µm sieve. The 63-150 µm samples were separated from the >150 µm samples. Only the >150 µm samples were used for this research as age and biostratigraphic control are based on quantitative planktonic foraminiferal analysis of sample splits of approximately 300 specimens from the >150 µm size fractions (Keller, 2004). The samples were subsequently bottled and labelled.

Figure 3.2: Laboratory oven

Figure 3.3: Petri dish on left, sieve on right.

3.3.2 Quantitative Analyses

For estimating the relative abundance of each species, the >150 µm size-fraction was analysed. Where necessary each sample was split using a random splitter, this splitter divided each run into equal halves and in some cases many runs were required to bring the split fraction down to the ideal quantity of 300 planktonic foraminiferal specimens (Keller, 2004). The split fraction was recorded and carefully performed to allow accuracy. The specimens were then deposited onto a picking tray (Figure 3.5) With the aid of a stereo microscope, equipped with SWF2OX lens, on average 300 complete specimens of planktonic foraminifera were subsequently picked onto a Chapman slide using a 0000 size paint brush and deionised water. Each Chapman slide consists of 32 equal numbered compartments (Figure 3.4). Each specimen was identified and put into a separate compartment on the slide. When this procedure was completed the total number of species was counted and this data was inputted into Excel spread sheets for further analysis.

The samples showed no outward signs of dissolution and on average the planktonic foraminiferas were relatively well preserved morphologically. All fragmented specimens, if found were excluded from the foraminiferal census counts. Furthermore, it is important to note the taxonomy that was utilised to identify the planktonic foraminifera in this research. The taxonomy regulated by Hemleben *et al*. (1989) was practiced here. Only the white and pink variants of *G. ruber* were identified. The two coiling varieties (dextral and sinstral) of *G. truncatulinoides* and *N. pachyderma* were also determined.

Figure 3.4: Stereo microscope with a Chapman slide on top

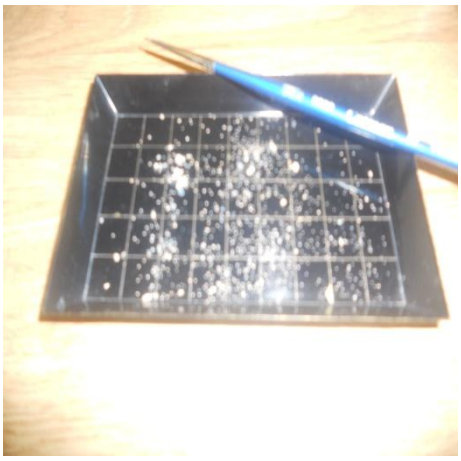

Figure 3.5 Picking tray and 0000 brush

3.4 Radiocarbon Dating

The method mostly employed to date marine fossils and sediments spanning the last 50k yrs. is radiocarbon dating. This system was developed in the late 1940s by William F. Libby, an American chemist. Carbon has three natural isotopes, ^{12}C, ^{13}C and ^{14}C. ^{12}C and ^{13}C are stable isotopes while ^{14}C is a radioactive isotope that is formed in the upper atmosphere, where it merges with oxygen to form carbon dioxide (Hua, 2009). All living things comprise of ^{14}C. In nature, ^{14}C forms when high-energy atomic particles called cosmic rays collide into the earth's atmosphere, causing atoms in the atmosphere to collapse into electrons, neutrons, protons and other particles. Some neutrons strike the nuclei of nitrogen atoms in the atmosphere. Each of these nuclei absorbs a neutron and then drops a proton. In this way, a nitrogen atom becomes a ^{14}C atom. Following its

production, ^{14}C is conveyed to all the carbon reservoirs, such as the biosphere and oceans. Living organisms take up ^{14}C through the food chain and other metabolic processes and they preserve a content of ^{14}C in balance with that available in the atmosphere until the moment of death (Hua, 2009). Similar to all radioactive substances ^{14}C atoms decay at a precise and unchanging rate. With the passing of time, newly created ^{14}C in the atmosphere is constantly replacing ^{14}C as it decays but once the organism dies this supply is cut off from the ^{14}C source (Wilson *et al.*, 2005). Subsequently, the concentration of ^{14}C in the organism begins to decrease by radioactive decay. It takes approximately 5,700 years for ^{14}C to decay by half, a period referred to as the half-life (Bell and Walker, 2005).

After scientists measure an object's or fossil's ^{14}C content and assuming that the rate of decay and replenishment are constant, they compare it with the ^{14}C in tree-rings whose ages are known. This technique enables them to counterbalance for variations of ^{14}C content in the atmosphere at various times in the past and to gain a more precise date. Initially, significant inaccuracies between the age of samples based on ^{14}C dating and dendrochronology were discovered. In the 1960s, scientists measuring the radioactivity of a known age in tree rings found inconsistencies in the ^{14}C concentration up to a maximum of ±5% over the previous 1500 years (Higham, 2002). These chronological fluctuations led to the calibration of radiocarbon dates to other known aged materials. German and Irish oak trees have been dated over recent years to produce a tree ring based ^{14}C calibration data set IntCal98, which now extends back over 10,000 years. This also enables the calibration of dates to solar or calendar dates (Higham, 2002; Kromer, 2009).

According to Walker, (2005) accuracy and precision underline the quality of ^{14}C dating. Accuracy relates to the level of agreement between the real age of a given sample and that created by the dating process. Precision relates to the geometric indecision with any physical or chemical analysis that is used to interpret age (Walker, 2005). There are two principal techniques used to measure ^{14}C of any given sample, namely beta counting and Accelerator Mass Spectrometry (AMS). Beta particles are products of radiocarbon decay and this method of dating can be controlled in two different ways. Firstly, the carbon sample is converted to CO_2 before measurement in gas proportional counters take place. Liquid scintillation counting is the second method, for this procedure, the sample is in liquid form and a scintillator is added. A flash of light is produced when the scintillator interacts with a beta particle. AMS is the chosen dating technique for this study, mainly because of its accuracy and time

efficiency. AMS laboratory measurements can be obtained in a matter of hours and can date samples accurately without compromising analytical precision (Walker, 2005).

3.4.1 Accelerator Mass Spectrometry

In the 1980s, AMS was developed and this is a direct method of ^{14}C isotope counting. This utilises particle accelerators as mass spectrometers to count the relative number of ^{14}C atoms in a sample as opposed to decay products (Walker, 2005). The central advantages of the AMS method-dating is that milligram sized samples are required for dating. The ability to analyse small samples offered opportunities to date new materials such as foraminifera from marine sediments and other fossilised resources (Hua, 2009). Also, compared to the radiometric method, AMS has benefits in the speed and efficiency in which samples can be treated in a matter of hours rather than a few days. AMS governs the isotope ratio of ^{14}C relative to that of the stable isotopes of ^{13}C and ^{12}C and the age is then determined by relating this ratio with that of a standard of known ^{14}C content (Walker, 2005). This is frequently referred to as isotope ratio mass spectrometry.

The tandem accelerator encompasses two separate phases of acceleration and is the most commonly used system. Pre-treated samples are changed to carbon dioxide and then graphite in a forced circulation system. These graphite particles are then installed on a metal disc awaiting AMS measurement (Walker, 2005). With the support of a van de Graff generator, the particles are then accelerated at high speeds, allowing the separation of the ^{14}C signal from that of the other two isotopes, ^{12}C and ^{13}C (Walker, 2005). AMS then concludes the ratio of ^{14}C relative to the other two isotopes. Radiocarbon ages are then obtained by comparing this ratio of the sample material with that of an internationally accepted standard of known ^{14}C content, usually NBSoxalic acid (Walker, 2005).

Understandably, there are sources of error associated with this method. For example, contamination refers to the addition of younger or older carbon to the sample material and can occur during or prior to field sampling, in the laboratory due to fungal growth or through modern contamination by dust and skin (Walker, 2005). Contaminants, such as soils and sediments, dissolved carbonates and humic acids must be removed before samples are processed for dating, this denotes the pre-treatment step (Hua, 2009). Bioturbation by organisms on a lake or ocean floor can allow for the downward movement of younger sediments which can cause major miscalculations in radiocarbon dates. The addition of 1% modern carbon to a 17,000 year old sample has

the ability to reduce the age by 600 years (Walker, 2005). A modern sample with the addition of the same amount of carbon will increase the age by approximately 80 years. Radiocarbon laboratories have inflexible modern procedures in place to safeguard against the hazard of contamination (Walker, 2005).

The concentration of ^{14}C differs between the key carbon reservoirs, such as the biosphere, ocean and atmosphere. The residence time of carbon in each of the reservoirs is different. The deep ocean, with a residence time of approximately 800 years has much lower ^{14}C content than that of the atmosphere (Broecker, 2000). ^{14}C becomes integrated into sea water in the form of dissolved carbonate, subsequently sinking without replenishing resulting in the sea water having a deceptive age (Walker, 2005). As a result, materials from the ocean have to be modified for the age of sea water. In the case of the surface ocean and due to the interaction between the two reservoirs, the atmosphere and ocean, surface waters have higher intensities of ^{14}C (Hua, 2009). Recent studies have shown that marine samples have radiocarbon dates that are older than contemporary terrestrial samples. The extent of the marine offset is repeatedly accessed as over 400 years but can fluctuate from place to place depending on the degree of ocean mixing (Pilcher *et al.*, 2005). Surface ocean organisms such as planktonic foraminifera appear younger than their synchronous deep ocean matter but older than their coexistent terrestrial samples (Hua, 2009). To report chronological concerns, calibration of ^{14}C ages is usually undertaken using a computer programme. CALIB 5.0.1 is one such example which can convert ^{14}C into calendar years using the INTCAL 98 calibration curve which is mainly based on dendrochronological records. However, this calibration curve stops at 24,000 cal yr B.P. (Bard *et al.*, 2004). To calibrate a ^{14}C date for a surface ocean sample, the Marine04 calibration curve or the INTCAL04 can be utilised (Hughen *et al.*, 2004; Hua, 2009).

The chronological framework of this research is based on seven ^{14}C-AMS dates. A minimum of 10-20 mg of clean mixed planktonic foraminifera was sampled for each ^{14}C date in cores ODP 964A (four ^{14}C dates) and 973A (three ^{14}C dates). The dates were converted into calendar years using the programme CALIB 5.01, which includes a reservoir age of 400 years (Geraga *et al*., 2008). This age is consistent with the reservoir age proposed by Siani *et al*. (2001) for the Adriatic Sea.

3.5 Artificial Neural Networks

Artificial Neural Networks (ANN), were first developed in 1959 by Rosenblatt and expanded in 1974 by Werbos and over the past few decades has undergone rapid

advancement and is now widely used in many fields (Dayhoff and DeLeo, 2001). This computer based system and form of artificial intelligence can determine the relationship between two sets of variables, by the inputting of a calibration dataset, resulting in the prediction of an output value and in distinguishing a pattern in multifactorial data (Hayes *et al.*, 2005).

Hayes *et al.* (2005), in their research on the reconstruction of Mediterranean Sea surface temperatures (SST) during the last glacial maximum (LGM) used ANN as a basis for reconstruction. Reconstructions were based on an expanded data set of 273 samples in 37 cores with a uniform minimum level of age control (Hayes *et al.*, 2005). This technique proved reliable when compared to conventional computational techniques as prediction errors were at a minimum (0.5-1.1°C). Siccha *et al.* (2009) investigated the distribution of planktonic foraminifera in the surface sediments of the Red Sea. With the use of ANN technique a high correlation between faunal composition and such variables as salinity, temperature, stratification and oxycline depth was established with a high average accuracy of (15%). For the purpose of this study, quantitative downcore variations in eastern Mediterranean Sea planktonic foraminiferal assemblages were investigated by comparison to a modern calibration dataset in an effort to reconstruct Quaternary SSTs in the eastern Mediterranean Sea.

3.5.1 The Calibration Dataset

The calibration data set used in this research is based on census counts of planktonic foraminiferal species in three cores from the eastern Mediterranean Sea, (964A, 969A and 973A) and also on the calibration dataset of Hayes *et al.* (2005). All samples within the calibration data set were picked from the >150 µm fraction. For calibration functions, Hayes *et al*. (2005) used annual, winter (January-March) and summer (July-September) SST data from the World Ocean Atlas (WOA, Vol. 2) and WOA 98 sample software was subsequently utilised (http://www.palmod.uni-bremen.de/csn/woasample.html). The calibration data set of Hayes *et al*., (2005) includes 145 Mediterranean and 129 North Atlantic core tops. To reduce the effect of lumping of cryptic genetic species and to ensure the inclusion of sub-polar water assemblages, Atlantic core tops were taken within the range of ~25-70° N and between ~5° E-30°W (Hayes *et al*., 2005). Furthermore, these core tops are included to provide analogues for glacial Mediterranean Sea assemblages which contain species that are devoid in the Mediterranean Sea today. Samples from upwelling regions were excluded from the data set because these species are governed by unusual physical constraints

(Ufkes *et al*., 1998; Hayes *et al*., 2005). Also excluded were the core tops recording >70% of *N. pachyderma* (sinstral), since such associations have never been identified in the Mediterranean Sea (Hayes *et al*., 2005).

Chapter 4: Presentation of Results

4.1 Introduction

This chapter presents the chronological framework upon which this research is based. It will present the planktonic foraminiferal faunal assemblage and SST results for the three eastern Mediterranean deep-sea cores.

4.2 Chronostratigraphy

The following section will illustrate how the chronological framework for this research was obtained. The age models are based on 7 ^{14}C-AMS dates (Table 4.1) from cores 964A and 973A. Currently, there is only one AMS date for core 969A, which is insufficient to create a chronological record.

Core	Depth (cm)	Corrected depth (cm)	^{14}C (yrs BP)	Mean Calendar Age (cal BP)
964A	2.5	2.5	1250± 30	795
964A	46.5	9.5	2360± 30	1975
964A	102.5	65.5	13050± 60	15000
964A	134.5	87.5	17730± 80	20800
973A	2.5	2.5	1390± 30	930
973A	46.5	21.5	3370± 30	3240
973A	102.5	77.5	14450± 50	17055
969A	34.5		9700± 40	10565

Table 4.1: The 8 ^{14}C-AMS dating control points utilised in this research. Corrected depth (cm) refers to the depth (cm) after the subtraction of turbidites.

Turbidite systems are well developed along the continental margins of the Mediterranean Sea, with many deposits forming during the Quaternary Period (CIEMS, 2002). The mountain ranges surrounding the Mediterranean Sea, along with rapidly changing climatic conditions, impact heavily on sedimentation rates within the basin.

When examined, cores 964A and 973A displayed evidence of turbidites. Photographs obtained for this study illustrates core 964A highlighting this. Numerous fine to medium turbidites were identified, in core 973A, including one 14m thick interval of sand and nannofossil clay during the Ocean Drilling Programme (Emeis *et al*., 1996). The sedimentological characteristics and position of the major turbidites was recorded during this drilling programme and colour scanning aided the identification of the thicker turbidite beds (Emeis *et al*., 1996). As these deposits are instantaneous they can be subtracted from the depth of studied sections without it affecting the age-models.

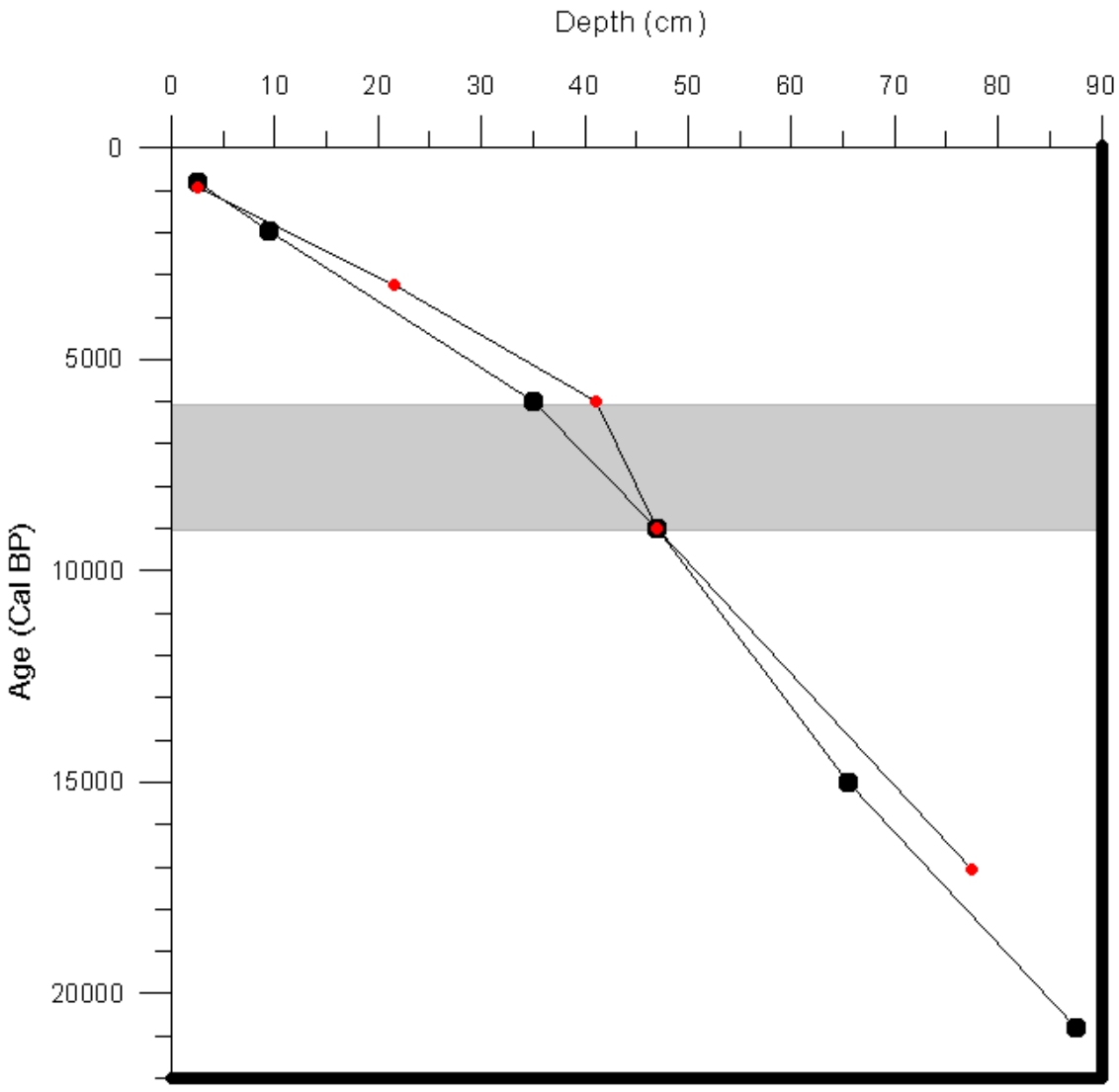

Figure 4.1: The age model for core 964A: (shown in black) is based on four ^{14}C AMS dates while the age model for core 973A: (shown in red) is based on three ^{14}C AMS dates. Both cores have two additional dating control points at 9000 and 6000 cal yrs BP (the known dates of S1, Principato, 2003). The grey shaded area represents S1 deposited between 9,000-6,000 cal yrs BP (Principato, 2003).

Core	Depth (cm)	Sedimentation Rate (cm/kyr)	Average rate of sedimentation (cm/kyr)
964A	2.5 - 9.5	5.9	
964A	9.5 - 65.5	4.3	
964A	65.5 - 87.5	3.8	
964A			4.7
973A	2.5 - 21.5	8.2	
973A	21.5 - 77.5	4	
973A			6.1

Table 4.2: Table illustrating the sedimentation rates for cores 964A and 973A. Sedimentation rates were initially calculated for each interval using the dating control points outlined in Figure 4.1. This enabled the average sedimentation rate to be calculated for each core.

Sedimentation rates in the eastern Mediterranean Sea are generally low (3-4cm/kyrs) (Principato, 2003). Nijenhuis and de Lange (2000) have analysed seventeen sapropels recovered during ODP Leg 160 from sites 964, 966, 967, and 969. These authors acknowledged that sedimentation rates were low (1.66- 4.23cm/kyrs) and did not change significantly during sapropel formation. Resulting from these low sedimentation rates are the lack of high-resolution studies for the last 15,000 cal yrs BP (Vergnaud-Grazzini *et al*., 1988; Troelstra *et al*., 1991; Principato, 2003). The average sedimentation rates from the Ionian Sea are slightly higher compared to other cores extracted from the eastern Mediterranean basin (Table 4.2).

4.3 Results

Planktonic foraminiferal faunal assemblage results for 13 species will now be discussed in the following paragraphs. *G. ruber* (white and pink), *G. siphonifera*, *N. pachyderma* (dextral and sinistral), *G. rubescens*, *O. universa*, *G. truncatulinoides* (dextral and sinistral), and *G. sacculifer,* are subsequently presented for the three eastern Mediterranean cores. Other species represented are *G. bulloides, G. glutinata, G.*

inflata, T. quinqueloba and *G. scitula.* All 13 species are illustrated versus age in cal yrs BP for cores 964A and 973A. Core 969A will be plotted against depth. Relative abundances of each species will be expressed as percentages in all three cores. Furthermore, mean annual, summer and winter SST results, based on the ANN transfer function, are also presented for the three eastern Mediterranean cores. Summer SSTs correspond to the months of June, July and August. Winter SSTs correspond to the months of December, January and February. Annual SSTs correspond to the annual average results. Again, cores 964A and 973A graphs are illustrated versus age in cal yrs BP. Core 969A will be plotted against depth and all SSTs will be recorded in degrees Celsius (°C). As outlined in chapter 3, section 3.5, the error associated with the ANN technique ranges between 0.5°C (winter SSTs) and 1.0°C (summer SSTs). As such, these errors must be taking into account when analysing the SST records to avoid over interpretation of the climate signals. Telford *et al.* (2012) have argued that quantitative palaeoecological reconstruction lack major testing as a transfer function for any variable will generate a reconstruction for any fossil data where some common species exist. These authors claim that the depth habitats of planktonic foraminifera may affect reconstructed temperatures. Transfer functions for palaeoenvironmental reconstruction make a number of assumptions (Birks *et al.*, 2010). Telford *et al*. (2012) have stated that planktonic foraminifera found in sediment can be correlated to different seasons and water depths. Their composition underpins the thermal structure of the upper ocean layers, therefore it would be unforeseen if temperature reconstruction from one depth in one season secured SST changes through space and time. If thermal structure remains the same, transfer functions based on a fixed calibration depth should not be affected. The significance of some of these inferences for planktonic foraminifera-derived SST has been examined. Spatial autocorrelation may make reconstructions appear more certain than confirmed by the data (Telford *et al*., 2012). Guiot and de Vernal (2011) have responded to the above argument and have continued to defend climatic variables in relation to transfer functions. These authors have argued that when climatic variables are strongly correlated, they also show similar spatial structure. In their research, they found that latitude and longitude accounted for 98% of the winter temperature variance, 90% of the winter salinity, 99% of the summer temperature and 94% of the summer salinity.

This section will include the description of results of each core; along a west-east transect beginning with the most westerly site, 964A.

4.4 ODP core 964A

4.4.1 Faunal results

Planktonic foraminiferal faunal abundances for core 964A are presented in figure 4.2. The observed faunal record begins at ~20,800 cal yrs BP. The planktonic foraminiferal assemblage is dominated by eight species, *G. ruber* (white)*, G. siphonifera, O. universa, G. sacculifer, G. bulloides, G. glutinata, G. inflata,* and *N. pachyderma.* High concentrations (12-70%) of the warm water species, *G. ruber* (white), is evident throughout the Holocene and late Pleistocene in core 964A, with a major peak abundance of ~70% in the middle of S1 (Figure 4.2a). This correlates well with the findings of Melki *et al.* (2009). High frequencies of this species suggest that surface waters were dominated by an oligotrophic mixed layer for most of the year (Ariztegui *et al.*, 2000). *G. ruber* (pink), another warm water species, typically resides in waters of >24°C (Figure 4.2a) (Bé, and Tolderlund 1971). This species is absent from the assemblage until approximately 12,000 cal yrs BP where it exhibits a marked increase reaching frequencies of approximately 10% in S1 at ~6,600 cal yrs BP. This indicates optimum temperature conditions during the termination of S1 (Thunell *et al.*, 1977; Rohling, 1993). However, during the late Pleistocene and from ~12,000 cal yrs BP onwards this species exhibits a marked decrease in population and becomes absent from the faunal record.

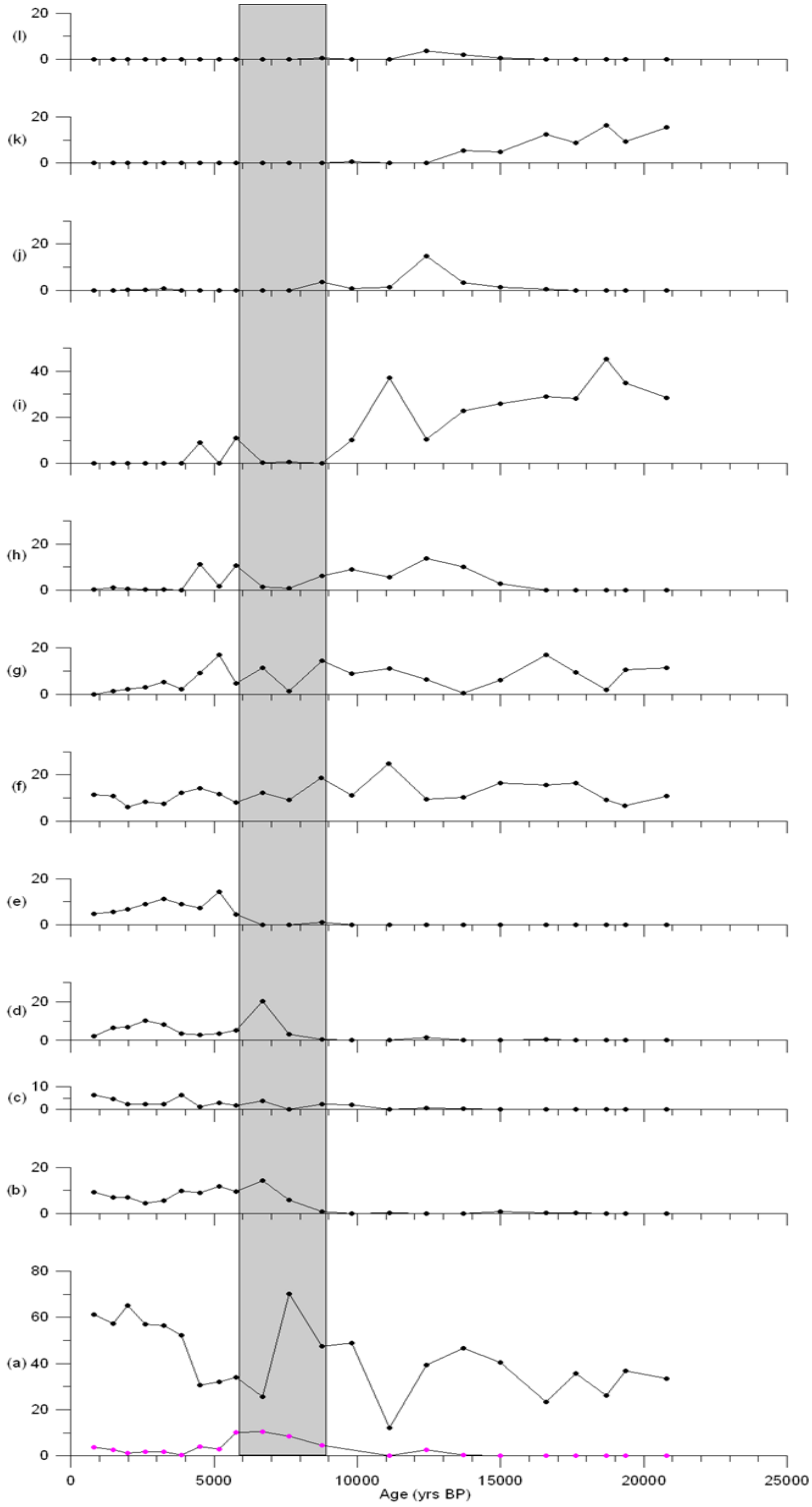

Figure 4.2: Planktonic foraminiferal relative faunal abundances (%) for core 964A. (a) = *G. ruber* (black line represents white variant, pink line represents pink variant), (b) = *G. siphonifera*, (c) = *G. rubescens,* (d) = *O. universa*, (e) = *G. sacculifer*, (f) = *G. bulloides*, (g) = *G. glutinata,* (h) = *G. inflata*, (i) = *N. pachyderma* (dextral), (j) = *G. truncatulinoides*, (k) = *G. scitula,* (l) = *T. quinqueloba*. The chronology for these faunal occurrences is based on ^{14}C AMS dating. The grey shaded area represents S1 deposited between 9,000-6,000 cal yrs BP (Principato, 2003).

G. siphonifera is absent during the late Pleistocene before climbing to a peak of ~14%

within S1 at ~7000 cal yrs BP (Figure 4.2b). Frequencies of this species remain between 5-12% for the remainder of the Holocene. Darling and Wade (2008) found the highest frequencies of *G. siphonifera* dominate the tropical zone with their range terminating towards the lower temperatures of the transitional zone. *G. rubescens* is also indicative of warm waters and low abundances of this species are observed, in particular, during the late Pleistocene and never exceed 6% during the Holocene. During the formation of S1, low frequencies of *G. rubescens* (~2%) are observed (Figure 4.2c). *O. universa* has a temperature range of between 10 and 30°C and has a wide distributional range from the transitional to the tropical zones (Figure 4.2d) (Darling and Wade, 2008). Another species indicative of warm surface waters is *G. sacculifer* (Figure 4.2e). This species was almost non-existent during the deposition of S1 but displayed its highest frequencies of ~14% after the deposition of this sapropel. Kuroyanagi and Kawahata (2004) have observed that *G. sacculifer* prefers warmer water and is more prevalent at shallower depths, and at higher light intensity than *G. ruber*. *G. sacculifer* has been observed at the top of S1 in most cores from the eastern Mediterranean Sea and this correlates well with the occurrence of a surface pycnoline during that period (Geraga *et al.*, 2005). Several studies on eastern Mediterranean cores have inferred that warm water foraminiferal species dominate surface waters during the deposition of most sapropels (Thunell *et al.*, 1977, 1982; Rohling and Gieskes, 1989; Rohling *et al.*, 1993). *G. bulloides and G. glutinata* show almost similar trends throughout the entire faunal assemblage (Figure 4.2f and g). Both species have moderate (~7-17%) and low (~1-6%) faunal frequencies and are more abundant during the late Pleistocene. These species show a gradual increase at the onset of S1 deposition. This increase can be attributed to lower oxygen content within the photic zone as *G. bulloides* can survive in a lower oxygen environment (Geraga *et al.*, 2005). *G. inflata*, associated with cool deep mixed waters (Figure 4.2h), exhibits a marked presence throughout the late Pleistocene (from ~15,000 – 4,500 cal yrs BP) reaching frequencies of approximately ~14%. A sharp decline of this species is evident throughout the duration of S1 and the temporal increase at the termination of S1 can be attributed to deep water ventilation (Geraga *et al.*, 2005). *N. pachyderma* (dextral) shows a marked presence in the late Pleistocene where it exhibits high frequencies of ~45% (Figure 4.2i). In contrast this species appears in low percentages (<4%), or is absent, during the Holocene until approximately 4,000 cal yrs BP. The absence of *N. pachyderma* during S1 in core 964A is in agreement with the study of Ariztegui *et al.* (2000), possibly indicating that a deep chlorophyll maximum (DCM) could not

develop. *G. truncatulinoides* (dextral and sinistral) (Figure 4.2j) displays a similar pattern to that of *T. quinqueloba* in core 964A. The percentage of *G. truncatulinoides* is minimal throughout the faunal record except where it reaches a peak abundance of 11% at ~12,000 cal yrs BP. This may reflect a cooling period as this species prefers a cool well mixed layer with intermediate to high nutrient levels (Pujol and Vergnaud Grazzini, 1995). This species is controlled mainly by winter convection and vertical mixing (Geraga *et al.*, 2005). According to Darling and Wade (2008) *G. truncatulinoides* and in particular the sinistral variant is largely restricted to warm sub-tropical waters. *G. scitula,* another cold water, sub-polar species, shows a distinct presence during the late Pleistocene, reaching a peak frequency of ~16% at approximately 19,000 cal yrs BP before disappearing from the faunal assemblages at approximately 14,000 cal yrs BP (Figure 4.2k). The species is absent from the faunal records during S1 and throughout the Holocene. This pattern corresponds well to observations by Geraga *et al*. (2005), who note peak abundances of this species at 18,000 cal yrs BP. *T. quinqueloba* is indicative of cool waters, and is tolerant of fairly low salinities and enhanced fertility in surficial waters (Figure 4.2l) (Geraga *et al.*, 2008). In core 964A, this species never exceeds frequencies of 1% in the late Pleistocene but displays a marked increase of ~5% at approximately 11,000 cal yrs BP prior to becoming almost non-existent in the Holocene.

4.4.2 Sea Surface Temperature Results

The SST results for 964A are presented in figure 4.3. The average annual SSTs are ~19°C, the average winter SSTs are ~15°C and the average summer SSTs are ~24°C. The lowest winter SST (10.99°C) is recorded at ~ 11,000 cal yrs. BP. The highest summer SST (26.25°C) is recorded at ~2,606 cal yrs BP (Figure 4.3).

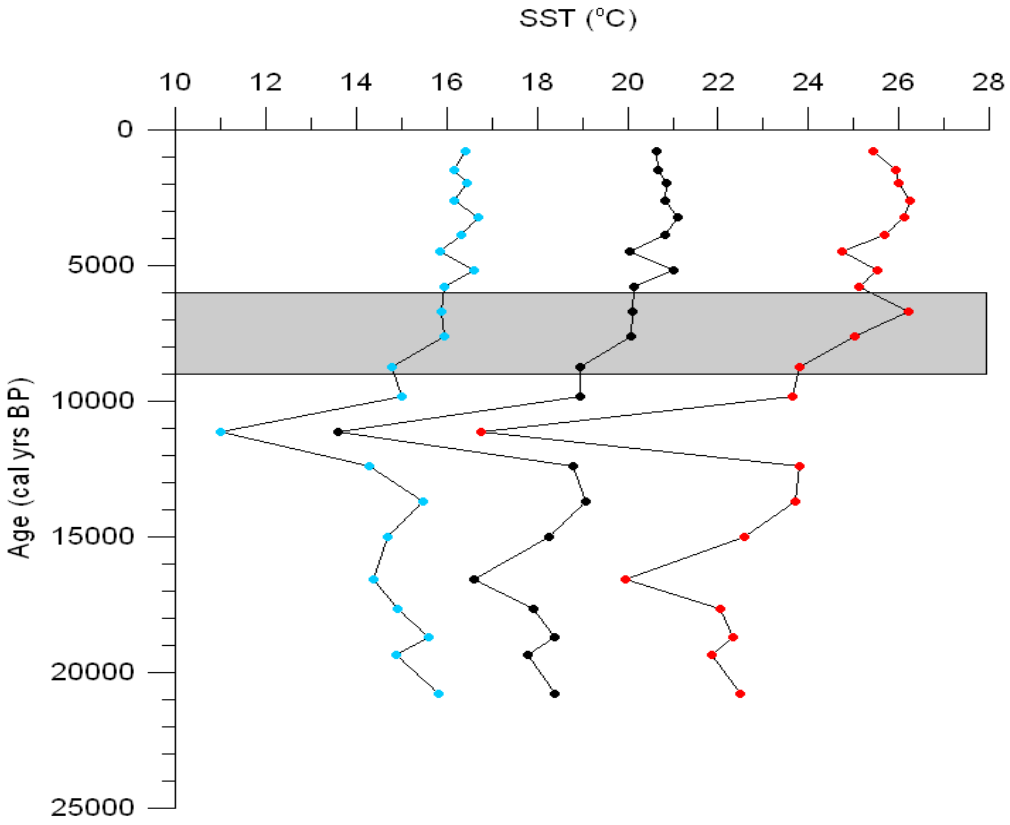

Figure 4.3: Graph depicting Late Quaternary SSTs for Core 964A. The graph is reconstructed from downcore variations in planktonic foraminiferal abundances utilising ANN and the calibration dataset of Hayes *et al.* (2005). The black line represents annual SSTs, the red line represents summer SSTs and the blue line represents winter SSTs. The grey shaded area represents S1 deposited between 9,000-6,000 cal yrs BP (Principato, 2003).

A general cooling is observed from the start of the record with annual temperatures decreasing by ~ 2°C by 17,000 cal yrs BP. Over the following 3,000 years average temperatures increased culminating at ~ 19°C at 13,000 cal yrs BP. A period of significant cooling occurred at ~11,000 cal yrs BP with annual temperatures decreasing by ~ 5.5°C. This decrease in temperature is more pronounced in the summer record. Coinciding with the present interglacial, from ~11,000 cal yrs BP temperatures increased abruptly to ~ 19°C. Since then a general trend of warming is evident throughout the remainder of the Holocene. This warming appears somewhat more pronounced during the deposition of S1, between 9,000 and 6,000 cal yrs BP, particularly in the summer SST record.

4.5 ODP Core 973A

4.5.1 Faunal Results

This section presents the planktonic foraminiferal assemblage results for core 973A. Here, the observed faunal record begins at 17,055 cal yrs BP (Figure 4.4). The planktonic foraminiferal faunal record is dominated by six distinct species. Of the warm water species, *G. ruber* (white) (Figure 4.4a) is the most dominant prevailing throughout the faunal record. This species is known to mainly dominate waters east of the Straits of Messina, frequently occurring as high as 69% (Cifelli, 1971). At ~16,000 cal yrs BP the percentage rate of this species dropped dramatically from ~30% to less than 5%. It increases again after approximately 2000 years. A subsequent increase culminates in high frequencies (~52%) at ~ 12,000 cal yrs BP. During S1, high concentrations of *G. ruber* are present, averaging ~47% with maximum abundances occurring at ~ 3,200 cal yrs BP and remaining the dominant species throughout the Holocene. An appearance of the species, *G. ruber* (pink) (Figure 4.4 a) is in response to warmer conditions in the early Holocene at approximately 8,000 cal yrs BP. There is a distinct presence of this species at ~5,500 cal yrs BP where it peaks at ~7%. This indicates that optimum temperature conditions prevailed after the deposition of S1 (Thunell, 1977; Rohling, 1993).

An interesting observation in this core is that *G. siphonifera, O. universa* and *G. sacculifer* are absent from the faunal record in the late Pleistocene. This correlates significantly with numbers of the same species discovered in core 964A. *G. siphonifera* and *G. sacculifer* (Figure 4.4b and e) increased to reach peak frequencies between ~4,000-5,000 cal yrs BP. *G. bulloides,* (Figure 4.4f) which is a eutrophic species and can survive in an environment where oxygen has been rapidly consumed (Principato, 2003), is one of the most common species in high productivity and upwelling zones (Fraile *et al*., 2008). Throughout this core, *G. bulloides* has a continuous but moderate presence throughout the faunal record. It never comprises more than 22% of the faunal assemblage and reached its peak at ~1000 cal yrs BP.

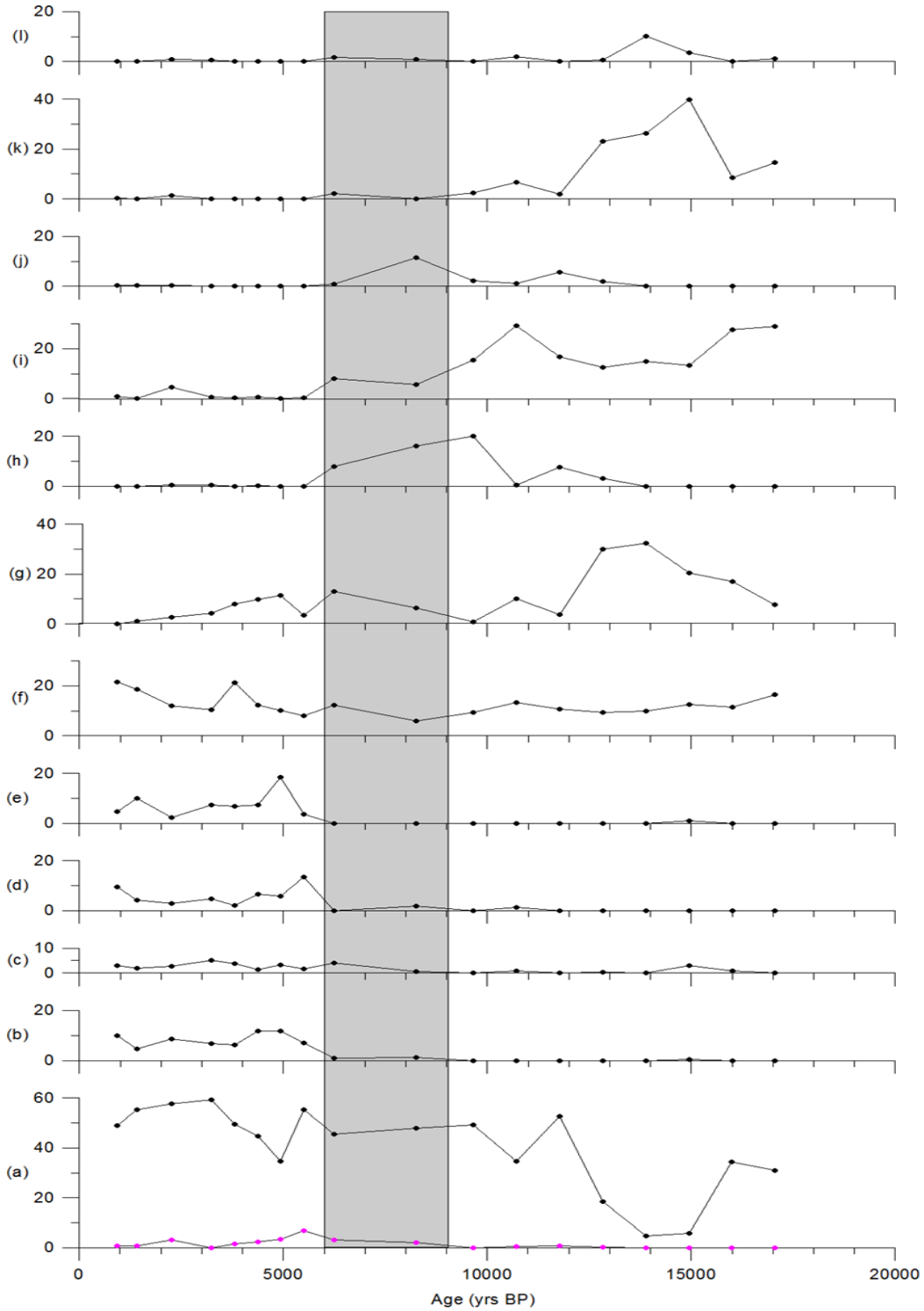

Figure 4.4: Planktonic foraminiferal relative faunal abundances (%) for core 973A. (**a**) = *G. ruber* (black line represents white variant, pink line represents pink variant), (**b**) = *G. siphonifera*, (**c**) = *G. rubescens*, (**d**) = *O. universa*, (**e**) = *G. sacculifer*, (**f**) = *G. bulloides*, (**g**) = *G. glutinata,* (**h**) = *G. inflata*, (**i**) = *N. pachyderma* (dextral), (**j**) = *G. truncatulinoides*, (**k**) = *G. scitula,* (**l**) = *T. quinqueloba*. The chronology for these faunal occurrences is based on ^{14}C AMS dating. The grey shaded area represents S1 (from 9,000-6,000 cal yrs BP) (Principato, 2003).

G. glutinata, (Figure 4.4g) is present in low densities and occurs in nutrient rich waters in the present-day Mediterranean (Pujol and Vergnaud Grazzini, 1995). However, in

core 973A, this species is more prevalent during the late Pleistocene where it reaches a peak of over 30% at ~14,000 cal yrs BP. A slight increase is observed towards the end of S1 before decreasing for the remainder of the late Holocene. Again, *G. glutinata* (Figure 4.4g) which thrives in colder waters shows similar traits to *N. pachyderma* (dextral) in that it dominates significantly in the late Pleistocene in core 973A. *G. inflata* is considered a cool water species however, this species displays a varied temperature tolerance (Cifelli, 1971) (Figure 4.4h). This species is non-existent in the faunal assemblage until approximately 13,000 cal yrs BP. It displays high concentrations (~20%) before the onset of S1 at ~10,000 cal yrs BP. This pattern has been interpreted as the onset of modern-day hydrographic conditions by Ariztegui *et al.* (2000). *G. inflata* gradually decreases after the deposition of S1 before tapering off to almost non-existent in the late Holocene. Similar to core 964A, this disappearance can be attributed to a lack of mixing in the water column and this is a pattern which corresponds well to that observed by Ariztegui *et al.* (2000). While *N. pachyderma* (dextral) normally dominates assemblages of planktonic foraminifera in polar and sub-polar eutrophic zones a general consistency in the fluctuations of this species has been observed during the Pleistocene within this core (Ufkes *et al*., 2000). It increases to just over 29% at ~17,000 cal yrs BP and again at ~10,000 cal yrs BP. *N. pachyderma* (dextral) are virtually absent in the sapropel sediments of this core. The species are more prevalent in the glacial sediments. *G. truncatulinoides* (Figure 4.4j) only make minor contributions to the foraminiferal faunal assemblage in core 973A. This species is generally scarce in the eastern Mediterranean and this pattern corresponds well with that observed in core 964A (Cifelli, 1971). This species' presence in the late Pleistocene is non-existent but exhibits an increase in S1, peaking at ~8,000 cal yrs BP with ~11%. Furthermore, *G. scitula* has a similar pattern within the foraminiferal faunal assemblage of core 973A, occuring at frequencies of less than 2%. *G. scitula* reached high frequencies of between 20-40% within the late Pleistocene, while occurring at frequencies of less than 2% during the Holocene (Figure 4.4k). Finally, another cold water species, *T quinqueloba*, is the least abundant species in this core but demonstrates high frequencies of ~10% at approximately 14,000 cal yrs BP before declining to almost non-existent in the Holocene (Figure 4.4l).

4.5.2 Sea Surface Temperature Results

The SST results for 973A are presented in Figure 4.5. The average annual SSTs are ~19°C, the average winter SSTs are ~15.48°C and the average summer SSTs are

~23.28°C. The lowest winter SST (12.71°C) is recorded at ~13,886 cal. yrs. BP. The highest summer SST (26.34°C) is recorded at ~4,938 cal. yrs. BP. The highest annual SST average (~26°C) is at ~5,000 cal yrs BP and the lowest (~14°C) is at ~17,000 cal yrs BP.

Beginning at ~ 17,000 cal yrs BP, annual SSTs illustrate a significant decrease (~ 5°C) culminating in the lowest recorded SSTs at ~ 14.000 cal yrs BP. This decrease appears more pronounced in the summer record. A return to warmer temperatures (~ 19°C) ensues in the following 4,000 yrs punctuated briefly by a minor cooling episode (~ 2°C) centred at ~ 11.000 cal yrs BP A notable peak (3°C) in SST occurs after the termination of S1 before returning to average annual SSTs of ~ 20°C for the remainder of the Holocene.

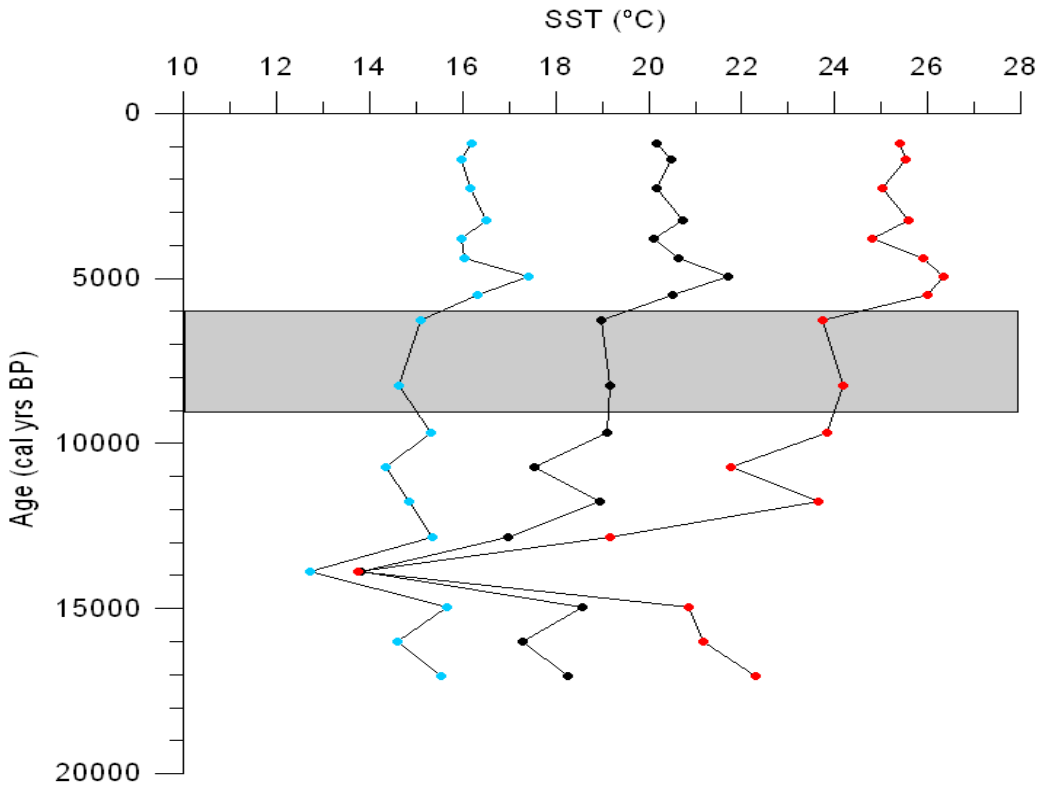

Figure 4.5: Graph depicting Late Quaternary SSTs for Core 973A. The graph is reconstructed from downcore variations in planktonic foraminiferal abundances utilising ANN and the calibration dataset of Hayes *et al*. (2005). The black line represents annual SSTs, the red line represents summer SSTs and the blue line represents Winter SSTs. The grey shaded area represents S1 deposited between 9,000-6,000 cal yrs BP (Principato, 2003).

4.6 ODP core 969A

4.6.1 Faunal Results

This section presents the planktonic foraminiferal assemblage results for core 969A

(Figure 4.6). Although there is no established chronological record for this core, one ^{14}C AMS date and the occurrence of S1 allows a basic interpretation of the timeframe involved. The Quaternary planktonic foraminiferal faunal record is dominated by six distinct species. Similar to the other two cores, 964A and 973A, *G. ruber* (white) (Figure 4.6a) is the most dominant species prevailing throughout the faunal record. High concentrations of this species (20-66%) are evident throughout the faunal record. This species is more abundant in tropical and sub-tropical oligotrophic waters. *G. ruber* (pink) (Figure 4.6a) shows a moderate presence and similar to the other two cores, this species appears in low percentages in the late Pleistocene until approximately at 32.5cm in depth where it exhibits a marked increase reaching frequencies of ~16% (Figure 4.6a). In all three cores, 964A, 973A, and 969A, *G. siphonifera, G. rubescens, O. universa* and *G. sacculifer* show little or no presence during the late Pleistocene. These warm species exhibit a clear but moderate presence during the Holocene ranging from ~17-70%. *G. siphonifera* reaches its peak (~14%) after the termination of S1 at approximately 18.5cm (Figure 4.6b). *G. rubescens* (Figure 4.6c), while showing almost similar traits to *G. siphonifera* and *G. sacculifer*, has a weak presence in the late Pleistocene until it exhibits an increase in frequency at 28.5cm reaching ~13%. *O. universa* is virtually non-existent throughout the faunal record of the late Pleistocene until approximately at 48.5cm where it begins to show a weak presence throughout the remainder of the faunal record with frequencies of >6% (Figure 4.6d). *G. sacculifer,* the tropical species, is absent from the assemblage in the late Pleistocene until ~10,000 cal yrs BP after which it reaches a high frequency of ~17% at 22.5cm in depth (Figure 4.6e). There is a distinct presence of this species throughout the Holocene. Low abundances of this species are observed throughout the late Holocene and it never reaches more than 6%. *G. bulloides* (Figure 4.6f) was especially well developed in core 969A, reaching a peak frequency of 16% in the Pleistocene. Similar to *G. ruber*, this species prevailed throughout the core. *G. glutinata* (Figure 4.6g) dominates the Pleistocene before reaching frequencies of ~20% at ~10,000 cal yrs BP (34.5cm). However, it remains less significant in the late Holocene (>9%), but compares well to the same species observed in cores 964A and 973A.

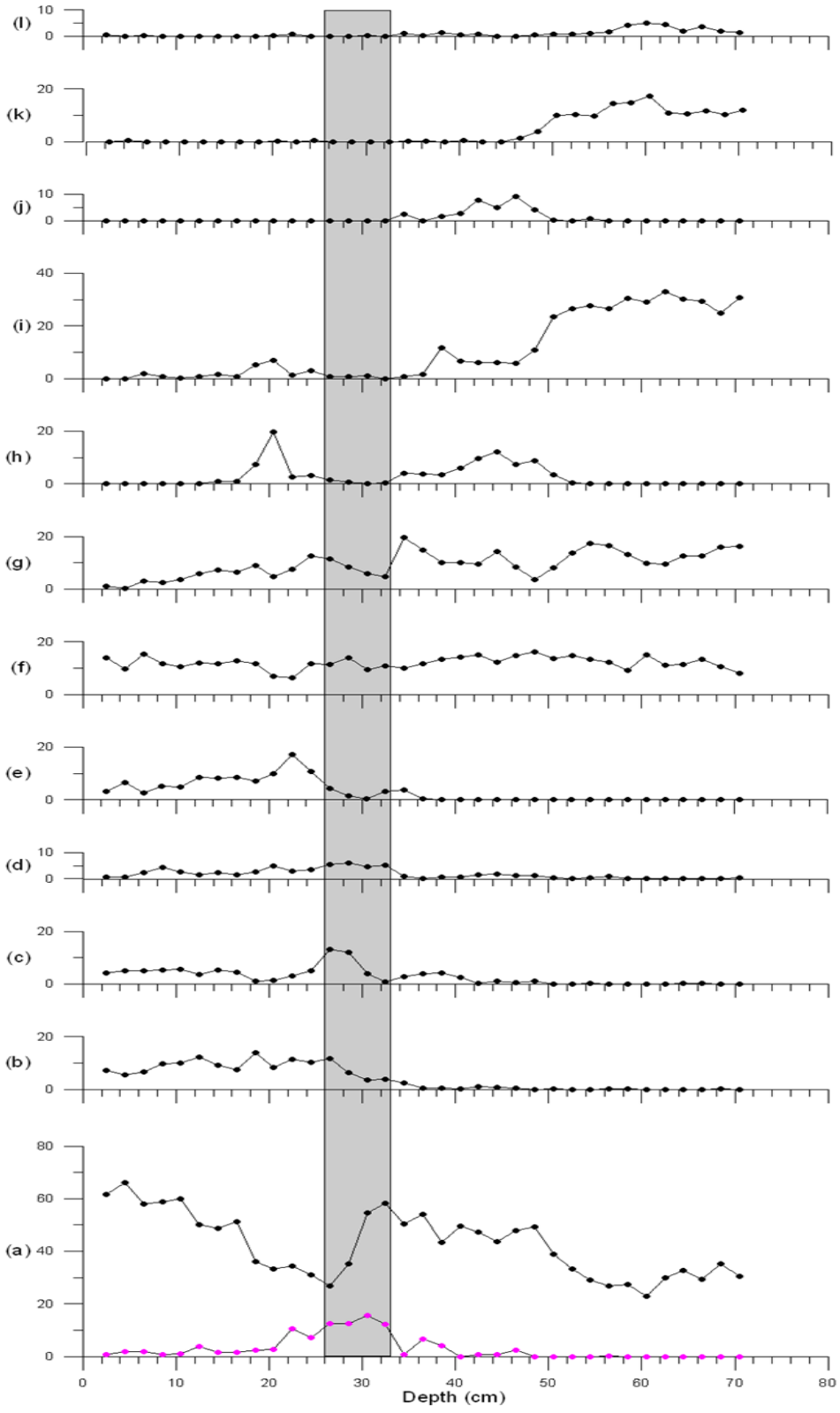

Figure 4.6: Planktonic foraminiferal relative faunal abundances (%) for core 969A. (a) = *G. ruber* (black line represents white variant, pink line represents pink variant), (b) = *G. siphonifera*, (c) = *G. rubescens*, (d) = *O. universa*, (e) = *G. sacculifer*, (f) = *G. bulloides*, (g) = *G. glutinata,* (h) = *G. inflata*, (i) = *N. pachyderma* (dextral), (j) = *G. truncatulinoides*, (k) = *G. scitula,* (l) = *T. quinqueloba*. The grey shaded area represents S1 deposited between from 9,000-6,000 cal yrs BP (Principato, 2003).

Another cool water species, *G. inflata* (Figure 4.6h) had two dramatic increases, one in

the Pleistocene of ~12% and one in the Holocene of almost 20% at 20.5cm This species is virtually absent in S1 (Figure 4.6h). The eutrophic *N. pachyderma* (dextral) (Figure 4.6i) has a continuous presence throughout the late Pleistocene reaching frequencies of ~30%. A marked decrease in this species is obvious at 46.5cm where it continues to show a consistent but weak presence for the remainder of the faunal record. This species disappears from the assemblage at 4.5cm. *G. truncatulinoides* (Figure 4.6j) only makes minor contributions to the faunal assemblage, while *G. scitula* exhibits high frequencies in the late Pleistocene (~17%) at 60.5cm before tapering off at 48.5cm to almost non-existent throughout the remainder of the Holocene record (Figure 4.6k).

4.6.2. Sea Surface Temperature Results

The SST results for 969A are presented in Figure 4.7. The average annual SSTs are ~18°C, the average winter SSTs are ~15.°C and the average summer SSTs are ~24°C. The lowest winter SST (~14°C) is recorded at 54.5cm. The highest summer SST (~26°C) is recorded at ~25cm. The highest annual average SST is 22~°C at ~19cm and the lowest (~17°C) is recorded at 55.5cm The SST record for core 969A displays a general cooling trend from the start of the record culminating in the lowest recorded annual SSTs (~ 15°C) at 54.5cm. A subsequent abrupt increase in temperatures is observed, with summer temperatures increasing from 20°C to 24°C. The highest SSTs are recorded just after the termination of S1 before returning to average annual temperatures of ~ 20°C for the remainder of the Holocene.

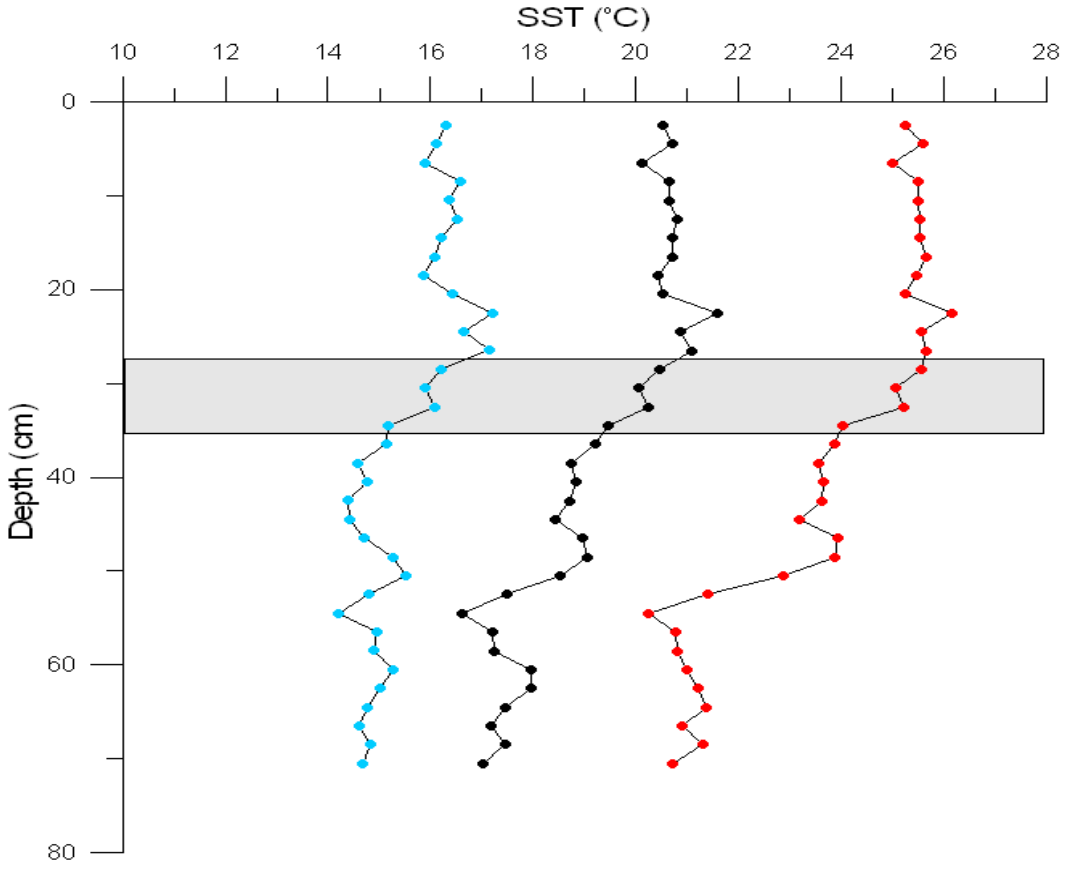

Figure 4.7: Graph depicting Late Quaternary SSTs for Core 969A. The graph is reconstructed from downcore variations in planktonic foraminiferal abundances utilising ANN and the calibration dataset of Hayes *et al*. (2005). The black line represents annual SSTs, the red line represents summer SSTs and the blue line represents winter SSTs. The grey shaded area represents S1 deposited between 9,000-6,000 cal yrs BP (Principato, 2003).

Chapter 5: Discussion

5.1 Introduction

It is now widely acknowledged that palaeoenvironmental reconstruction utilising foraminifera relies on the assumption that assemblages mirror the environment at the time of deposition.Visual inspection of downcore compositional changes in planktonic foraminiferal assemblages facilitates a palaeoenvironmental reconstruction of the Ionian Sea during the late Quaternary period. The observed faunal records consists of 13 species (Figures 5.2, 5.4, 5.6), only the faunal signatures of those that exhibit significant trends will be discussed in this chapter. The Ionian Sea palaeoenvironmental reconstruction allowed the presentation of four distinct time frames, the late Pleistocene (~20,000-13,000 cal yrs BP), the glacial/interglacial transition (~13,000-9,000 cal yrs BP), Sapropel 1 (~9,000-6,000 cal yrs BP) and the late Holocene (~6,000 to present cal yrs BP). Each individual sample taken from the cores was 1cm in thickness and represents approximately ~220 cal yrs BP in core 964A and ~180 cal yrs BP in core 973A. There is no evidence for the '8.2 ky BP event' in all three cores studied, potentially this climatic event should be evident as its duration was ~150 years. Therefore, as the sampling resolution was every 4cm in cores 964A and 973A, it is likely that the event was missed. Only major, multi-decadal events can be identified in this palaeoenvironmental reconstruction. Available proxy data and model simulations frequently suggest that the '8.2 ky BP event' has registered stronger in the high to middle latitudes around the North Atlantic Ocean as a result of colder, drier conditions (Pross *et al*., 2009).

This chapter will also discuss the relevance of other studies in regard to the results of this research.

5.1.1 Late Pleistocene Interval (~20,000-13,000 cal yrs BP)

A general consistency in the fluctuation of cold water species is observed in the faunal assemblages from the Ionian Sea during the late Pleistocene. The reconstructed SST record for this interval in both 964A and 973A show a cooling episode at ~ 17,000 cal yrs BP that may be associated with Heinrich event 1. This is harder to determine in core 969A due to a lack of a definitive age model. Emeis *et al*. (2000) estimated that SSTs were between 13-9°C in the Ionian Sea during this interval. This contrasts with this research which estimates annual average temperatures to be between 19-14°C. Possible dating errors can be observed in the cores, for example, the minimum temperature inferences in cores 964A (~11,000 cal yrs. BP) and 973A (~14,000 cal yrs. BP) and at

~55cm in 969A are thousands of years apart but are likely the same climatic event, The Younger Dryas. Consequently, the faunal assemblages are dominated by cold water species such as *N. pachyderma* (dextral), *G. scitula* and *T. quinqueloba*, reflecting these cold glacial conditions. *N. pachyderma* (dextral) is known to be associated with cool eutrophicated waters and the occurrence of a Deep Chlorophyll Maximum (Thunell, 1978; Pujol and Grazzini, 1995; Geraga *et al*., 2005). In addition, this species reflects significant productive surface conditions as a result of a high terrestrial input (Triantaphyllou *et al*., 2009). Both *G. scitula* and *T. quinqueloba* are indicative of cool subpolar waters and as such reflect the intensification of cold, glacial conditions at this time. In addition *T. quinqueloba,* a eurythermal species, is known to proliferate during the spring in association with diatom blooms (Sauter and Thunell, 1991; Stefanelli *et al*., 2005). However, this species only makes a minor contribution (~5%) to the faunal record in core 969A and has a moderate peak of ~10% at approximately 14,000 cal yrs BP in core 973A. Although the late Pleistocene is characterised by cool temperatures, *G. ruber*, a warm water species, displays significant frequencies throughout the interval. Research undertaken by Numberger *et al*. (2009) in the eastern Mediterranean also found an abundance of *G. ruber* during the late Pleistocene. They attributed the presence of this species to different habitat preferences due to different morphotypes of *G. ruber* (white) in the eastern Mediterranean Sea. Other studies have indicated that this warm, shallow dwelling species (0-50m) tends to be abundant at the end of the summer months when surface waters are well stratified (Pujol and Vergnaud-Grazzini, 1995; Stefanelli *et al*., 2005). It has also been identified in low salinity waters. During the late Pleistocene, *G. bulloides* has an average relative abundance of ~17% in all three cores. Thunell (1978) emphasised that *G. bulloides* is present in surface sediments throughout the entire Mediterranean Basin. However, the warmer, more saline eastern basin is defined by an observed reduction (5-20%) of this temperature dependent species, with the lowest percentage of this species located where summer sea surface temperatures reach 25-26°C (Thunell, 1978). *G. glutinata* is one of the most ubiquitous species within the Mediterranean Sea, accounting for less than 5% of surface faunal assemblages (Thunell, 1978).

The interval between ~15,000-13,000 cal yrs BP corresponds to the Bölling/Alleröd and is synchronously recognised in the central and eastern Mediterranean Sea. This interval is characterised by temperate warm water species (Rouis-Zargouni *et al*., 2009). The high abundance of *G. ruber* and to a lesser degree, *G. rubescens* reflects this warming interval. High frequencies of *G. ruber* (white)

(~47%) are observed in core 964A during this time while *G. rubescens* only makes minor contributions (~1-3%) to the faunal assemblages in the three studied cores.

5.1.2 Glacial/ Interglacial Transition (~13,000-9000 cal yrs BP)

The reconstructed SST record for this interval illustrates an increase in temperatures An abrupt increase in temperature is observed in cores 964A and 973A at ~14,000 cal yrs BP, with annual average temperatures of between 17-16°C (Figures 4.3, 4.5). Glacials are characterised by cold polar conditions with interglacials reflecting generally warmer, drier conditions. The last glacial-interglacial transition (13,000-9,000 cal yrs BP) was characterised by many climatic fluctuations. Following deglaciation at the termination of the last cold stage (~14,000 cal yrs BP), temperatures were comparable to the present day (Turney *et al*., 2008). An abrupt cold climatic event known as the Younger Dryas, occurred at approximately 12,500-11,500 cal yrs BP. This has been defined and accelerated by the readvancement of glaciers in the Northern Hemisphere (Turney *et al*., 1998). A warming period ensued post 11,500 cal yrs BP.

In core 964A and during this glacial-interglacial interval, *G. ruber* (white) dominates the faunal assemblage but shows an abrupt decrease at ~11,000 cal yrs BP, going from ~40% to ~12% in core 964A (Figure 5.2) but has high frequencies of over 40% in the other two cores throughout the faunal record. The appearance of *G. ruber* (pink) at ~12,000 cal yrs BP with a low 2% implies maximum warm temperatures. Similarities occur within the three cores in relation to the appearance of *G. ruber* (pink) with percentages of less than 1% evident in cores 973A and 969A. Similar to *G. ruber* (white) this species disappears at ~11,000 cal yrs BP in core 964A. Interestingly, the lowest winter SST (10.99°C) is recorded at ~11,000 cal yrs BP in core 964A. This decrease in fluctuation of *G. ruber* (white and pink) may suggest that the species are temperature controlled. Pujol and Vergnaud-Grazzini (1995) have acknowledged that the eastern basin with its oligotrophic conditions promotes an increase in predatory foraminiferas such as *G. ruber* (white and pink). In modern day environments this species will prevail where summer surface temperatures exceed 24°C and will peak in a well stratified water column (Thunell, 1978). *G. bulloides* and *N. pachyderma* (dextral) have peaks of 25% and 37% respectively in this Ionian core. *G. bulloides* generally resides in sub-polar waters but can show significant increase in the Mediterranean Sea in winter and during episodes of high fertility while *N. pachyderma* (dextral) is known to favour cooler water temperatures (Fairbanks and Wiebe, 1980; Stefanelli *et al*., 2005). In core 973A, *G. bulloides* and *N. pachyderma* (dextral) show similar trends

with both species displaying between ~10-17%. The cool temperate water species *G. truncatulinoides* makes an abrupt entry into the faunal assemblage with a peak of 11% at ~12,000 cal yrs BP before becoming non-existent in the faunal record. This contrasts considerably with core 973A in that the species peaks after this transition interval. We know from modern day environments that this species prevails in winter assemblages in the Ionian basin, preferring a well-mixed water column (Pujol and Vergnaud-Grazzini, 1995). In core 969A, this species makes minor contributions to the faunal record but moreover, it only makes its presence within this transition period. This species infers changing climatic conditions, with sinistral forms reflecting warm conditions and dextral forms indicating cooler conditions.

The Younger Dryas is a well-defined climatic cooling episode that occurred between 12,800-11,500 cal yrs BP. It is thought that this interval is represented by the lowest SSTs (~14°C) in both cores 964A and 973A (Figure 4.3, 4.5). This significant cooling interval is well reflected by the dominance of the sub-polar species *N. pachyderma*. In modern day environments an abundance of *N. pachyderma* is indicative of the presence of a Deep Chlorophyll Maximum (DCM) (Sprovieri *et al*., 2003). Presently, this species exists where winter SSTs are less than 13.5°C (Thunell, 1978). At ~10,000 cal yrs BP *N. pachyderma* illustrates a decrease in frequencies of approximately 30% in core 964A and by ~15% in core 973A. In core 969A this species decreases by ~10% at a depth of 36.5cm which may correspond to the end of the Younger Dryas. This abrupt decrease in frequencies coincides with the start of the warm current interglacial. *G. scitula* is present in the late Pleistocene until it exits at ~11,000 cal yrs BP; this again reflects the transition from glacial conditions to the warmer Holocene. The gradual increase in both *G. ruber* (white and pink) and the weak presence of *G. inflata* is indicative of a slow recovery of deep vertical mixing in the water column during winter (Sprovieri *et al*., 2003). This correlates with the results from cores 964A, 973A and 969A. Geraga *et al*. (2008) have also emphasised that this interval is characterised by a gradual increase of *G. ruber* (white) (up to 38%), and all three eastern Ionian Sea cores are in general agreement with this however, there are some discrepancies. *G. inflata* shows a weak presence in the three cores 964A and 969A during this cold event. It has been observed by Rouis-Zargouni *et al.* (2009) that an abrupt but brief increase in *G. inflata* of 5-40% occurred at the transition of the Younger Dryas and the Holocene. This is evident in core 973A but is not observed in cores 964A and 969A. *G. bulloides* is present in the three cores examined, though its frequencies are highly variable and so of little importance for correlation purposes, a

pattern which corresponds well to that observed by Hayes *et al*. (1999). The cooling of the Younger Dryas is also depicted by cool dinocyst species such as *Nematosphaeropsis labyrinthus* (35%). A maximum abundance of these species was observed by Rouis-Zargouni *et al*. (2009) which underpins an increase in nutrient supply. An increase of semi-desert vegetation is also recorded at this time, suggesting a dry climate (Fletcher *et al*., 2009; Rouis-Zargouni *et al*., 2009).

The early Holocene is characterised by the Climate Optimum between approximately 10,000-8,000 cal yrs BP, which precedes the deposition of S1. The reconstruction of SSTs depicts this warming interval more so in core 964A (Figure 4.3) where an abrupt increase in temperatures is evident. The air temperature in the mid-latitudes of the northern hemisphere is thought to have been 1-3°C higher than at present with significant change occurring in the atmospheric circulation system (Sbaffi *et al*., 2004). The onset is marked by the significant increase in warm water planktonic foraminiferal species. In this study, *G. ruber* (pink) displays a dramatic increase in cores 964A and 969A with frequencies of ~6% and ~12% respectively. Core 973A showed a low frequency of > 1%. This species is indicative of optimum warm conditions and the stratification of the water column (Principato *et al*., 2003). *G. ruber* (white) shows high frequencies between ~35-58% in all three Ionian Sea cores which again reflects warm conditions. Geraga *et al*. (2008) suggested that the sharp increase in the abundance of *G. ruber* (white) was the initiation of the formation of stratified waters. SSTs varied at the beginning of the Holocene but increased to 17-18°C during the formation of S1 which coincided with this Climatic Optimum (Principato *et al*., 2003). *G. rubescens* made their entry into the faunal record at this time in core 969A with ~4%, further cementing optimum climatic conditions. *G. inflata* peaked in core 973A with ~20% and had a moderate presence in cores 964A and 969A. *G. bulloides* and *N. pachyderma* show similar traits in all three cores with frequencies of between 10-20%. Rouis-Zargouni *et al*. (2009) have acknowledged that warming was at its strongest at ~10,000 cal yrs BP. This is further corroborated in pollen records which highlights the appearance of *Pistacia* in the Mediterranean forests at this time. Similarly the presence of warm dinocyst species such as *Impagidinium paradoxum* (5-10%) and *Impagidinium aculeatum* (10-25%) suggest a significant rise in winter temperatures (Rossignol-Strick., 1995; Watts et al., 1996; Rouis-Zargouni *et al*., 2009).

5.1.3 The formation and deposition of S1 (~9,000-6,000 cal yrs BP)

The sediments of the eastern Mediterranean Sea contain organic-rich distinctive layers which have been identified as sapropels (Thompson *et al*., 1999). The Holocene sapropel S1 (~9,000-6,000 cal yrs BP) can be dated by ^{14}C measurements which is precise and well calibrated. The deposition of this sapropel began during the Holocene Climatic Optimum which followed the cold Younger Dryas event (Principato *et al.*, 2003).

Planktonic foraminiferal sapropel assemblages are normally depicted by a peak in frequency of *G. ruber* (white) (Negri *et al*., 1999). An increase in this species has been observed in the Holocene in all faunal records throughout the entire Mediterranean Sea (Hayes *et al*., 1999; Geraga *et al*., 2005). This correlates especially well to core 964A where a peak abundance (~70%) of this species is evident. Cores 973A and 969A have also high frequencies of this species (~27-58 % and ~45-50%) respectively. An increase in the number of this species has been interpreted as an indicator of enhanced productivity in modern day oceanography. *G. ruber* (white) can survive in a wide range of temperatures but thrives in well stratified and oligotrophic waters (Pujol and Vergnaud-Grazzini, 1995; Geraga *et al.*, 2008). The beginning of S1 is marked not only by the increase in *G. ruber* (white) but also with an increase of *G. ruber* (pink) (Principato *et al*., 2003). The moderate frequency of this species displays a pattern which is consistent between the three Ionian Sea cores. *G. ruber* (pink) increases in abundance especially in core 969A with ~12-16% depicting optimum climatic conditions during the formation of S1. *O. universa,* another warm species, is known to frequent tropical to transitional zones, with its highest frequencies occurring in upwelling areas (Thunell, 1978), peaks at ~20% at ~6,600 cal yrs BP in core 964A. Core 969A has a low frequency of this species while the species is almost non-existent in core 973A at this time. It has been noted by the above authors that *O. universa* accounts for between 1-10% of the population over both the western and eastern basins with the exception of the north western basin and the Aegean Sea, the coolest regions within the Mediterranean Sea. *G. siphonifera* peaks at ~14% in core 964A and core 969A shows similar trends. *G. sacculife*r, which has strong temperature dependence, signifies a general warming period and indicates the possibility of a shallow pycnocline following a wet period and abundant runoff from the Nile (Principato *et al*., 2003). Thunell, (1978) has stated that this species is most abundant (5-10%) in the warm eastern basin where SSTs range between 23.5-26.5°C. *G. sacculife*r, is less frequent in regions associated with bottom water formation such as the Aegean Sea. A frequency

increase of this species is observed from west to east emphasising its temperature dependence (Thunell, 1978). The reappearance of *G. inflata* at the end of S1 suggests that the Ionian Sea became well ventilated at this time (Ariztegui *et al*., 2000). In the present day environment, this species has a preference for a cool, well mixed water layer with intermediate to high nutrient supply. In the three cores examined in this study, *G. inflata* had a moderate frequency of ~16% in core 973A, cores 964A and 969A showed similar traits of low frequencies throughout this interval. An increase in this species between 7,000-8,000 cal yrs BP has been interpreted as the beginning of modern hydrographic conditions (Ariztegui *et al*., 2000). *N. pachyderma* (dextral) which thrives today where SSTs are below 7°C was observed in low percentages throughout this interval in the cores examined. Ariztegui *et al*. (2000) noted that an absence of this species in both the Adriatic and Ionian assemblages indicated that a DCM could not develop. However, in contrast to this finding, *N. pachyderma* (dextral) is evident throughout the S1 interval in the Tyrrhenian records, suggesting contrasting oceanographic conditions between the western and eastern basins (Ariztegui *et al*., 2000). *G. truncatulinoides* has a peak frequency of ~9% in core 973A, the coiling direction of this species generally infers changing climatic conditions, sinstral forms being warm markers and dextral forms cold markers (Thunell, 1978). An abundance of this species shows the presence of a well-developed deep and cold mixed layer (Principato *et al*., 2003). Mixed deciduous forests and an increase in aquatic palynomorph contents have indicated a humid climate prevailing during this interval (Triantaphyllou *et al*., 2009). Abrupt decreases of warm micro fauna and microflora was observed and pollen data indicating forest decline has been noted at ~8,200 cal yrs BP, suggesting a short cold and dry period interrupting this warm interval (Fletcher *et al*., 2009; Rouis-Zargouni *et al*., 2009).

5.1.4 The Late Holocene (6,000 cal yrs to present)

SST reconstruction clearly indicates that the Holocene is defined by climatic instability. The highest SSTs are recorded just after the termination of S1 before returning to average annual temperatures of ~20°C for the remainder of the Holocene in core 969A (Figure 4.6). Again in core 973A, a notable peak (3°C) in SST occurs after the termination of S1 before returning to average annual SSTs of ~ 20°C for the remainder of the Holocene. This interval is mainly dominated by warm water planktonic foraminiferal species. In core 964A, warm water species are in abundance, *G. ruber* (white) decreases after the termination of S1 at ~6,000 cal yrs BP to frequencies of

~30% but increases again at approximately 3,000 cal yrs BP to over 60%. Core 969A correlates well with this finding and in both cores, this species reaches over 60% at ~1000 cal yrs BP. *G. ruber* (pink) peaks at ~10% at ~6,000 cal yrs BP. In core 973A a similar pattern is evident. *G. ruber* (white) decreases at ~5,000 cal yrs BP to ~35% and *G. ruber* (pink) has a moderate peak of ~10% at ~5,500 cal yrs BP before decreasing to low frequencies throughout the late Holocene. *G. ruber* (pink) decreases at ~5000 cal yrs BP in all three cores, possibly depicting cooler climatic conditions. Geraga *et al*. (2005) has concluded that during the Holocene, *G. ruber* (white) remains the most abundant species (>20%) in the faunal records. This data indicate that during the late Holocene, surface waters in the eastern Mediterranean Sea were dominated by an oligotrophic mixed water layer (Ariztegui, *et al*., 2000).

Other minor warm planktonic indicators in the three cores are: *G. siphonifera, G. sacculifer, G. rubescens,* and *O. universa. G. siphonifera* has similar traits in cores 964A and 973A with peaks of ~12-14% at ~5,000 cal yrs BP. In core 969A, at 18.5cm (~4,200 cal yrs BP) this species had the highest peak of ~14% in the faunal assemblage. A low frequency (>10%) of this species is evident throughout the remainder of the late Holocene in all three cores investigated. *G. sacculifer*, which is frequent in the warm eastern basin occurs where an oligotrophic mixed water layer exists (Ariztegui *et* al., 2000). In cores 964A, 973A and 969A, this species has high peaks (14-19%) at similar times of ~5,000 cal yrs BP. This high occurrence of *G. sacculifer* may signify a new run-off stage when anoxic conditions were still prevailing in the eastern Mediterranean Sea (Principato *et al*., 2003). *G. rubesce*ns is present in all three cores at low frequencies (1-6%) throughout the late Holocene. *O. universa*, a species associated with tropical to transitional zones and indicative of warm conditions, is evident in low abundances (~1-10%) throughout the faunal record in the three Ionian cores. Geraga *et al*. (2008) have observed high percentages of this species throughout the Holocene record. The appearance of *N. pachyderma* (dextral) and *G. inflata* and the increasing trend in the abundance of *G. glutinata* with the decreasing trend in the abundance of some warm water species, signifies the prevalence of cold, well mixed, nutrient-rich waters in winter over warm, well stratified and oligotrophic waters in summer. This seasonal contrast has been accounted for in all Adriatic Sea records (Geraga *et al.*, 2008). At ~5,000 cal yrs BP in cores 964A and 973A, *G. glutinata* has high peaks of (~17 and 11% respectively) before decreasing to low values throughout the late Holocene. A similar trend is observed in 969A with ~13% at 22.5cm preceding a decrease for the remaining faunal record of this core. It has been noted that at ~5,000

cal yrs BP, a wetter phase in the mid-Holocene occurred, lake and precipitation levels were higher. Precipitation levels rose to >500mm/yr at ~4,800 cal yrs BP (Frumkin *et al*., 1994; Robinson *et al*., 2006). However, records from the Mediterranean do not correlate with this. *N. pachyderma* (dextral) and *G. inflata* disappeared in the Adriatic Basin during the late Holocene and decreased in the Tyrrhenian Sea assemblages (Ariztegui *et al.*, 2000). This correlates with the findings in the three Ionian cores where low frequencies of these two species are observed during this interval. Rouis-Zargouni *et al*. (2009) has concluded that *G. inflata* increased from 10 to 30% in the central Mediterranean and was the dominant species from 6,500 cal yrs BP onwards in the Holocene. This greatly contrasts with the three Ionian cores examined in this research. A rapid and temporal increase of *G. inflata* after the termination of S1 is observed in most east Mediterranean cores (Geraga *et al*., 2005). In core 969A, a high spike of this species is evident (~20%) at ~5,000 cal yrs BP and at a depth of 20.5cm is visible. A similar trend in 964A is obvious with a peak of ~11% at ~5,000 cal yrs BP while core 973A has low frequencies throughout the faunal assemblage of the late Holocene. In core 973A, *G. bulloides*, has a high peak of ~20% at approximately 1,000 cal yrs BP. In core 964A the species has increased by ~4% at 1,000 cal yrs BP and in core 969A the species has a frequency of ~14% at this time. In present day environments the presence of this species indicates sub-polar water masses, upwelling areas, strong seasonal mixing and freshwater inputs (Lourens *et al*., 1994, Geraga *et al*., 2005).

In conclusion, the results from the three Ionian cores show a minor level of association when compared to other studies. It is somewhat apparent that the distribution patterns influence the palaeoenvironmental characteristics in the area where the species reside.

Chapter 6: Conclusions and Further Work

6.1 Conclusions

The primary aim of this research was to investigate Late Quaternary palaeoenvironmental change in the Ionian Sea. A variety of techniques were utilised to achieve this aim. A biostratigraphical description and interpretation of palaeoenvironmental change in the Ionian Sea, using Planktonic foraminiferal analyses was generated. The chronology of all palaeoenvironmental change was established by this research and validated by ^{14}C-AMS dating. SST reconstruction was employed, based on the use of ANN and the calibration dataset of Hayes *et al*. (2005).

This research distinctly illustrates evidence of palaeoenvironmental change during an interval of previously considered climatic stability. The palaeoenvironmental reconstruction of this research divides this time frame (~20,000-to present) into four distinct intervals. The late Pleistocene (~20,000-13,000 cal yrs BP) is depicted by cool temperatures and a mixed water column prevailing in the Ionian Sea. This is intercepted by the warmer Bölling/Alleröd and a rise in sea surface temperatures may have been evident at the termination of this event. The glacial-interglacial transition (~13,000-9,000 cal yrs BP) is characterised by rising temperatures comparable to the present day. The cooling of the Younger Dryas is revealed by the abundance of cool water planktonic foraminifera, cool dinocyst species and an increase in semi-desert vegetation during this event. The onset of the Holocene is marked by a general warming and the abundances of warm dinocyst and planktonic foraminiferal species. Optimum warm conditions at approximately 10,000 cal yrs BP is evident with the appearance of *G. ruber* (pink), this species also indicates the stratification of the water column. The reconstruction of the formation and deposition of S1 (~9,000-6,000 cal yrs BP) suggests a warm interval underpinned by the abundance of *G. ruber* (white) and an increase in *G. ruber* (pink). The increase in abundance of this species represents further evidence of water column stratification. A humid interval is evident by the presence of mixed deciduous forests and aquatic palynomorph contents. Finally, the reconstruction of the late Holocene (~6,000-to present cal yrs BP), is defined by a general warming

period superimposed on this are the rapid climatic fluctuations. The presence of warm water planktonic foraminiferal species and the dominance of *G. ruber* during this interval suggests warm temperatures and an oligotrophic mixed water layer in the Ionian Sea during this interval.

Interestingly, comparison of our biostratigraphical results shows some association with other eastern Mediterranaen studies, suggesting that planktonic foraminiferal analyses can be considered relevent in relation to a basin-wide scale. Palaeoenvironmental and hydrographical characteristics of a region underpins the abundance distribution patterns of planktonic foraminiferal organisms. SST graphs produced by this research show significant late Quaternary variability. There is ample evidence of cooling in the late Pleistocene and a general warming in the Holocene.

6.2 Further Work

6.2.1 Recommendations for further work

During the course of this research, some areas where further work would be advantageous were distinguished.

1. ^{14}C-AMS dates could be produced and utilised in all the examined cores, in particular to core 969A where only one ^{14}C-AMS is available. This would provide a more authentic chronological framework.

2. The application of Oxygen isotope analyses on all three cores would provide more information in obtaining a more accurate chronological framework.

3. Additional eastern Mediterranean cores could be examined for correlation purposes.

Bibliography

Ariztegui, A. Asioli, J. J. Lowe, F. Trincardi, L. Vigliotti, F. Tamburini, C. Chondrogianni, C. A. Accorsi, M. Bandini Mazzanti, A. M. Mercuri, S. Van der Kaars, J. A. McKenzie, F. Oldfield. 2000. Palaeoclimate and the formation of S1: inferences from Late Quaternary lacustrine and marine sequences in the central Mediterranean region. *Palaeogeography, Palaeoclimateology, Palaeoecocology,* Vol. 158: 215-240.

Armstrong, H. A. and M. D. Brasier. 2005. Microfossils-Second Edition. London: Blackwell Publishers.

Bard, E., F. Rostek and G. Ménot-Combes. 2004. Radiocarbon calibration beyond 20,000 ^{14}C yr B.P. by means of planktonic foraminifera of the Iberian Margin. *Quaternary Research,* Vol. 61: 204-214.

Baudin, F., N., Combourieu-Nebout and R. Zahn. 2007. Signatures of rapid climatic changes in organic matter records in the western Mediterranean Sea during the last glacial period. *Bulletin de la Societe Geologique de France*, Vol. 178(1): 3-13.

Bé, A. W. H. 1969. Planktonic foraminifera in distributions of selected groups of marine invertebrates in waters south of 35° S latitude: Antarctic Map Folio Service, *American Geographical Society*, Folio 11: 9-12.

Bé, A. W. H. and Tolderlund, D. S., 1971. Seasonal distribution of planktonic foraminifera in the western North Atlantic. *Micropaleontology, Vol.*17: 297-329.

Bé, A. H. W. 1977. 'An ecological, zoogeographic and taxonomic review of recent planktonic foraminifera', in Ramsay, A. T. S., (eds) Oceanic Micropalaeontology. London: Acedemic Press.

Beavington, S. J. and P. A. Racey. 2004. Ecology of extant nummulitids and other

larger benthic foraminifera: applications in palaeoenvironmental analysis. *Science Direct*, Vol. 67: 219-265.

Bell M., and M.J.C. Walker. 2005. Late Quaternary Environmental Change-physical and human perspectives-Second Edition. Glasgow: Prentice Hall.

Birks, H. J. B., Heiri, O., Seppä, H, and Bjune, A. 2010. Strengths and weaknesses of quantitative climate reconstructions based on Late-Quaternary biological proxies. *Open Ecology Journal,* Vol 3: 68-110.

Boscolo, R., and H., Bryden. 2001. Causes of long-term changes in Aegean sea deep water. *Oceanologicaacta*, Vol. 24: No. 6, 519-527.

Bradley, R. 1999. Paleoclimatology: Reconstructing Climates of the Quaternary. Second Edition. London: Elsevier.

Broecker, W. S., 2000. Was a change in thermohaline circulation responsible for the Little Ice Age? *Proceedings of the National Academy of Sciences of the United States of America,* Vol. 97: 1339-1342.

Cacho, L., J. O. Grimalt, M. Canals, L. Sbaffi, N. J. Shackleton, J. Schonfeld, and R. Zahn. 2001. Variability of the western Mediterranaen Sea surface temperature during the last 25,000 years and its connection with Northern Hemisphere climatic changes. *Palaeoceanography*, Vol. 16: 40-52.

Calvert, S.E. 1983. Geochemistry of the Pleistocene sediments from the eastern Mediterranean. *Oceanologica* Acta, Vol. 6: 255-267.

Campins, J., A. Jansá and A. Genovès. 2006. ThreDimensional structure of western Mediterranean cyclones. *International Journal of Climatology*, Vol. 26: 323-343.

Capotondi, L., A. M. Borsetti and C. Morigi. 1999. Foraminiferal ecozones, a high resolution proxy for the late Quaternary biochronology in the central Mediterranean Sea. *Marine Geology*, Vol. 153: 253-274.

Cita, M. B., M. A. Chienici, G. Ciarupo, Z. M. Moncharmont, S. D'Onofrio, S. Ryan,

and R. Scorziello. 1973. Quaternary record in the Ionian and Tyrrhenian basins of the Mediterranaen Sea. Initial Report Represents Deep Sea Drilling Project, Vol. 13:1263-1339.

Cheney, R.E. and R.A. Doblar.1982. Structure and variability of the Alboran Sea frontal system. *Journal of Geophysical Research*, Vol. 87: 585-594.

CIESM. 2012. (Online) Turbidite systems and deep-sea fans of the Mediterranean and the Black seas. Ciesm Workshop Series, No.17 120 pages, Monaco. www.ciesm.org/publications/BucharestO2.pdf (accessed on 30.10.12)

Cifelli, R., 1971. On the temperature relationships of planktonic foraminera. *Journal of Foraminiferal Research*, Vol. 1: No. 4: 170-177.

Cifelli, R., 1974. Planktonic foraminifera from the Mediterranaen and adjacent Atlantic waters (Cruise 49 of the Atlantis 11, 1969). *Journal of Foraminiferal Research*, Vol. 4: No. 4: 171-183.

Cita, M.B., and G. Alosi. 2000. Deep-sea tsunami deposits triggered by the explosion of Santorini (3500y BP), eastern Mediterranean. *Sedimentary Geology,* Vol. 135: 181-203.

Climap. 1976. The surface of the Ice-Age Earth. *Science*, Vol. 191: 1131-1137.

Comas, M.C., R. Zahn, and A. Klaus. 1996. Proceedings of the Ocean Drilling Programme. *Initial Reports*, 161.

Cramp, A., M. Collins, and R. West. 1988. Late Pleistocene-Holocene sedimentation in the NW Aegean Sea: A palaeoclimatic palaeoceanographic reconstruction. *Palaeogeography, Palaeoclimateology, Palaeoecocology,* 68: Issue 1: 61-77.

Darling, K. F., and C. M. Wade. 2008. The genetic diversity of planktic foraminifera and the global distribution of ribosomal RNA genotypes. *Marine Micropalaeontology*, Vol. 67: Issue 3, 216-238.

Dayhoff, J.E., and J.M. DeLeo. 2001. Artificial Neural Networks. *American Cancer Society*, Vol 91: 1615-1635.

Dick, C., V. Ediger, D. Fabbri, A. F. Gaines, G. D.Love, A. McGinn, C. McRae, I. P. Murray, B. J. Nicol and C. E. Snape. 2002. Eastern Mediterranean sapropels: chemical structure, deposition and relation to oil-shales. *Fuel,* Vol. 81: 431-448.

Doyle, P. 2005. Understanding Fossils - An Introduction to Invertebrate Palaeontology. London: John Wiley & Sons Ltd.

Dymond, J., E. Suess and M. Lyle. 1992. Barium in the deep-sea sediment: A geochemistry proxy for paleoproduction. *Paleoceanography*, Vol. 7: 163-181.

Earththreats. 2012. (Online). http://earththreats.com/2012/07/54-migrants-stranded-in-the-mediterranean-sea-die-of-dehydration (accessed on 05.11.2012).

Ellison, C. R. W., M. R. Chapman, and I. R. Hall. 2006. Surface and deep ocean interactions during the Cold Climate Event 8,200 years ago. *Science*, Vol. 312: 1929-1932.

Emeis, K., A. Camerlenghi, J. A. McKennzie, D. Rio, and R. Sprovieri. 1991. The occurrence and significance of Pleistocene and upper Pleistocene sapropels in the Tyrrhenian Sea. *Marine Geology,* Vol. 100: Issue (1-4), 155-182.

Emeis, K. C., A. H. F., Robertson, C. Richter *et al*. 1996. Proceedings of the Ocean Drilling Programme. *Initial Reports*, Vol. 160.

Emeis, K., T. Sakamoto, R. Wehausen and H-J. Brumsack. 2000. The sapropel record of the eastern Mediterranean Sea- results of Ocean Drilling Program Leg 160. *Palaeogeography, Palaeoclimateology, Palaeoecocology,* Vol. 158: 371-395.

Emelyanov, E. M., 2005. Calcite Compensation Depth in the Barrier Zones of the Ocean. Springer: USA.

Eumestat. 2012.(Online).

http://oiswww.eumetsat.org/WEBOPS/iotm/iotm/20051004_convection/20051004_convection.html (accessed on 05/11/2012).

Fairbanks, R. G., and P. H. Weibe. 1980. Foraminifera and Chlorophyll maximum: vertical distribution, seasonal succession, and palaeoceanographic significance. *Science*, Vol. 209: 1524-1526.

Fletcher, W. J., M. F. Sanchez-Goni, O. Peyron, and L. Dormoy. 2009. Abrupt climate changes of the last deglaciation detected in a western Mediterranean forest record. *Climate of the past discussions*, Vol. 5: 203-235.

"Foraminifera". 2011. (Online). Available: http://www.bowserlab.org/foraminifera/forampage2.htm (accessed on 28.03.2011).

"Foraminifera". 2011. (Online). Available: http://www.ucl.ac.uk/GeoSci/micropal/foram.html (accessed on 28.03.2011).

Fortey R. 2002. Fossils: The Key to the Past. 3rd edition. London: The Natural History Museum.

Fraile, I., M. Schulz, S. Mulitza and M. Kucera. 2008. Predicting the global distribution of planktonic foraminifera using a dynamic ecosystem model. *Biogeosciences*, Vol. 5: 891-911.

Francois R., S. Honjo, S. Manganini and G.E. Ravizza. 1995. Biogenic barium fluxes to the deep sea: Implication for palaeoproductivity reconstruction. *Global Biochemistry,* Cycles 9, 289-303.

Frigola, J., A. Moreno, I. Canals, F.J. Sierro, J.A. FloresJ, .O. Grimalt, D.A. Hodell and J.H. Curtis. 2007. Holocene climate variability in the western Mediterranean region from a deepwater sediment record: *Paleoceanography*, Vol. 22: 1-16.

Frumkin, A., I. Carmi, I. Zak, and M. Magaritz. 1994. Middle Holocene environmental change determined from the salt caves of Mount Sodon, Israel. In: Bar-Yosef, O., and R. S., Kra. (Eds.), late Quaternary Chronology and Palaeoclimates of the eastern Mediterranaen. *Radiocarbon*, 315-332.

Gallego-Torres, D., F. Martinez-Ruiz, A. Paytan, F. J. Jimenez-Espejo, and M. Ortega-Huertas. 2006. Pliocene- Holocene evolution of depositional conditions in the eastern Mediterranean: Role of anoxia vs. Productivity at time of sapropel deposition. *Palaeogeography, Palaeoclimateology, Palaeoecocology,* 04205: 1-16.

Gallego-Torres, D., F. Martinez-Ruiz, G. J., de Lange, F.J., Jimenez-Espejo, and M. Ortega-Huertas. 2010. Trace-elemental derived paleoceanographic and paleoclimatic conditions for Pleistocene Eastern Mediterranean sapropels. *Palaeogeography, Palaeoclimateology, Palaeoecocology,* Vol. 293: Issues 1-2, 76-89.

Georgopoulos, D., G., Chronis, G., Zervakis, V., Lykousis, V., Poulos, A., Iona. 2000. Hydrology and circulation in the southern Cretan Sea during CINCS experiment. Prog. Oceanography, Vol. 46: 89-112.

Geraga, M., S. Tsaila-Monopoli, C. Iokim and G. Papatheodorou. 2005. Short-term climate changes in the southern Aegean Sea over the last 48,000 years. *Palaeogeography, Palaeoclimatology, Palaeoecology,* Vol. 220: 311-332.

Geraga, M., G. Mylona, S. Tsaila-Monopoli, G. Papatheodorou, and G. Ferentinos. 2008. Northeastern Ionian Sea: Palaeoceanographic variability over the last 22ka. *Journal of Marine Systems,* Vol. 74: 623-638.

Giorgi, F. and P. Lionello. 2008. Climate change projections for the Mediterranean region. *Global and Planetary Change*, Vol. 63: 90-104.

Guiot, J., and A. De Vernal. 2011. Is spatial autocorrelation introducing biases in the apparent accuracy of palaeoclimatic reconstructions? *Quaternary Science Reviews*, Vol. 30: 3214-3216.

Haslett, S. K. 2002. 'Palaeoceanographic applications of planktonic sarcodine protozoa: radiolarian and foraminifera', in Haslett, S. K. (eds). Quaternary Environmental Micropalaeontology. London: Arnold.

Hayes, A., E.J Rohling, S. De Rijk, D. Kroon, W.J. Zachariasse. 1999. Mediterranean

planktonic foraminiferal faunas during the last glacial cycle. *Marine Geology*, Vol. 153: 239-252.

Hayes, A., M. Kucera, N. Kallel, L. Sbaffi and E. J. Rohling. 2005. Glacial Mediterranean Sea surface temperatures based on planktonic foraminiferal assemblages. *Quaternary Science Reviews,* Vol. 24: 999-1016.

Hemleben, C., M. Spindler, and O.R. Anderson. 1989. Modern Planktonic Foraminifera. New York: Springer.

Higham, T. 2002. Web-inforadiocarbon. (Online). Available: www.c14dating.com (accessed: 12.10.2012).

Hilgen, F. J., 1991. Astronomical calibration of Gauss to Matuyama sapropels in the Mediterranaen and implications for the Geomagnetic Polarity Time Scale. *Planet Earth*, Vol. 104: 226-244.

Hua, Q., 2009. Radiocarbon: A chronological tool for the recent past. *Quaternary Geochronology,* Vol. 4, 378-390.

Hughen, K., M. Baillie, E. Bard, A. Bayliss, J. Beck, C. Bertrand, P. Blackwell, C. Buck, G. Burr, K. Kutler, P. Damon, R. Edwards, R. Fairbanks, M. Friedrich, T. Guilderson, B. Kromer, F. McCormac, S. Manning, C. Bronk Ramsey, P. Reimer, S. Remmele, J. Southon, M. Stuiver, S. Talamo, F. Taylor, L. van der Plicht, and C. Weyhenmeyer. 2004. Marine04 Marine radiocarbon age calibration, 20-0 ka BP. *Radiocarbon,* Vol. 46: 1059-1086.

Hurrell, J. W., Y. Kushnir, G. Ottersen, and M Visbeck. 2003. An overview of the North Atlantic Oscillation. *Geophysical Monograph*, Vol. 134.

Istrianet. 2012. (Online). http://www.istrianet.org/istria/geosciences/meteorology/winds/tech-notes.htm (accessed 06.01.2011)

Jalut, G., J. J. Dedoubat, M. Fontugne, and T. Otto. 2008. Holocene circum-

Mediterranean vegetation changes: Climate forcing and human impact. *Quaternary International*, Vol. 200. 4-18.

Jorissen, F. J., 1999. Benthic foraminiferal succession across Late Quaternary Mediterranean sapropels. *Marine Geology*, Vol. 153: 91-101.

Katz, E. J.,1972. The Levantine intermediate water between the Strait of Sicily and the Strait of Gibraltar. *Deep Sea Research and Oceanographic Abstracts*, Vol.19: Issue 7, 507-520.

Keller, G. 2004. Low-Diversity, Late Maastrichtian and Early Danian Planktic foraminiferal Assemblages of the eastern Tethys. *Journal of Foraminiferal Research,* Vol.34, No. 1: 49-73.

Kromer. B., 2009. Radiocarbon and dendrochronology. *Dendrochronologia*, Vol. 27: Issue 1, 15-19.

Kroon, D., I. Alexander, M. Little, L. J. Lourens, A. Matthewson, A. H. F. Robertson and T. Sakamoto. 1998. Oxygen isotope and sapropel stratigraphy in the eastern Mediterranean during the last 3.2 million years. *Proceedings of the Ocean Drilling Programme, Scientific Results,* Vol. 160: 181-189.

Kucera, M. 2002. 'Planktonic foraminifera as tracers of past oceanic environments', in Hillaire-Marcel, C., and A. De Vernal (eds). Proxies in Late Cenzoic Palaeoceanography. USA: Elsevier.

Kullenberg, B., 1952. On the salinity of water contained in marine sediments. *Medd. Oceanography,* Institution Göteberg, Vol. 21: 1-38.

Kuroyanagi, A., and H. Kawahata. 2004. Vertical distribution of living planktonic foraminifera in the seas around Japan. *Marine Micropaleontology*, Vol. 53: Issues 1–2, 173-196.

Lascaratos, A., R.G. Williams and E. Tragou, 1993. A Mixed-Layer Study of the Formation of Levantine Intermediate Water. *Journal of Geophysical Research*, Vol. 98:

14,739-14,749.

Lascaratos, A., W., Roether, W., Nittis and B., Klein. 1999. Recent changes in deep water formation and spreading in the eastern Mediterranean Sea: a review. *Prog. Oceanography,* Vol.44: 5-36.

La Violette, P., 1994. Overview of the Major Forcings and Water Masses of the Western Mediterranean Sea. *Seasonal and Interannual Variability of the Western Mediterranean Sea Coastal and Estuarine Studies,* Vol. 46: 1-11.

Lionello, P., P Malanotte-Rizzoli and R. Boscolo, P. Albert, V. Artale, L. Li, J. Luterbacher, W. May, R. Trigo, M. Tsimplis, U. Ulbrich, and E. Xoplaki. 2006. 'The Mediterranean Climate: an overview of the main characteristics and issues' in Lionello, P., P Malanotte-Rizzoli and R. Boscolo (eds). Mediterranean Climate Variability, Oxford: Elsevier.

Lourens, L .J., F. J. Hilgen, L. Gudjonsson, and W. J. Zachariasse. 1994. 'Late Pliocene to Early Pleistocene astronomically forced sea surface productivity and temperature variations in the Mediterranean' in Lourens, L. J., (eds), Astronomical forcing of Mediterranaen climate during the last 5.3 million years. *Universiteit Utrecht*. 37-58.

Lourens, L.J., 2004. Revised tuning of Ocean Drilling Programme Site 964 and KC01B (Mediterranean) and implications for the delta 0-18, tephra, calcareous nonnofossils and geomagnetic reversal chronologies of the past 1.1 Myr. *Paleoceanography,* Vol. 1-2: 49-78.

Malanotte-Rizzoli, P., M. R. D'Alcala, A. Theocharis, A. Bergamasco, D. Bregant, G. Budillon, G. Civitarese, D. Georgopoulos, A. Michelato, E. Sansone, P. Scarazzato, and E. Souvermezoglou.1997. A synthesis of the Ionian Sea hydrography, circulation and water mass pathways during POEM-Phase I. *Progress in Oceanography*, Vol. 39: Issue 3, 153-204.

Malanotte-Rizzoli, P. and A. Hecht. 1988. Large-scale properties of the eastern Mediterranean: a review. *Oceanologica Acta*, Vol.11(4): 323-335.

Mamo, B., L. Strotz, and D. Dominry-Howes. 2009. Tsunami sediments and their assemblages. Earth Science Reviews, Vol. 96: Issue 4: 263-278.

Martinez-Ruiz, F., A. Payton, M. Kastner, J. M. Gonzalez-donoso, D. Linares, S. M. Bernasconi and F. J. Jimenez-Espejo. 2003. *Palaeogeography, Palaeoclimateology, Palaeoecocology,* Vol. 190: 23-37.

Melki, T., N. Kallel, F.J. Jorissen, F. Guichard, B. Dennielou, S. Berné, L. Aabeyrie and M. Fontugne. 2009. Abrupt climate change, sea surface salinity and paleoproductivity in the western Mediterranean Sea (Gulf of Lion) during the last 28kyr. *Palaeogeography, Palaeoclimatology, Palaeocology,* Vol. 279: 96-113.

Miller, A.R. 1963. Physical Oceanography of the Mediterranean Sea: A discourse. *Rapp. Comm. Int. Mer Mèdit*, Vol. 17: 857-871.

Monserrat, S., J. L. Lopez-Jurado, and M. Marcos. 2008. A mesoscale index to describe the regional circulation around the Balearic Islands. *Journal of Marine Systems*, Vol. 71: 413-420.

Mulitza, S., T. Wolff, J. Patzold, W. Hale and G. Wefer. 1998. Temperature sensitivity of planktic foraminifera and its influence on the oxygen isotope record. *Marine Micro-paleontology,* Vol.33: 223-240.

Murat, A., and H. Got, 2000. Organic carbon variations of the eastern Mediterranean Holocene sapropel: a key for understanding formation processes. *Palaeogeography, Palaeoclimateology, Palaeoecocology*: 241-257.

National Oceanography Centre. 2012. (Online). Available: www.noc.soton.ac.uk/soes/teaching/courses/oa432_624/basics.pdf (accessed: 12.10.2012).

Naval Research Laboratory. 2012 (Online). http://www.nrlmry.navy.mil/~medex/tutorial/toc/toc.html (accessed on 5/11/2012)

Negri, A., L. Capotondi and L. Keller. 1999. Calcareous nannofossils, planktonic foraminifera and oxygen isotopesin the Late Quaternary sapropels of the Ionian Sea.

Marine Geology, Vol. 157: 89-103.

Nijenhuis, I. A., S. J. Schenau, C. H. Van der Weijden, F. J. Hilgen, L. J. Lourens and W. J. Zachariasse. 1996. On the origin of upper Miocene sapropelites: A case study from the Faneromeni Section, Crete (Greece). *Paleoceanography,* Vol. 11: 633-645.

Nijenhuis, I. A., H-J. Boch, J. S.Sinninghe Damstè, H-J. Brumsack and G. J. De Lange. 1999. Organic matter and trace element rich sapropels and black shales: a geochemical comparison. *Earth Planet, Science Letter,* Vol. 169: 277-290.

Nijenhuis, I. A. And G. J. De Lange. 2000. Geochemical constraints on Pliocene sapropel formation in the eastern Mediterranean. *Marine Geology,* Vol. 163: 41-63.

Numberger, L., C. Hemleben, R. Hoffmann, A. Mackensen, H. Schulz, J. M. Wunderlich, and M. Kucera. 2009. Habitats, abundance patterns and isotopic signals of morphotypes of the planktonic foraminifer Globigerinoides ruber (d'Orbigny) in the eastern Mediterranean Sea since the Marine Isotopic Stage 12. *Marine Micropaleontology*, Vol. 73: Issues 1–2, *90-104.*

Ocean Drilling Program. 2012. (Online) Available: http://www-odp.tamu.edu/publications/161_SR/chap_32/c32_f1.htm (accessed on 12.10.2012).

Olausson, E., 1961. Studies in deep sea cores. *Deep sea expedition 1947-1948,* Vol. 8: 337-391.

Ozsoy, E., 1981. On the atmospheric factors affecting the Levantine Sea. *European Centre for medium range weather forecasts, Technical Report*, Vol. 25: 29.

Ozturgut, E., 1976. The source and spreading of the Levantine Intermediate Water in the eastern Mediterranaen. *Saclant ASW Research Centre Memorandum SM-92, La Spanzia*, Italy, 45.

Passier, H. F., J. J. Middelburg, G. J. De Lange, and M. E. Bõttcher. 1999. Modes of sapropel formationin the eastern Mediterranean: Some constraints based on pyrite properties. *Marine Geology,* Vol. 153: 199-219.

Pawlowski, J. 2009. Foraminifera. University of Geneva.

Paytan, A., F., Martinez-Ruiz, M. Eagle, A. Ivy, S. D.Wankel. 2004. Using sulfur isotopes in barite to elucidate the origin of high organic matter accumulation events in marine sediments. *Sulfur Biogeochemistry, GSA Special Paper,* Vol. 379: 151-160.

Pilcher, J.R., 2005. 'Radiocarbon Dating and Environmental Radiocarbon Studies', in Mackay, A., R. Battarbee, J. Birks and F. Oldfield (eds). Global change in the Holocene. London: Hodder .Arnold

Pinardi, N. and E. Masetti. 2000. Variability of the large scale general circulation of the Mediterranean Sea from observations and modelling: a review. *Palaeogeography, Palaeoclimatology, Palaeoecology,* Vol. 158: 153-173.

Principato, M. S., S. Giunta, C. Corselli, and A. Negri. 2003. Late Pleistocene - assemblages in three box-cores from the Mediterranean Ridge area (west-southwest of Crete): palaeoecocological and palaeoceanographic reconstruction of sapropel S1 interval. *Palaeogeography, Palaeoclimatology, Palaeoecology*, Vol. 190: 61-77.

Principato, M. S. 2003. Late Pleistocene-Holocene Planktonic foraminifera from the eastern Mediterranean Sea: towards a high-resolution planktonic foraminiferal assemblage zonation for the late Quaternary of the Mediterranean. *Rivista Italiana di Paleontologia e stratigrafia*, Vol. 109: Issue 1, 111-124.

Pross, J., U. Kotthoff, U.C. Müller, O. Peyron, I. Dormoy, G. Schmiedl, S. Kalaitzidis, and A.M. Smith. 2009. Massive perturbation in terrestrial ecosystems of the Eastern Mediterranean region associated with the 8.2 kyr B.P. climatic event. *Geological Society of America*, Vol. 37, No. 10: 887-890.

Pujol C. and C. Vergnaud Grazzini. 1989. Palaeoceanography of the last deglaciation in the Alboran Sea (western Mediterranean). Stable isotopes and planktonic foraminiferal records. *Marine Micropalaeontology*, Vol. 15: Issue 1-2, 153-179.

Pujol C. and C. Vergnaud Grazzini. 1995. Distribution patterns of live foraminifera as related to regional hydrography and productive systems of the Mediterranaen Sea.

Marine Micropalaeontology, Vol. 25: 187-217.

Robinson, S. A., W.G. Leslie, A. Theocharis and A. Lascaratos. 2001. Mediterranean Sea Circulation. *Ocean Currents*, Vol. 1-19.

Robinson, S. A., S. Black, B. W. Sellwood, and P.J. Valdes. 2006. A review of palaeoclimates and palaeoenvironments in the Levant and eastern Mediterranaen from 25,000 to 5,000 years BP: setting the environmental background for the evolution of human civilisation. *Quaternary Science Review*, Vol. 25: 1517-1541.

Rohling, E. J., and W. W. C. Gieskes. 1989. Late Quaternary changes in Mediterranaen Intermediate Water density and formation rate. *Palaeoceanography*, Vol. 4: 531-545.

Rohling, E. J., 1991. Shoaling of the eastern pycnocline due to reduction of excess evaporation: implication for sapropel formation. *Paleoceanography,* Vol. 6: 747-753.

Rohling, E., and F.J. Hilgen, 1991. The eastern Mediterranean climate at times of sapropel formation: A review. *Geology,* **Vol.** 70: 253-264.

Rohling, E. J., F. J. Jorissen, C. Vergnaud Grazzini, and W. J. Zachariasse. 1993. Northern Levantine and Adriatic Quaternary planktic foraminifera; Reconstruction of paleoenvironmental gradients. *Marine Micropaleontology*, Vol. 21: Issues 1–3, 191-218.

Rohling, E. J., M. Den Dulk, C. Pujol, and C. Vergnaud-Grazzini. 1995. Abrupt hydrographic changes in the Alboran Sea (western Mediterranaen) around 8000 yrs BP. Deep Sea Results, Vol. 42: 1609-1619.

Rohling, E.J., 2001. The Dark Secret of the Mediterranean –a case history in past environmental reconstruction, http://www.iasonnet.gr/abstracts/rohling.html (accessed on 15.01. 2011)

Rohling, E. J. , T. R. Cane, S. Cooke, M. Sprovieri, I. Bouloubassi, K. C. Emeis, R. Schiebel, D. Kroon, F. J. Jorissen, A. Lorre, A. E. S. Kemp. 2002. African monsoon variability during the previous interglacial maximum. *Earth and Planetary Science*

Letters, Vol. 202: Issue 1, 61-75

Rohling, E., R. Abu-Zied, J. Casford, A. Hayes and B. Hoogakker, 2009. The Marine Environment: Present and Past, in J.C.Woodward (ed.), *The Physical Geography of the Mediterranean.* Oxford University Press, Oxford, 33-67.

Rossignol-Strick, M., W. D. Nesteroff, P. Olive, and C. Vergnaud-Grazzini. 1982. After the deluge: Mediterranean stagnation and sapropel formation. *Nature*, Vol. 295: 105-110.

Rossignol-Strick, M., 1985. Mediterranean Quaternary Sapropels, an immediate response of the African monsoon to variation of insolation. *Palaeogeography, Palaeoclimateology, Palaeoecocology,* Vol. 49:237-263.

Rossignol-Strick, M., 1987. Rainy periods and bottom water stagnation initiating brine accumulation and metal concentrations, 1. The Late Quaternary. *Palaeoceanography*, Vol 2: 333-360.

Rossignol-Strick, M., 1995. Sea land correlation of pollen records in the eastern mediterranean for the glacial-interglacial transition: biostratigraphy versus radiometrictime-scale. *Quaternary ScienceReviews*, Vol, 14: 893-915.

Rouis-Zargouni, I., J. L. Turon, L. Londeix, L. Essallami, N. kallel, and M. A. Sicre. 2010. Environmental and climatic changes in the central Mediterranaen Sea (Siculo-Tunisian Strait) during the last 30 ka based on dinoflagellate cyst and planktonic foraminifera assemblages. *Palaeogeography, Palaeoclimateology, Palaeoecocology,* Vol. 285: 17-29.

Ryan, W. B. F., 1972. Stratigraphy of Late Quaternary sediments in the eastern Mediterranean in: The Mediterranean Sea: A National Sedimentation Laboratory, edited by Stanley, D.J.Dowden, Hutchinson and Ross, Stroudsburg, 149-169.

Sancetta, C. 1999. Oceanography: The mystery of the sapropels. *Nature*, Vol. 398: 27-29.

Santinelli, C., L. Nannicini, and A. Seritti. 2010. DOC dynamics in the meso and bathypelagic layers of the Mediterranean Sea. *Deep Sea Research Part II: Topical Studies in Oceanography*, Vol. 57: Issue 16, 1446-1459.

Sarmiento, J. L., T. Herbert, J. R. Toggweiler. 1988. Mediterranean nutrient balance and episodes of anoxia. *Global Biochemistry,* Vol. 2: 427-444.

Sautter, L. R., and R. C. Tunell. 1991. Seasonal variability in the upwelling environment sediment trap results from the San Pedro basin, southern California Bight. *Palaeoceanography*, Vol. 6: 307-334.

Sbaffi, L., F. C. Wezel, G. Curzi, and U. Zoppi. 2004. Millennial- to centennial-scale palaeoclimatic variations during Termination I and the Holocene in the central Mediterranean Sea. *Global and Planetary Change*, Vol. 40: Issues 1–2, 201-217.

Schenau, S. J., A. Antonarakou, F. J. Hilgen, L. J. Lourens, I. A. Nijenhius, C. H. Van der Wrijden and W. J. Zachariasse. 1999. Organic rich layers in the Metochia section (Gavdos, Greece): Evidence for a single mechanism of sapropel formation during the past 10 Myr. *Marine Geology,* Vol. 153: 117-135.

Schiebel, R., and C. Hemleben. 2005. Modern planktic foraminifera. *Palaontologische Zeitschrift*, Vol. 79: Issue 1, 135-148.

Schmiedl, G., A. Mitschele, S. Beck, K-C Emeis, C. Hemleben, H. Schulz, M. Sperling, and S. Weldeab. 2003. Benthic foraminiferal record of ecosystem variability in the eastern Mediterranean Sea during times of sapropel S5 and S6 deposition. *Palaeogeography, Palaeoclimateology, Palaeoecocology*, Vol. 190: 139-164.

Shaw, H. F., and G. Evans. 1984. The nature, distribution and origin of a sapropelic layer in sediments of the Cilicia basin, northeastern Mediterranean. *Marine Geology*, Vol. 61: 1-12.

Siani, G., M., Paterne, M.E., Sulpizio, R., Sbrana, A., Arnold, and M. Haddad. 2001. Mediterranean Sea surface radiocarbon reservoir age changes since the last glacial maximum. *Science*, Vol. 294: 1917-1920.

Siccha, M., G. Trommer, H. Schulz, C. Hemleben and M. Kucera. 2009. Factors controlling the distribution of planktonic foraminifera in the Red Sea and implications for the development of transfer functions. *Marine Micropaleontology, Vol.* 72: 146-156.

Sprovieri, R., E. Di Stefano, A. Incarbona, and M. E. Gargano. 2003. A high-resolution record of the last deglaciation in the Sicily Channel based on foraminifera and calcareous nannofossil quqntitative distribution. *Palaeogeography, Palaeoclimateology, Palaeoecocology,* Vol.202: 119-142.

Stanley, S. M. 2005. Earth System History- Second Edition. New York: W.H. Freeman and Company.

Stefanelli, S, L. Capotondi, and N. Ciaranfi. 2005. Foraminiferal record and environmental changes during the deposition of the Early-Middle Pleistocene sapropels in southern Italy. *Palaeogeography, Palaeoclimateology, Palaeoecocology,* Vol. 216: 27-52.

Tang, C. M., and L. D. Stott. 1993. Seasonal salinity changes during Mediterranean sapropel deposition 9000 years B.P.: evidence from isotopic analyses of individual planktonic foraminifera. Paleoceanography, Vol. 8: Issue (4), 473-493.

Telford, R. J., C. Li, and M. Kucera. 2012. Mismatch between the depth habitat of planktonic foraminifera and the calibration depth of SST transfer functions may bias reconstructions. *Climate of the Past Discussions*, Vol. 8: 4075-4103.

Theocharis, A., E., Balopoulos, E., Kioroglou, S., Kontoyiannis and H., Iona, A. 1999b. A synthesis of the circulation and hydrography of the south Aegean Sea and the straits of the CretanArc. *Prog Oceanography*, Vol. 44: 469-509.

Thiede, J. 1978. A glacial Mediterranean. *Nature*, Vol. 276: 680-683.

Thomson, J., N. C. Higgs, T. R. S. Wilson, I. W. Croudace, I. W. De Lange and P. J. M. Santvoort. 1995. Redistribution and geochemical behaviourof redox-sensitive elements around S1, the most recent eastern Mediterranean sapropel. *Geochemistry. Cosmochemistry. Acta,* Vol. 59: 3487-3501.

Thomson, J., D. Mercone, J. G. De Lange, and P. J. M.Van Santvoort. 1999. Review of recent advances in the interpretation of eastern Mediterranaen sapropel S1 from geochemical evidence. *Marine Geology*, Vol. 153: 77-89.

Thunell, R. C., D. F. Williams, and J. P. Kennet. 1977. Late Quaternary palaeoclimatology stratigraphy and sapropel history in eastern Mediterranaen deep-sea sediments. *Marine Micropaleontology,* Vol. 2: 371-388.

Thunell, R. C., 1978. Distribution of recent planktonic foraminera in surface sediments of the Mediterranaen Sea. *Marine Micropaleontology,* Vol. 3: 147-173.

Thunell, R. C., 1982. Carbonate dissolution and abyssal hydrography in the Atlantic Ocean. *Marine Geology*, Vol. 47: Issues 3–4, 165-180

Thunell, R. C., D. F., Williams, and P. Belayea. 1984. Anoxic events in the Mediterranean Sea in relation to the evolution of late Neogene climates. *Marine Geology,* Vol. 59: 105-134.

Triantaphyllou, M. V., A. Antonarakou, K. Kouli, M. Dimiza, G. Kontakiotis, M. D. Papanikolaou, P. Ziveri, P. G. Mortyn, V. Lianou, V. Lykousis, M. D. Dermitzakis. Late Glacial–Holocene ecostratigraphy of the south-eastern Aegean Sea based on plankton and pollen assemblages.*Geology Marine Lette*r, Vol. 29: 249-267.

Triantaphyllou, M. V., M. Dimiza, and C. Anagnostou. 2010. Calcareous nannofossils and planktonic foraminiferal distributional patterns during deposition of sapropels S6, S5 and S1 in the Libyan sea (eastern Mediterranean). *Geo-Marine Letters*, Vol. 30: Issue 1, 1-13.

Troelstra, S. R., O. M. Ganssen, K., Van der Borg, and A. F. M. De Jong. 1991. A late Quaternary stratigraphic framework for easterm Mediterranaen sapropel S1 based on AMS 14C dates and stable oxygen isotopes. *Radiocarbon*, Vol. 33: 15-21.

Turney, C. S. M..1998. Extraction of rhyolitic ash from inerogenic lake sediments. *Journal of Palaeolimnology*, Vol. 19: 199-206.

UCAR. 2012. (Online) http://eo.ucar.edu/spotlight/nao/page3.html (accessed on

05/11/2012)

Ufkes, E., J.H.f., Jansen, G.J., Brummer. 1998. Living planktonic foraminifera in the eastern South Atlantic during spring: indicators of water masses, upwelling and Congo (Zaire) River plume. *Marine Micropaleontology,* Vol.33: 27-53.

Ufkes, E., J. H. F. Jansen, R. R. Schneider. 2000. Anomalous occurrences of Neogloboquadrina pachyderma (left) in a 420-ky upwelling record from Walvis Ridge (Se Atlantic). *Marine Micropalaeontology,* Vol. 40: 23-42.

Van Os, B. J. H., J. J. Middelburg, and G. J. de Lange. 1991. Possible diagenetic mobilisation of barium in sapropelic sediment from the eastern Mediterranean. *Marine Geology*, Vol. 100: 125-136.

Vargas-Yáñez, M., P. Zunino, K. Schroeder, J. L. López-Jurado, F. Plaza, M. Serra, C. Castro, M. C. García-Martínez, F. Moya, J. Salat. 2012. Extreme western intermediate water formation in winter 2010. *Journal of Marine Systems*, Vol.105–108: 52-59.

Vergnaud-Grazzini, C. Ryan, and W. B. F., Cita. 1977. Stable isotopic fractionation, climate change and episodic stagnation in the eastern Mediterranean during the late quaternary. *Marine Micropalaeontology,* Vol. 2: 353-370.

Vergnaud-Grazzini, C., M. Devaux, and J. Znaidi. 1986. Stable isotope 'anomolies' in Mediterranaen Pleistocene records. *Marine Micropaleontology*, Vol. 10: 35-69.

Vergnaud-Grazzini, C., A. M. Borsetti, F. Cati, P. Colantoni, S. D'Onofrio, J. F. Saliege, R. Sartori, R. Tampieri. 1988. Palaeoceanographic record of the last glaciation in the Strait of Sicily. *Marine Micropaleontology*, Vol. 13: Issue 1, 1-21.

Walker, M., 2005. Quaternary Dating Methods. John Wiley and Sons Ltd. Chichester: England.

Watts, W. A., J. M. R. Allen, B. Huntley, and S. C. Fritz. 1996. Vegetation history and climate of the last 15,000 years at laghi di Monticchio Southern Italy. *Quaternary Science Reviews*, Vol, 15: 113-132.

Williams, M., D. Dunkerley, P. De Deckker, P. Kershaw, and J. Chappell. 1998. Quaternary Environments-Second Edition. London: Arnold Publishers.

Wilson, R.C .L., S.A. Drury and J.L. Chapman. 2005. The Great Ice Age-Climate Change and Life. Cornwall: Routledge.

Wu, P., K., Haines, N., Pinardi. 2000. Toward an understanding of deep-water renewal in the eastern Mediterranean. *Journal Physics Oceanography*, Vol. 30: 443-458

Žarić, S., B. Donner, G. Fischer, S. Mulitza and G. Wefer. 2005. Sensitivity of planktic foraminifera to sea surface temperature and export production as derived from sediment trap data. *Marine Micropaleontology,* Vol. 55: 75-105.